ABSTRACT

SOHIL ARORA. Development of Dielectric Elastomer based Prototype Fiber Actuators (Under the guidance of Dr. Tushar K. Ghosh, Dr. John F. Muth and Dr. Richard Kotek)

Dielectric elastomer based prototype fiber actuators have been developed based on the concept of cylindrical dielectric elastomer actuators (DEAs). The prototype fiber actuators have been built using commercially available dielectric elastomer tubes, having wall thickness in the range of 100-200 microns, and applying appropriate compliant electrodes to inner and outer wall of these tubes.

Actuation behavior of prototype fiber actuators has been studied under different boundary conditions and as a function of applied electric field. Actuation behavior constitutes axial and radial actuation strains as well as blocking forces produced in the prototype upon actuation. Different boundary conditions were achieved by applying different prestrains on the dielectric elastomer tubes. Two types of prestrains, uniaxial and uniform, at different levels were applied. Uniaxially prestrained prototypes were fabricated by prestraining the dielectric elastomer tubes along the axial direction. Two dielectric elastomers, silicone and polyurethane, with compliant polymer based inner and outer electrodes were used for fabrication. Uniformly prestrained prototypes were fabricated by inflating the dielectric elastomer tubes with an inflation medium. To keep the actuator design simple, inner electrode was used as the inflation medium. A strong electrolyte was used as the inner electrode whereas a polymer based electrode was used as the outer electrode.

An experimental set-up was designed to conduct the actuation experiments and evaluate the actuation behavior of prototype fiber actuators. Actuation strains were measured using image analysis techniques and actuation blocking forces were measured using a load cell coupled to the prototype fiber actuator. A parabolic relationship was observed between applied electric field and axial actuation strains, radial actuation strains and actuation blocking force for the developed prototypes.

Upon actuation of the uniaxially prestrained prototypes it was observed that axial strains and actuation blocking force decreased with the increase in uniaxial prestrain levels, and radial strains increased with the increase in uniaxial prestrain levels. Also, silicone based uniaxially

prestrained prototype fiber actuators showed much higher actuation strains than the polyurethane based. In uniformly prestrained prototypes, axial actuation strains, radial actuation strains and actuation blocking force, all three, showed a decrease with increase in inflation pressure.

To characterize the tubular actuators for their utility and to validate the experimental technique used in this study the prototype fiber actuators were tested for any hysteresis in their actuation behavior. No hysteresis was observed in the actuation behavior of both silicone and polyurethane based prototype fiber actuators.

DEVELOPMENT OF DIELECTRIC ELASTOMER BASED PROTOTYPE FIBER ACTUATORS

by

SOHIL ARORA

A thesis submitted to the Graduate Faculty of

North Carolina State University

In partial fulfillment of the

Requirements for the degree of "Master of Science"

In

TEXTILE MANAGEMENT AND TECHNOLOGY

Raleigh, NC

July 2005

Approved by:

_____

Dr. Tushar K. Ghosh
Chair of Advisory Committee

_____

Dr. John F. Muth
Co-Chair of Advisory Committee

_____

Dr. Richard Kotek
Member of Advisory Committee

DEDICATION

I dedicate this thesis to my, parents Mrs. Arti Arora and Mr. Ved Prakash Arora, brother Ankit Arora and 'to be' life partner Ms. Mini Mehta. It is for their love, support and strong belief in my abilities that I have reached where I am today.

BIOGRAPHY

Sohil Arora was born on 2nd October 1980 in Faridabad, India. He completed his high school from APEEJAY School, Faridabad in the year 1998. He pursued his undergraduate degree in Textile Technology from one of India's most prestigious institutes of higher education, Indian Institute of Technology (IIT), Delhi. He completed his Bachelor of Technology degree from IIT in May 2002. After completing his bachelors, he worked as a textile engineer in the garment manufacturing industry in India for one year. In the Fall of 2003 he joined masters program in Textile and Apparel, Technology and Management department of North Carolina State University. He completed his masters' degree in Textile Management and Technology in August 2005. After graduation he will begin working with Select Comfort Corporation at their corporate headquarters in Minneapolis, MN.

ACKNOWLEDGEMENTS

I would like to thank Chair of my advisory committee, Dr. Ghosh for his guidance, support and encouragement through out these two years. He has taught me invaluable lessons that I will carry with myself for the rest of my life. I would like to thank Co-Chair of my advisory committee, Dr. Muth for his guidance through out the course of this project. I also wish to extend my appreciation to Dr. Kotek for his time as a member of my advisory committee.

I wish to thank all my colleagues, especially, Saurabh Chapparwal, Jeesang Hwang, Mehmet Cuneyt and Ravi Shankar for their insightful discussions and motivation at every step.

I also wish to thank all the staff of TATM office, especially, Rob Cooper and Tywanna Johnson for their cooperation during these two years of mine at College of Textiles.

TABLE OF CONTENTS

LIST OF TABLES

LIST OF FIGURES

1 INTRODUCTION

Use of polymers as actuator material has been an area of research for quite some time now. Many polymers are known that show dimensional changes in response to an electrical simulation. These polymers are called electroactive polymers or EAPs. Various actuators have been developed based of different actuation principles of EAPs, such as piezoelectric, electrostrictive, and magnetostrictive behavior, etc. In the past decade, a class of EAPs has drawn particular interest of the researchers because of their high actuation strains and energy densities. These are so called dielectric elastomers, and the actuators built using these are known as dielectric elastomer actuators or DEAs. The performance of DEAs very closely matches that of biological muscles in terms of strains, energy densities, pressure and speed [35] and can be used to develop actuators with muscle-like capabilities. Because of their muscle like actuation behavior DEAs have acquired the moniker 'Artificial Muscles'.

DEAs that are currently reported in literature can be broadly classified as planar or cylindrical DEAs. In the literature, several different configurations of planar and cylindrical DEAs have been developed and used to perform muscle like operations [34, 36, 46, 13, 1, 47, 37, 35]. Even though performance of the reported DEAs matches very closely to that of biological muscles, their size is far from the size of a biological muscle, which limits their applications and scope of operations. Dielectric elastomer fiber actuators conceptualized here, which in principle are cylindrical DEAs, will overcome the size disadvantage of DEAs as manufactured polymeric fibers of today are geometrically very close to size of biological muscles. These fiber actuators when bundled together will not only have the potential to give biological muscle like performance, like currently reported DEAs, and will be geometrically much closer to biological muscles, but will also provide more degrees of freedom than current DEAs. These fiber actuators can also be incorporated in conventional textiles to produce active, smart structures. Dielectric elastomer fiber actuators can be realized easily because technology to produce multicomponent fibers already exists and can be potentially adapted to produce dielectric elastomer fibers as actuators.

In this thesis, working prototypes of dielectric elastomer based fiber actuators have been developed, and their actuation behavior has been studied.

2 BACKGROUND

Polymers have many attractive characteristics; they are lightweight, inexpensive, fracture tolerant, and pliable. Further, they can be configured into almost any conceivable shape and their properties can be tailored to suit a broad range of requirements. For several decades, it has been known that certain polymers show change in shape in response to electrical simulation. These polymers have been referred to as Electro Active Polymers or EAP's. Initially, EAP's were capable of inducing only a relatively small strain; however in the last decade many new polymers have emerged which respond to electrical simulation with a significant shape or size change. Table 2.1 shows comparison of performance of EAP's with that of biological muscle and other actuator technologies.

Table 2.1 Comparison of EAP's with other actuator technologies [25]

	Actuator Type (specific example)	Typical (Max.) Strain (%)	Typical (Max.) Stress (MPa)	Typical (Max.) Specific Elastic Energy Density (J/g)	Typical (Max.) Elastic Energy Density (J/cm^3)	Typical (Max.) Avg. Specific Power Density at 1 Hz (W/g)	Peak Strain rate (%/s)	Elastic Modulus (MPa)	Est. Max. Efficiency (%)	Relative Speed (full cycle)
NATURAL MUSCLE	Mammalian Skeletal Muscle	20 (40)	0.1 (0.35)	0.041 (0.08)	0.041 (0.08)	0.041 (0.08)	> 50	10–60	20%	Medium
ELECTROACTIVE POLYMER	Dielectric elastomer	25 (> 300)	1.0 (7.0)	0.1 (3.4)	0.1 (3.4)	0.1 (3.4)	> 450	0.1–10	60–90	Med. - Fast
	Electrostrictive Polymer	3.5 (7.0)	20 (45)	0.17 (> 0.53)	0.3 (> 1.0)	0.17 (> 0.53)	> 2000	400–1200	60–90	Fast
	Electrochemo-mechanical Conducting Polymer	2 (20)	5 (200)	0.1 (1.0)	0.1 (1.0)	0.1 (1.0)	1	200–3000	< 5	Med. -Slow
	Ionic Polymer Metal Composite	0.5 (3.3)	3 (15)	(0.004)	(0.006)	0.004	3.3	50–100	1.5–3	Med. - Slow
	Mechano-chemical Polymer/Gels (Polyelectrolyte)	> 40	0.3	0.06	0.06	< 0.06	< 1	?	30	Slow
	Piezoelectric Polymer (PVDF)	0.1	4.8	0.0013	0.0024	0.0013	?	450	60–90	Fast
OTHER	Liquid Crystal Elastomer (Thermal)	19 (45)	0.12 (0.45)	0.003 (0.06)	0.003 (0.06)	< 0.003	37	0.3 – 4	< 5%	Slow
	Shape Memory Polymer	100	4	2	2	< 0.2	?	?	< 10	Slow
NONPOLYMER ACTUATORS	Electromagnetic									
	Direct (Voice Coil)	50	0.10	0.003	0.025	0.003	> 1000	NA	> 80	Fast
	Motor/transmission	50	NA	NA	NA	0.5	< 200	NA	> 50	Medium
	Piezoelectric									
	Ceramic (PZT)	(0.2)	(110)	(0.013)	(0.10)	(0.013)	> 1000	25,000–70,000	> 90	Fast
	Single Crystal (PZN-PT)	(1.7)	(131)	(0.13)	(1.0)	(0.13)	> 1000	9000	> 90	Fast
	Shape Memory Alloy (TiNi)	> 5	> 200	> 15	> 100	< 15	300 (one direction only)	20,000–80,000	< 10	Slow
	Thermal (Expansion)	1	78	0.15	0.4	< 0.15	Depends on heat transfer	> 70,000 (varies)	< 10	Slow
	Magnetostrictive (Terfenol-D, Etrema Products)	0.2	70	0.0027	0.025	>0.0027	>1000	40,000	60	Fast

2.1 ELECTRO ACTIVE POLYMERS (EAP'S)

As mentioned before, polymers that show change in shape on application of an electrical impulse have been called electro active polymers or EAP's. EAP's can be divided primarily into two groups: electronic and ionic.

2.1.1 Electronic EAP's

EAPs that are driven by electric field or coulomb forces are called electronic EAPs. They are capable of performing energy conversion between electric and mechanical form and hence can be used as solid-state electromechanical actuators and motion sensors. Different types of electronic EAPs are discussed below.

Ferroelectric Polymers

When a non-conducting crystal or dielectric material exhibits spontaneous electric polarization the phenomenon is called ferroelectricity [4], in other words, when a ferroelectric crystal is compressed along a certain axis a voltage is produced at the surface or when an external voltage is applied the crystal sustains an elongation. Some commonly used ferroelectric polymers are Poly (vinylidene difluoride) (PVDF) and its copolymers**.** Strains of nearly 2% have been reported in PVDF at large ac fields (~200MV/m) [3]. Higher strains (~ 5%) have been reported for P(VDF-TrFE) copolymer with defects introduced in its crystalline structure [44]

Electrets

An electret is a polymeric dielectric, which when subjected to an applied electric field can retain a state of polarization after the field is removed [14]. The process of polarizing a polymer dielectric is called direct or dc poling and is usually performed by placing two electrodes on opposite sides of the polymer material and applying required voltage to obtain the devised electric field. Some commonly used electrets are wax electrets and polymer electrets. Electrets have application in microphones, sensors, transducers and filters.

Electrostrictive Polymers

Electrostriction is defined as the change in shape of a body due to rearrangement of its molecules in presence of an external electric field. Materials showing actuation due to electrostriction are called electrostrictive materials.

Electrostrictive graft elastomers are polymers consisting of two components, a flexible macromolecule backbone and a grafted polymer that can be produced in a crystalline form, that exhibit high electric field induced strains (~4%) due to electrostriction [42]. Typically electrostrictive-grafted elastomer are used in combination with a piezoelectric poly(vinylidene fluoride-trifluoro-ethylene) copolymer to yield several compositions of a ferroelectric-electrostrictive molecular composite system [4].

Electrostrictive paper is another example where the principle of electrostriction is used to produce actuation. An electrostrictive paper is composed of a multitude of discrete particles, which are mainly of a fibrous nature forming a network structure. For example, silver laminated paper, whereby two silver laminated pieces of paper with silver electrodes are placed on the outside surfaces, show bending motion upon application of electric voltage to the electrodes [58].

Electroviscoelastic Elastomers

Electroviscoelastic elastomers are elastomers that have a shear modulus that can be controlled with an external electric field. These elastomers are cross-linked structures of composite of a polymer and a polar phase and are manufactured by applying an electric field during the time of curing, which orients and fixes the position of the polar phase in the elastomeric matrix keeping it in a solid state with a net shear modulus that can be controlled by applying an external electric field [40]. In the uncured state, electroviscoelastic elastomer behaves as electro-rheological fluids. Electro-rheological (ER) fluids are fluids that can be transformed from a liquid state into a solid state in milliseconds by applying an external electric field.. Similar to Electroviscoelastic effects magnetorheological effects can be induced in elastomers using magnetic fields and as much as 50% change in shear modulus can be induced [11, 56].

Liquid Crystal Elastomer (LCE)

LCEs are composite materials that can be electrically activable by inducing joule heating. They consist of monodomain nematic liquid crystal elastomers and conducting polymers distributed within their network structure [41]. The actuation mechanism of these materials involves phase transition between nematic and isotropic phases that exist in their crystal structure. Contractions of nearly 30% due to phase transition have been reported for LECs [39].

Dielectric EAP

Dielectric EAPs are polymers that show large mechanical deformations on application of an electric field. The actuation mechanism of dielectric EAPs is based on development of Maxwell pressure inside a charged capacitor. Dielectric EAPs will be discussed in detail in section 2.2.

2.1.2 Ionic EAP's

EAPs that are driven because of movement or migration of ions are called ionic EAPs. Some of the most commonly used ionic EAPs are discussed below.

Ionic Polymer Gels

Polymer gels are multi-phase materials consisting of a cross-linked polymer network and interstitial fluid. These materials show actuation by contracting or swelling in response to certain environmental stimuli, such as an electric field or a change in pH [29]. Actuation motions such as planar expansions and bending motions have been generated with ionic polymeric gels. Planar expansions of 300% [7, 27] and bending motions of greater than 90 deg [20] have been reported.

Ionomeric Polymer-Metal Composites (IPMC)

IPMCs typically produce a bending motion on application of an external electric field. The bending motion is produced due to movement of ions in the material when the electric field is applied.

An IPMC consist of a thin polymer membrane with metal electrodes plated on both faces. The polymer film has net charge from anions covalently fixed to the polymer chains in the base polymer, which is balanced by an amount of externally introduced counter ions. Two commonly used base polymers are Nafion® (perfluorosulfonate, made by DuPont) and Flemion® (perfluorocarboxylate, made by Asahi Glass, Japan) [4]. When an IPMC is subjected to a small potential (~5v), both the fixed anions and mobile counter ions are subjected to an electric field, with the counter ions able to diffuse towards one of the electrodes. As a result the composite undergoes a deformation towards the anode, followed by a slow relaxation in the opposite direction resulting in a bending motion of the IPMC. On the other hand, when the membrane is suddenly bent, a small voltage is produced across its faces.

Conducting Polymers

Conducting polymers are a class of materials that feature a conjugated backbone structure. Conducting polymers with appropriate dopant, such as hydrogen chloride or sulphuric acid, exhibit chemically and electrochemically controllable electronic conductivities. Doping is done in order to have ions that can flow across the covalently bonded conjugated polymer chain.

When an electric field is applied to doped conducting polymers with appropriate electrolyte, a reversible exchange of ions takes place between the conducting polymer and the electrolyte. Exchange of ions leads to oxidation or reduction reactions in the conducting polymer, which leads to significant changes in its volume [19]. For example, Otero and Sansinena developed a two-layer conducting polymer actuator by sandwiching an electrolyte solution between two polypyrrole electrodes [30]. When voltage was applied between the electrodes, oxidation occurred at anode and reduction at cathode, resulting in migration of ions between the electrolyte and electrodes. The migration takes place in order to balance the electric charge on the electrodes. Adding of ions resulted in swelling of polymer and removal resulted in shrinkage, which lead to bending of the actuator. Bilayer strips were made of 3-mg of Polypyrrole that lifted weights up to 300 times its own weight when activated by a 30-mA electric current.

Carbon Nanotubes

An ideal carbon nanotube can be thought of as a hexagonal network of carbon atoms that has been rolled up to make a seamless cylinder. Single-wall nanotubes can be thought of as the fundamental cylindrical structure, which form the building blocks of both multi-wall nanotubes and ordered arrays of single-wall nanotubes called ropes.

The actuation mechanism of a carbon nanotube is based on change in bond length of the carbon-carbon bond due to repulsion between similar charges developed on carbon atoms forming the nanotube. The net charge is developed on carbon atoms by suspending the nanotube in an electrolyte that forms an electric double layer with the nanotube and allows injection or removal of large. The repulsion between similarly charged adjacent carbon nuclei results in increase in the C-C bond length, which leads to increase in length and diameter of the nanotube [4]. Isotonic strains greater than 0.2% have been reported in bimorph cantilever actuators fabricated using single wall nanotube sheets in 1M NaCl solution [5].

Electro-Rheological Fluids (ERFs)

ERFs are made from suspensions of an insulating base fluid and particles of size in the order of 0.1 – 100 μm. When these fluids are subjected to an electric field the particles in the fluid align themselves along the field lines and change the consistency of the fluid from that of a liquid to a viscoelastic material or a solid. This phenomenon is called electrorheological effect or Winslow effect and is supposed to arise from difference in dielectric properties of the fluid and particles [55]. This control over rheological properties of a liquid offers new possibilities for actuation and control of mechanical motion.

2.2 DIELECTRIC ELASTOMER ACTUATORS (DEAs)

Elastomers are soft materials having rubber like elastic properties. Elastomers that show electromechanical response due to development of electrostatic pressures when subjected to an external electric field have been termed as dielectric elastomers. Dielectric elastomers have caught the attention of researchers because performance of actuators developed using dielectric elastomers have been found to be the closest to biological muscles as compared to other actuator technologies (see Figure 2.1).

Actuator	Strain	Actuation Pressure	Density	Efficiency	Speed (fast AND slow)
Natural Muscle	●	●	●	●	●
Electromagnetic	●	●	○	●	○
Piezoelectric	○	●	◐	●	●
Shape Memory Alloy	◐	●	◐	○	○
Magnetostrictive	○	●	○	●	○
Electrostatic	●	○	●	●	●
Dielectric Elastomers	●	●	●	●	●
○ = Poor		◐ = Fair		● = Good	

Figure 2.1 Comparison of natural muscle and man-made actuator technologies [35].

Several dielectric elastomers have been investigated for their performance as actuators including acrylics, silicones, ethylene propylene, polybutadiene and its copolymers, isoprene and urethanes (Table 2.2). Acrylic and silicone elastomers have emerged as the most promising polymers and have become the representative materials of this EAP class. These kinds of polymers are very compliant and have shown maximum deformations.

Table 2.2. Measured performance of various dielectrics [10]

Polymer Type	Energy Density (J/cm^3)	Pressure (MPa)	Strain (%)	Young's Modulus (MPa)	Maximum Electric Field (V/μm)
Polyurethane, Deerfield PT61 00S	0.10	1.9	11	17.0	160
Silicone, Dowcorning Sylgard 186	0.034	0.21	32	0.7	144
Flourosilicone Dow Corning 730	0.019	0.07	28	0.5	80
Fluoroelastomer Laurenl-143HC	0.0080	0.20	8	2.5	32
Polybutadiene Adrich PBD	0.011	0.19	12	1.7	76
Isoprene Natural Rubber Latex	0.0052	0.094	11	0.85	67

2.2.1 Principle of Operation

The operation of a DEA can be represented by a parallel plate capacitor, with the conducting electrodes as the two plates and elastomer as the dielectric medium, see Figure 2.2.

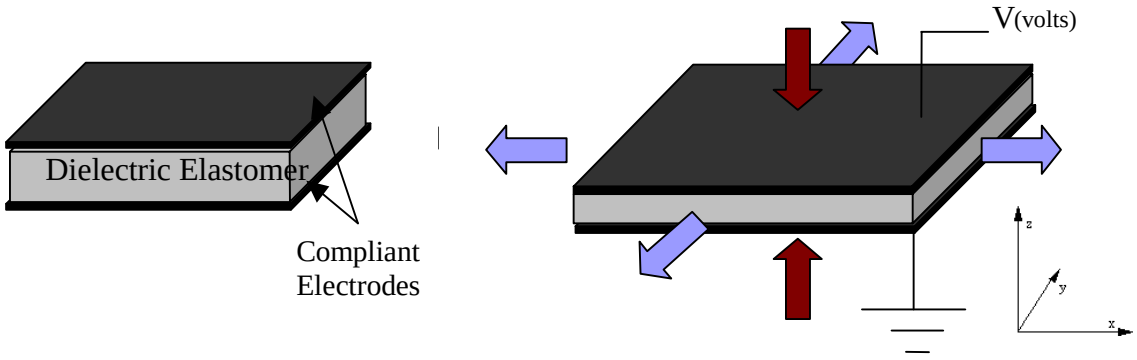

Figure 2.2 Schematic representation of operation of a DEA.

On application of voltage across the DEA the two electrodes develop opposite charge and attract each other because of coulomb forces. The attraction forces between the electrodes apply a pressure, called electrostatic pressure, *p*, on the dielectric film and squeeze the dielectric elastomer in the thickness direction. Change in thickness results in surface

expansion of the dielectric elastomer film as the volume of the elastomer is assumed to remain constant.

The electrostatic pressure (p) that compress the film in the thickness direction has been derived as change in electrostatic energy per unit area per unit displacement in the thickness direction, under the assumption that the dielectric film is perfectly elastic [33]. It is expressed as:

$$p = \varepsilon\varepsilon_0 E^2 \qquad \ldots(2.1)$$

Where ε is the dielectric constant of the dielectric EAP; E is the applied electric field; and ε_0 is permittivity of free space.

The behavior of dielectric EAP's upon application of voltage and different configurations of DEAs are discussed in detail in the following sections.

2.2.2 Actuation Behavior of DEAs

As discussed above, when a voltage is applied to a DEA it develops an electrostatic pressure, which results in change in shape of the DEA. This response of DEAs to applied voltage has been studied in the literature as actuation strains and blocking force (or pressure) developed in the actuator [34, 22, 1, 18, 10, 38]. Both actuation strains and blocking force (or pressure) developed in DEAs have been reported to depend on elastic modulus and dielectric constant of the elastomer, boundary conditions on the actuator and applied voltage (electric field) and are discussed in detail below.

Actuation strains

Actuation strains are defined as strains produced in an actuator upon actuation. As discussed earlier, actuation strains are produced in DEAs by applying a voltage across the two electrodes that results in change in dimensions of the dielectric elastomer. Actuation strains in DEAs have been reported in the literature in different ways depending on configuration of the DEA (different configurations of DEAs will be discussed later in section 2.2.3). In case of planar DEAs (section 2.2.3.1) actuation strains have been measured as strain along planar directions (x-direction and y-direction, see Figure 2.1) of the actuator [1, 31, 33, 32, 10] and as aerial strains produced in the active area of the actuator [32]. Under favorable boundary

conditions, planar strains as high as 215% and 117% have been reported along the length (x-directions) for acrylic and silicone based DEAs respectively and aerial strains as high as 158% and 93% have been reported for acrylic and silicone based DEAs respectively [32]. In case of cylindrical DEAs (Section 2.2.3.2) strains have primarily been measured along length (z-direction, see Figure 2.) of the actuator [10, 18, 38]. Axial strains of 5% have been reported for silicone based cylindrical DEAs [18] and axial strains as high as 25% have been reported for acrylic based rolled DEAs [38].

Actuation strains in DEAs have been reported to depend on various factors such as, dielectric elastomer (see Table 2.2), applied voltage and boundary conditions on the actuator (discussed in section 2.2.2.1) [10, 18, 38, 21, 32, 22]. Applied voltage is understood to directly affect the actuation strains because, according to equation 2.1, electrostatic pressures are directly proportional to the square of applied voltage and higher the electrostatic pressure higher is the actuation strain developed in the DEA. Boundary conditions are believed to affect actuation strains in a DEA as they change the mechanical and physical properties of the dielectric elastomer that in turn affects their actuation behavior. Boundary conditions of the DEA can be changed by changing prestrain or load on the actuator [21, 32, 33, 22]. Effect of prestrain on actuation behavior of DEAs is discussed in detail in section 2.2.2.1.

Several theoretical models have been reported in the literature that predicts actuation strains in planar DEAs [33, 21] and cylindrical DEAs [18]. All the models derive that actuation strains are directly proportional to the dielectric constant and square of applied voltage, and inversely proportional to modulus of the elastomer. But models reported so far are accurate only under specific boundary conditions and are limited in their scope. For example, the mathematical model developed by Capri and Rossi for actuation strains in a cylindrical DEA is accurate only at low prestrains and for linearly elastic and isotropic dielectric elastomer. This model will be discussed in detail in section 6.0. The reasons it is difficult to predict actuation strains in DEAs are that dielectric elastomers have non-linear elastic behavior, especially at large strains, and with application of prestrain that make these elastomers anisotropic, it becomes even more difficult to predict their actuation behavior.

Actuation blocking force

Actuation blocking force is defined as the force developed along the plane of a DEA (under isometric condition) due to electrostatic pressure, p, developed during actuation of the DEA. Blocking force is usually measured using a load cell coupled to a DEA. Different studies have reported several different numbers for blocking force developed in DEAs. For example, a 2.6 g of stretched acrylic film actuator has been reported to have developed blocking force of 29 N [31], a VHB^{TM} 4910 acrylic polymer film based bi-layer linear actuator mounted on a flexible frame and a linear bi-stable element, and having a weight (including dielectric elastomer and electrodes) of less than 0.1 g developed a blocking force of 1.5 N at 5.5 kV [1], and a rolled VHB^{TM} 4910 acrylic polymer film actuator, also called multifunctional elastomer rolls (MERs or Spring rolls), having 1.4 cms outer diameter, 6.8 cms axial length and 11g weight developed up to 15 N of blocking force [38]. Different configurations of DEAs will be discussed in detail in section 2.2.3.

Much like actuation strains, blocking force developed in DEAs depends on the type of dielectric material used, applied electric field and boundary conditions on the actuator. Theoretical models reported in literature derive blocking force to be directly proportional to dielectric constant of the dielectric elastomer and square of applied voltage [22, 31]. The mathematical model developed by Kofod et al. was developed for predicting blocking force developed in a planar acrylic based DEA that was prestrained along planar directions. No mathematical model was found for actuation blocking forces developed in a cylindrical DEA.

2.2.2.1 Effect of Prestrain on Actuation Behavior of DEAs

As mentioned earlier, prestrain is applied to the dielectric elastomer to change boundary conditions on the DEA. Application of prestrain has been reported to increase the actuation strains produced in DEAs, see Table 2.3 [32]. Besides changing the boundary conditions, application of prestrain serves two more purposes. Firstly, it reduces thickness of the elastomer. Reduction of thickness is based on the assumption of constancy of volume of the dielectric elastomer. Decrease in thickness of elastomer results in development of higher actuation strains and blocking force at same applied voltage as at lower thickness higher electric field is developed at the same voltage and higher the electric field, higher the electrostatic pressure developed in the DEA [22]. Secondly, it changes the modulus of the

dielectric elastomer along the direction of prestrain. Change in modulus is based on the stress-strain state of the elastomer after application of prestrain. Change in modulus of the elastomer changes the actuation strain response of the DEA as, based on the theory of linear elasticity, increase in modulus of elastomer decreases the strains produced in the elastomer for a constant stress and vise-a versa [24, 32].

Table 2.3. Measured strain response of prestrained dielectric elastomers [32].

Material	Prestrain (%)	Relative Area Strain (%)	Field Strength (MV/m)	Pressure (Mpa)	Estimated elastic energy, e (MJ/m^3)
Dow corning HS3 Silicone	(68,68)	93	110	0.3	0.098
	(14,14)	69	72	0.13	0.034
Nusil CF 19-2186 silicone	(45,45)	64	350	3.0	0.75
	(15,15)	33	160	0.6	0.091
3M VHB 4910 Acrylic	(300,300)	158	412	7.2	3.4
	(15,15)	40	55	0.13	0.022

Type of prestrain applied, such as a uniform prestrain or a biased prestrain, also affects actuation behavior of DEAs. A biased or non-uniform prestrain introduces anisotropy in the system thus affecting its actuation behavior along different directions. Pelrine et al. reported that in a non-uniformly prestrained system actuation occurs primarily in the direction with lower prestrain (see Table 2.4). The reason for this observed effect is believed to be increase in the local elastic modulus of the material with increased strain resulting in higher actuation in the direction with lower prestrain [32]. This observation was also made by Kofod G. in his work on actuation response of Polyacrylate based planar DEAs. He observed that increasing the prestrain along the width (x-direction) resulted in increase in maximum actuation strains along length (y-direction). Maximum actuation strains of 53%, 76% and 173% were reported for 300%, 400% and 500% x-direction prestrain respectively [21].

Hence, by applying a prestrain or changing the level of prestrain, actuation behavior of DEAs can be greatly modified.

Table 2.4. Actuation strains observed in non-uniformly stretched DEAs [32].

Material	Prestrain (%)	Relative Thickness Strain (%)	Relative Linear Strain (%)	Field Strength	Pressure (Mpa)	Estimated elastic energy, e (MJ/m^3)
Dow corning HS3 Silicone	(280,0)	54	117	128	0.4	0.16
Nusil CF 19-2186 silicone	(100,0)	39	63	181	0.8	0.2
3M VHB 4910 Acrylic	(540,75)	68	215	239	2.4	1.36

2.2.3 Dielectric Elastomer Actuator Configurations

Various configurations of DEAs have been reported in literature where deformation of dielectric polymer has been used in different ways to produce different kind of motions and perform desired functions [34, 13, 35, 23, 37, 38, 18, 16, 15, 48, 49, 50]. Even though DEAs can have several different configurations, the basic geometry is either a planar geometry or a cylindrical geometry. Hence, different configurations of DEAs can be broadly divided into two categories: planar and cylindrical DEAs; and are discussed in detail in following sections.

2.2.3.1 Planar dielectric elastomer actuators (single or multi layered)

Planar DEAs are fabricated by having one or more polymer films placed between compliant electrodes. The type of motion produced depends on the arrangement of layers and electrodes and the boundary conditions on the actuator. Some of the earliest planar DEAs, reported in US Patent 4400634, were manufactured with a film of dielectric material between two electrodes (unimorph) or with two dielectric elastomer films with an interspaced electrode and two electrodes on the two faces (bimorph). Figure 2.3 shows some of the planar DEAs reported [adapted from 34, 52 and 1].

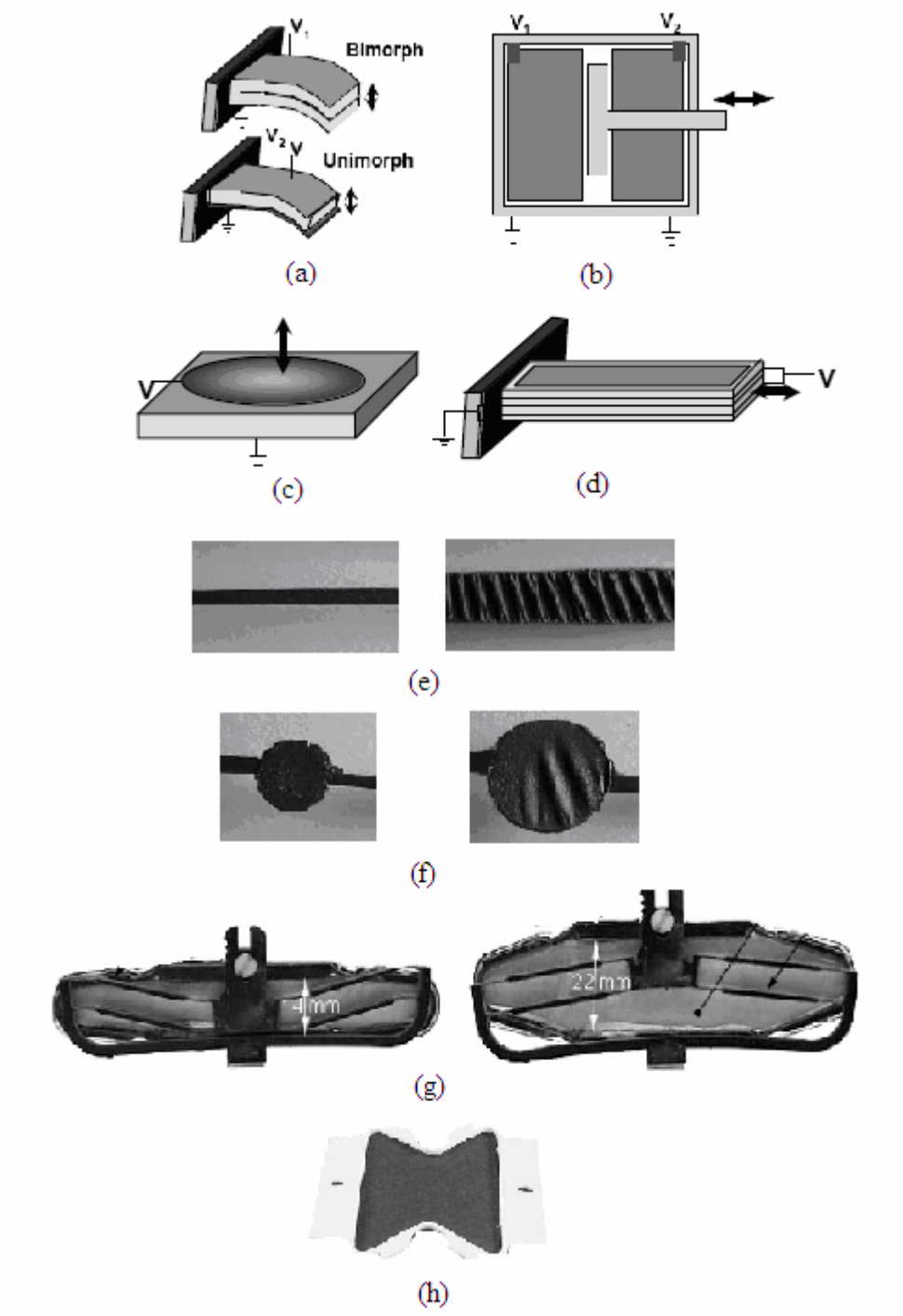

Figure 2.3. Planar Actuator Configurations (a) bimorph and unimorph [34] (b) stretched film based EAP electromechanical transducer [52] (c) diaphragm [34] (d) extender [34] (e) Linear motion stretched film [34] (f) circular motion stretched film [34] (g) embedded flexible frame actuator [1] (h) bow-tie [34]

Above configurations of dielectric elastomer actuators have been used to develop various devices. The diaphragm configuration (Figure 2.3 (c)) has been used to build acoustic actuators or loudspeaker systems that are well suited for applications such as noise cancellation and vibration control [47]. The operation of a dielectric elastomer diaphragm is based on out of plane movement of a dielectric film on application of an external electric field. The out of plane movement occurs because the actuator is constricted by rigid boundaries for in-plane movement. An array of diaphragm actuators on a surface can also be used to control flow of fluid over that surface by changing the shape and roughness of the surface (Figure 2.4).

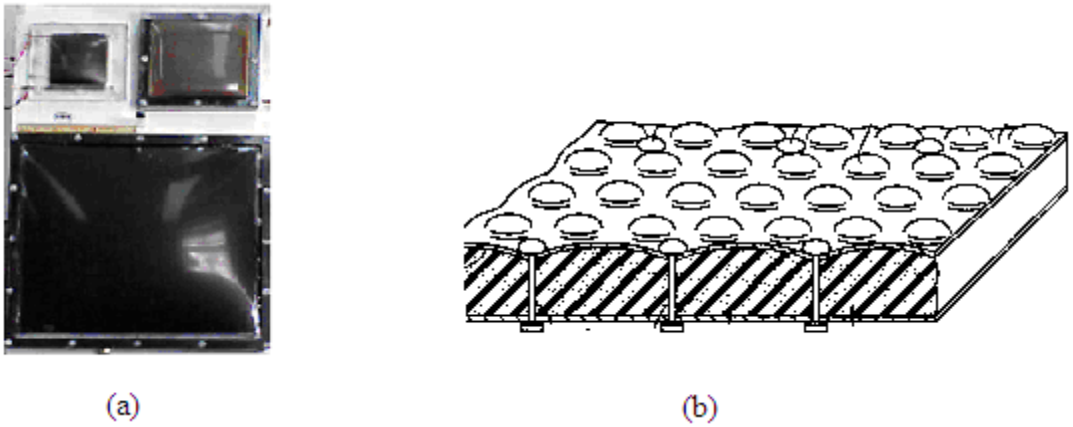

Figure 2.4. Dielectric elastomer diaphragm actuator (a) loudspeakers based on diaphragm dielectric actuator [4], (b) an array of diaphragm actuators on a surface that can be used for acoustic purposes or for controlling roughness of a surface [47].

The embedded flexible frame actuator (Figure 2.3 (g)) has been used to design high degrees of freedom (DOF) binary manipulators, which have been proposed to build light, inexpensive, simple, robust and easy to use robotic elements for future robotic systems [1]. The actuator consists of an integrated module (Figure 2.5 (a)) consisting of a dielectric polymer film, an elastic frame and a passive elastic element, and was used to build a prototype of a robotic element called Binary Robotic Articulated Intelligent Device (BRAID) (Figure 2.5 (b)). The active actuator area in each actuator module weighed 6 g, achieved

relative strains of 57% and developed blocking force of 1.5 N. A two-stage BRAID prototype was build using six actuator modules to show applicability of DEAs in building high DOF practical binary systems for future robotic systems (Figure 2.5 (c)).

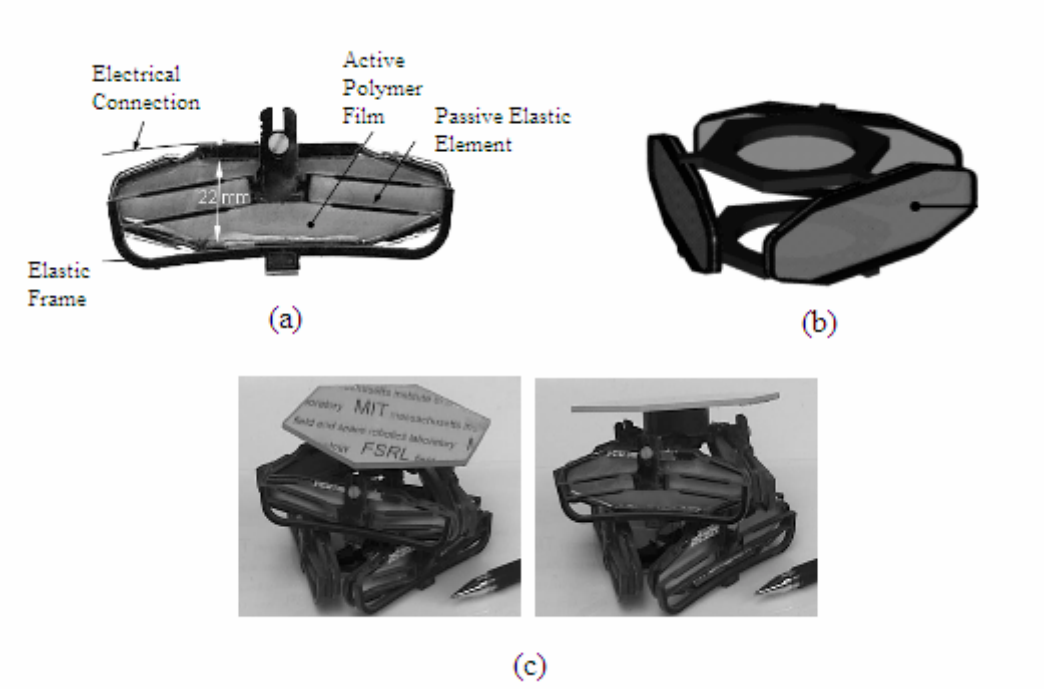

Figure 2.5 DEA based binary manipulators (a) embedded flexible frame actuator (b) schematic of a single stage Binary Robotic Articulated Intelligent Device (BRAID) (c) two-stage BRAID prototype [1]

The bow-tie configuration shown in Figure 2.2 (h) has been used to manufacture linear actuators, which are also called linear 'Artificial Muscle' (Figure 2.6). A bow-tie actuator is constructed using a dielectric elastomer film, having shape of a bow tie, with two compliant electrodes on its two surfaces. Application of an external electric field across the electrodes results in planar actuation of the actuator, which, because of a bow tie shape, translates into linear motion of the actuator. The linear 'artificial muscle' in Figure 2.6 was manufactured using a double bow tie structure, composed of two layers of acrylic film sandwiched together. It has a stroke of up to 10mm and force output of about 2N [4]. The linear 'artificial

muscle' actuator has been used to develop a self-contained hexapod robot (Figure 2.7 (a)) that mimics the motion of insect like walking [13] and an insect inspired flapping wing robot (figure 2.7 (b)) [35].

Figure 2.6. Linear 'Artificial Muscle' [34]

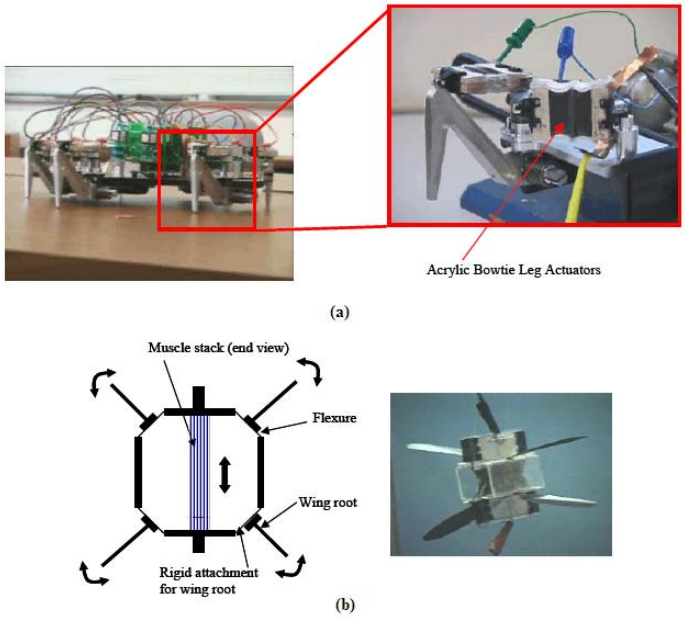

Figure 2.7. Devices built using bow-tie dielectric elastomer actuator (a) self-contained hexapod robot [13], (b) insect inspired flapping wing robot [35]

DEAs have also been used to manufacture various animated devices like an animated face, animated eye and animated skin [46]. Figure 2.8 shows a couple of animated devices manufactured using DEAs.

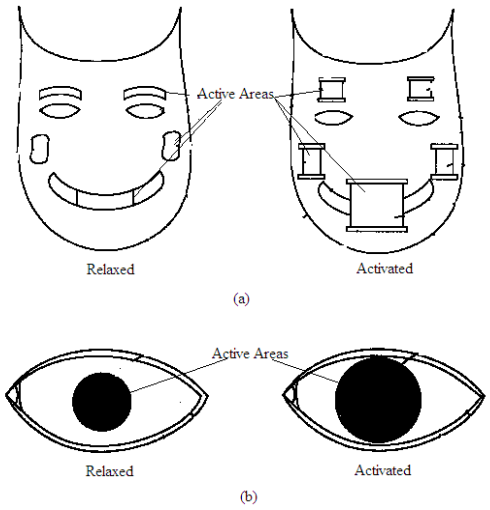

Figure 2.8. Animated devices built using DEAs (a) animated face, (b) animated eye [46]

Other applications of planar dielectric elastomer actuators that have been reported include a electromechanical transducer using two planar actuators coupled together, a serpentine robot and a solid state optical aperture based on stretched film circular actuator (see Figure 2.9).

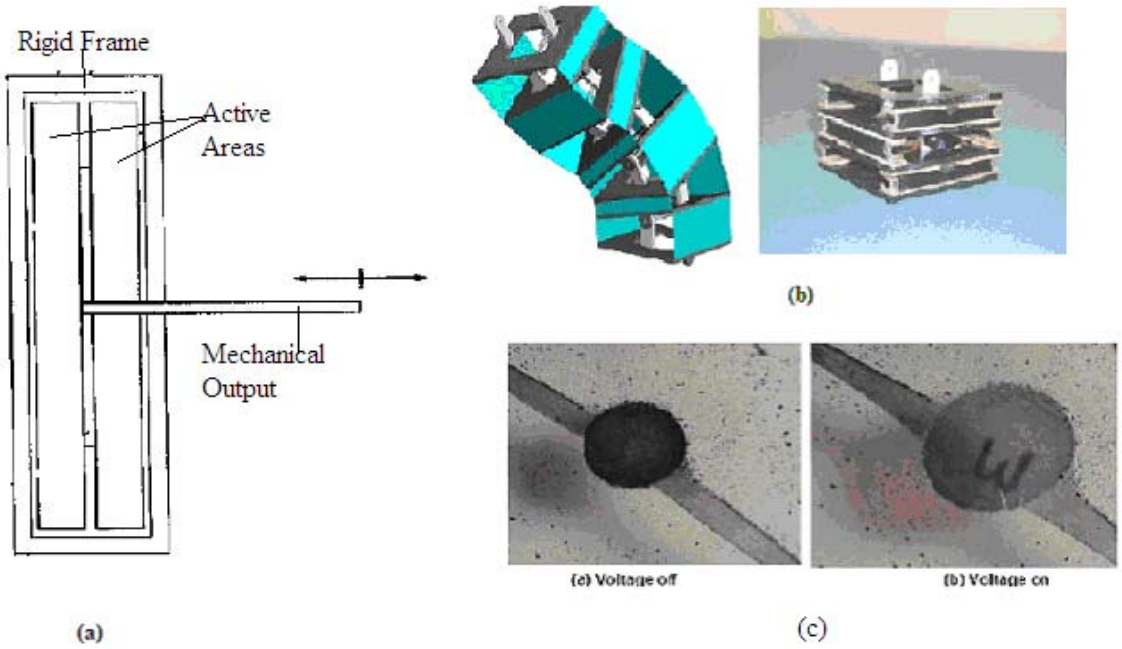

Figure 2.9. Devices made using planar dielectric elastomer actuators, (a) Schematic of a stretched film based EAP electromechanical transducer [52] (b) serpentine robot based on linear motion stretched film actuator [35], (c) Solid state optical aperture based on stretched film circular actuator [4]

2.2.3.2 Cylindrical dielectric elastomer actuators

Two different DEA configurations have been reported in the literature based on the cylindrical geometry: rolled DEAs and tubular DEAs (see, Figure 2.10) [23, 45, 38, 35, 15, 17]. Cylindrical DEAs are understood to provide a better way of manufacturing compact and efficient DEAs as they can be built without any frames for applying prestrain and also occupy less space than planar DEAs.

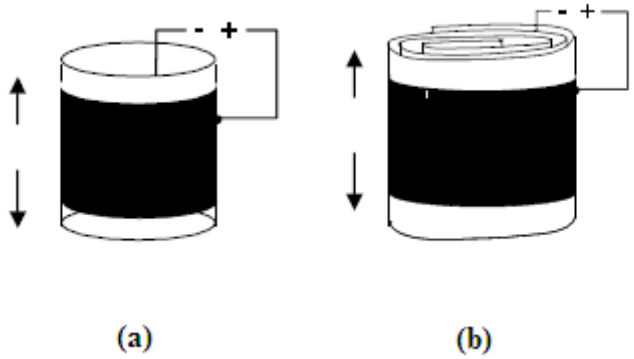

Figure 2.10. Cylindrical DEAs (a) tube and (b) roll

Rolled DEAs

Rolled DEAs, also called Multifunctional Elastomer Rolls (MERs) or Spring Rolls, are prepared by rolling a stretched acrylic film with two compliant electrodes onto itself or on a preloaded spring [45]. These actuators have one-degree of freedom and primarily function as linear actuators. Rolled actuators that have been fabricated have shown maximum strokes of 5-7% of their active lengths and forces ranging up to 1N [23].

Rolled DEAs with higher DOF have been reported [38]. Higher DOF are achieved by patterning the electrodes on the dielectric elastomer film before rolling such that after rolling the electrodes align radially on multiple circumferential spans of the rolls. Higher DOF can also be achieved by combining multiple rolled actuators with lower DOF. Pie et al. fabricated 2 DOF (Figure 2.11 (a, b and c) and 3 DOF rolled actuators by aligning the electrodes along two and four circumferential spans of the rolls respectively. The 2 DOF rolled actuator showed linear motion as well as a bending motion along one axes depending on which span of electrodes are activated. Similarly 3 DOF actuator showed linear motion and bending motion along two axes. Maximum bending angles of 90 degrees and 35 degrees and lateral forces of 1.68 N and 1 N were achieved with 2 DOF and 3 DOF rolled actuators respectively. Pie et al. also fabricated a ‘Sushi Roll’ with 8 DOF by putting four 2 DOF MERs in series (Figure 2.11 (d and e)).

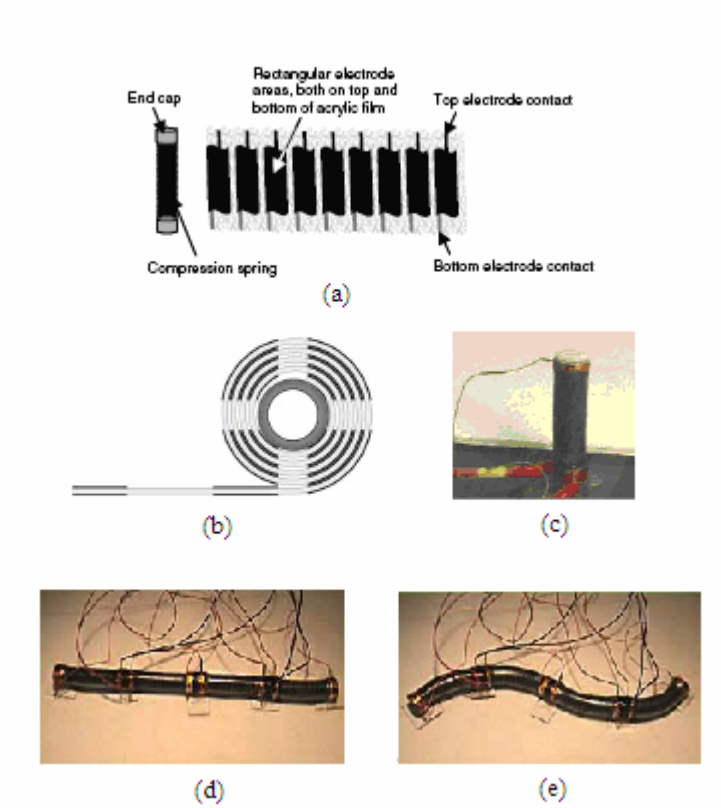

Figure 2.11. "A 2-DOF spring roll. (a) The central spring is compressed to solid length on a bolt with two end caps. Two acrylic films (3M VHB 4910) are highly prestrained and then patterned with rectangular electrode areas. The width of the rectangular electrode areas is increased incrementally. The two films are laminated and rolled around the spring and end caps. (b) During the rolling process, the electrode areas stack on top of each other and radially align on two circumferential spans of the roll. (c) The wire on top is the common electrode. The two contacts at the bottom control two circumferential spans that can be individually actuated." (d) Sushi roll fabricated using four 2 DOF MERs in relaxed state (e) sushi roll in activated state [38]

Linear and bending actuation motion of rolled actuators has been used as artificial muscles for robotic limbs, see Figure 2.12. Robots built using rolled actuators have proven to be faster and more efficient than robot based on bow-tie linear actuators [35, 37, 38].

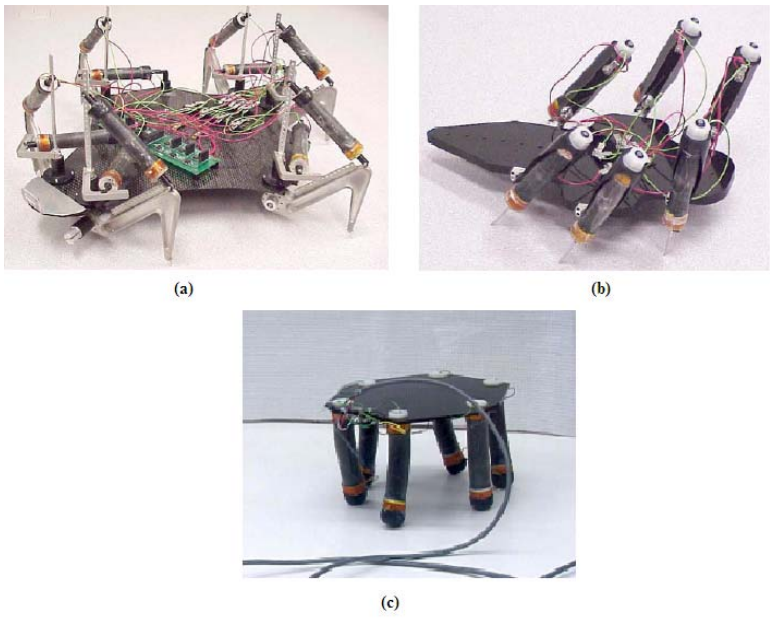

Figure 2.12. Robots built on using rolled dielectric elastomer actuators (a) FLEX-2 robot [35], (b) Skitter Robot using 6 rolled actuators [35] and (c) MERbot-a six legged robot with 2-dof spring rolls as legs [38].

Tubular DEAs

As it was mentioned earlier, all the rolled dielectric elastomer actuators have an electroded dielectric elastomer film that is rolled to make a cylindrical actuator. Another way of fabricating cylindrical DEAs that has been reported is to use dielectric elastomer tubes instead of a dielectric film. An obvious advantage of this technique is that it overcomes the difficulties in fabrication of rolled actuators [37, 38].

Carpi and Rossi have reported studies on cylindrical actuators that were fabricated using silicone tubes with compliant electrodes on the inner and outer wall of the tube (Figure 2.13). They reported linear actuation strains of up to 4.5% at 100V/μm with 5% prestrained silicone tubes [18].

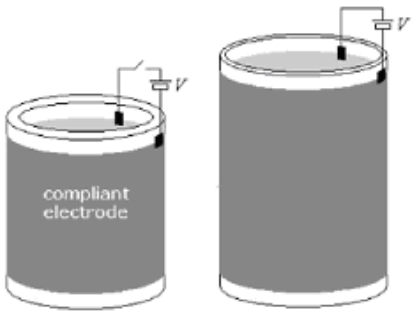

Figure 2.13. Schematic of a tube based cylindrical dielectric elastomer actuator [18]

In another study, Capri and Rossi reported a cylindrical DEA where the two electrodes were arranged as slightly displaced concentric coils inside the dielectric elastomer tube wall, see Figure 2.14 [15]. When a voltage difference was applied to the two electrodes in this DEA the electrostatic pressure generated between the two electrodes caused the dielectric material present between them to deform, but unlike all other DEAs mentioned before, the deformation of the dielectric material resulted in linear contraction and radial expansion of the dielectric elastomer tube. This motion is desirable as it closely matches the working of a biological muscle, which also contract when activated. According to the preliminary data that has been reported, linear contractions of up to 6% were achieved at 25V/μm (Figure 2.14 (c)) [12].

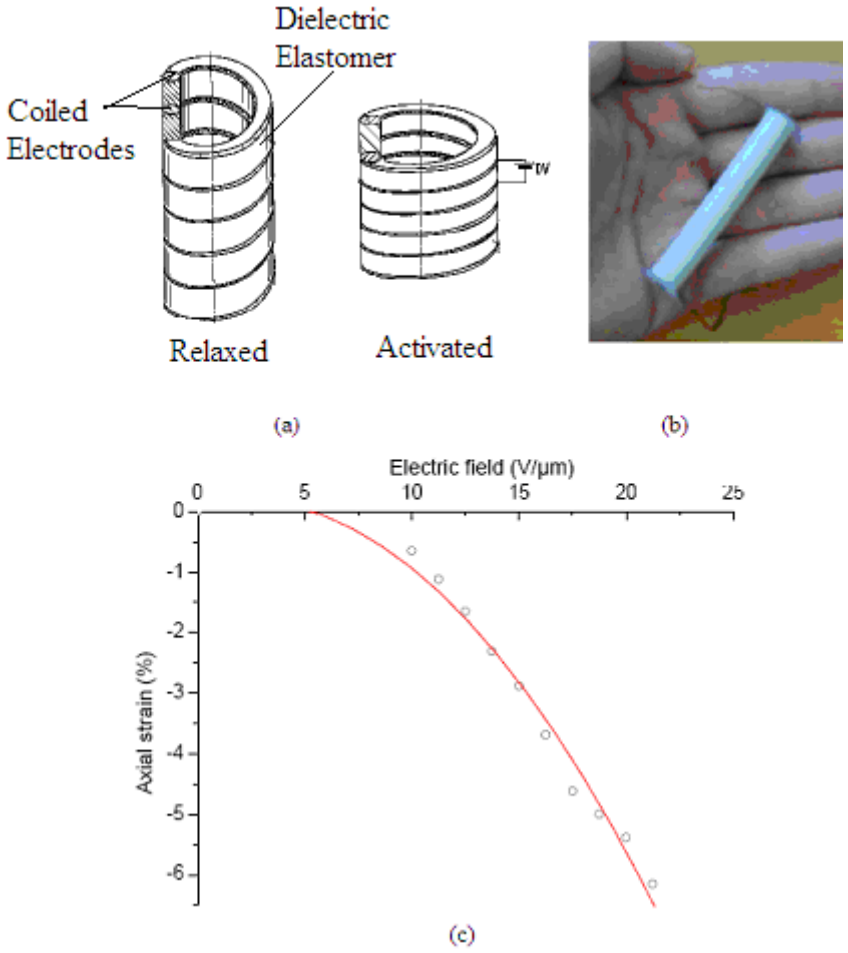

Figure 2.14. A new dielectric elastomer actuator configuration, (a) schematic of a contracting linear dielectric elastomer actuator [15] (b) a silicone-based prototype contracting linear dielectric elastomer actuator, (c) preliminary actuation results of developed prototype actuator [12].

2.3 COMPLIANT ELECTRODES FOR DEAS

A distinguishing characteristic of dielectric elastomer actuators is high strains produced upon actuation, in some cases as high as 200% [24]. In order for these actuators to perform at such high levels of strain it is important to have electrodes that can perform at similar strains. A compatible electrode needs to maintain its conductivity and be mechanically stable at high strains so as to not negatively affect the actuation behavior of DEAs. Different materials have

been used to prepare compliant electrodes in DEAs, such as metals, polymers and electrolytes, and will be discussed in detail in the following sections.

2.3.1 Metal Electrodes

In some of the earliest actuation experiments conducted with dielectric films, gold was used as electrode material. Polyurethane films with gold films, which could be gold metal film or sputtered gold films, were developed as actuators that showed actuation strains of ~ 3% at 20V/μm [28, 42]. Even though sputter deposited ultra thin gold/metal films formed uniform electrode with good conductivity, they had a high elastic modulus that cracked at strains greater than 4% and put a constraint on the polymer film during actuation. Hence, strains greater than 4% were difficult to achieve with gold films as electrode material.

Later, Benslimane and Gravesen reported compliant metallic electrodes for dielectric elastomer actuators that maintained their conductivity up to 33% strain [6]. The solution they came up with to solve the problem of failure of metal electrode at high strains was 3-D patterning of electrodes on the surface of the elastomer film such that they can extend along with the film and thus withstand high actuation strain. A corrugated pattern was developed on one of the surface of the dielectric film while it was being spun cast and a thin layer of electrode was then deposited on the corrugated surface to get the micrometer sized 3-D pattern of electrode (Figure 2.15 (a)). The electrode thus formed was compliant in the direction of the wave-pattern but stiff as a metallic layer in the perpendicular direction to the corrugation. The final actuator was manufactured by laminating two such films with flat sides in contact (figure 2.15 (b)). Silicone was used as the dielectric material and silver as the electrode material. The final actuator was reported to show elongation of up to 22% at an applied voltage of 3.6 kV and at constant load of 0.3Mpa.

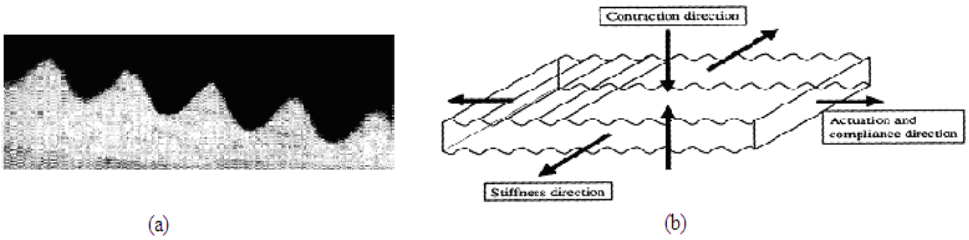

Figure 2.15. Dielectric EAP with smart metallic compliant electrodes (a) Optical microscope picture of the cross section of the mould (b) Schematic of the dielectric EAP with smart metallic compliant electrodes deposited on top and bottom side [6]

Kornbluh et al used a zigzag pattern of the electrode to facilitate high actuation strains with metal electrodes (Figure 2.16). They formed zigzag patterns of gold traces on a silicone EPAM by first sputtering the gold traces uniformly on the silicone film and then using photolithography to make the zigzag pattern. The electrodes thus formed were found to remain conducting till 80% strain [26].

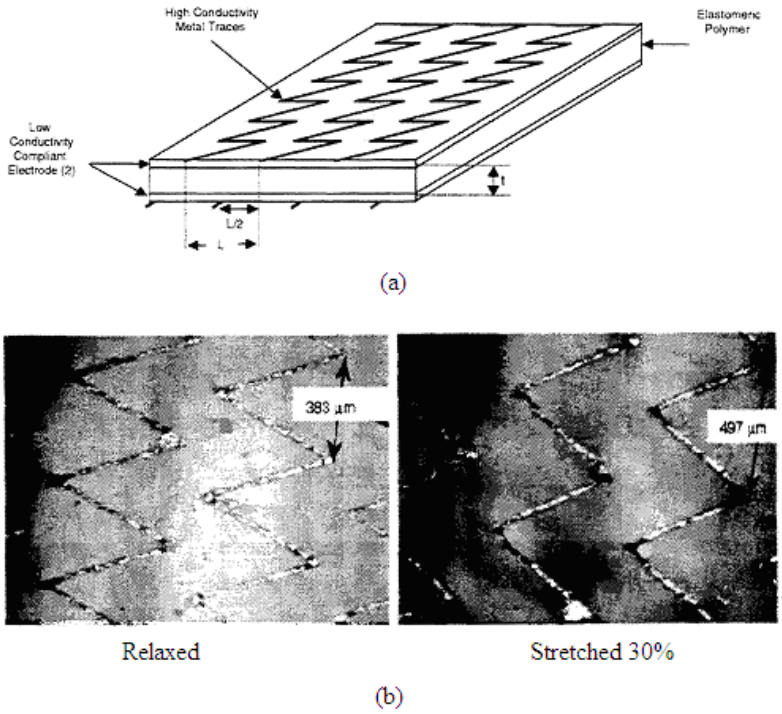

Figure 2.16. Dielectric EAP with patterned gold electrodes (a) schematic (b) Silicone elastomer with patterned gold electrodes under relaxed and stretched state [26]

2.3.2 Polymer Based Electrodes

Polymer based electrodes are relatively a newer class of materials being used for preparing compliant electrodes for DEAs. They have the potential of combining the electrical properties of metals with the processability of polymers. Use of two types of polymer-based electrodes has been reported: conducting polymers and conducting particles in a polymer matrix. The two types of polymer-based electrodes are discussed in detail below.

Conducting Polymers as electrodes

Polypyrrole and polyaniline are two conducting polymers that have been commonly reported being used as compliant electrodes for dielectric EAP's [8, 44, 54, 57]. The conducting polymer electrodes can be applied on the polymer film using in-situ polymerization technique. In in-situ polymerization, the polymer film on which conducting polymer is to be coated is dipped in a polymerization bath that has the monomer of the conducting polymer along with oxidizing agent and catalyst. Once the polymer film is dipped in the bath the conducting polymer monomer starts to polymerize on the surface of the film and forms a conducting layer that acts like an electrode.

Su et al. studied the performance of polyurethane based actuators with gold electrodes and polypyrrole electrodes [44]. The polypyrrole electrode was fabricated on the polyurethane surface using in-situ polymerization technique as discussed above, and had a resistivity of about 1000 Ω/cm. They reported that polyurethane film coated with Polypyrrole conducting polymer showed similar longitudinal strains as the one with gold electrodes. They also reported that, in case of both polyurethane film actuators with gold and polypyrrole electrodes, longitudinal strains produced in the polyurethane film actuator decreased with increase in frequency of applied voltage and increased with decrease in film thickness.

Even though Su et al. found longitudinal strain response of polyurethane based actuators with polypyrrole electrodes to be similar to that with gold electrodes, in another study done by Cheng Z.Y. et al. it was reported that transverse strain response of electron irradiated P(VDF-TrFE) copolymer films with conducting polymer electrodes was better than the one with gold-electrodes [9]. The comparative study was done for two conducting polymers: polypyrrole and PANI. The conducting polymer electrodes were applied using in-situ polymerization technique discussed above and gold electrode was applied by sputtering. Two

different set of experiments were performed, one with unstretched P(VDF-TrFE) film and another with stretched P(VDF-TrFE) film. In case of unstretched film, performance of P(VDF-TrFE) film with polypyrrole electrodes and gold electrodes was compared whereas in case of stretched film, performance of P(VDF-TrFE) film with PANI electrodes and gold electrodes was compared. Performance was studied for stretched film because it was known that stretched P(VDF-TrFE) film actuators showed larger transverse strains than the unstretched ones [9]. In case of unstretched film, transverse strain response of nearly 0.15% and 0.12% were reported for unstretched P(VDF-TrFE) film with polypyrrole and gold electrodes respectively. In case of stretched film, transverse strain response of nearly 0.7% and 0.6% were reported for stretched P(VDF-TrFE) film with PANI and gold electrodes respectively. The reason that actuators with conducting polymer electrode and gold electrode showed similar longitudinal strain response (as reported by Su et al.) but significantly different transverse strain response was reported to be higher elastic modulus of the gold electrodes, which had a clamping effect on the dielectric elastomer film in the transverse direction but did not have a direct affect on strains in the longitudinal direction [9].

As was reported for metal electrodes, conducting polymer electrodes also lost their conductivity with increase in strains and constrained the movement of the actuator [54]. Here also, much like metal electrodes, one of the solutions reported was to fabricate wrinkled electrodes that would smooth out at high strains and thus retain their conductivity and mechanical strength, and not constrict the movement of the actuator [54]. Watanabe et al. developed wrinkled polypyrrole electrodes by carrying out in-situ polymerization on the surface of a strained polyurethane film. In this way, after electrode formation, when the polymer film was relaxed, the conducting polymer layer that was formed on the surface of the film developed wrinkles to adjust for decrease in the surface area of the polymer film. When these actuators were actuated the wrinkled polymer electrode adjusted to change in dimensions by smoothening out (Figure 2.17), thus not breaking down mechanically or electrically, or constricting movement of the actuator. Wrinkled polypyrrole electrodes that were developed on surface of polyurethane film with 35% strain were reported to not lose their conductivity till 40% strain.

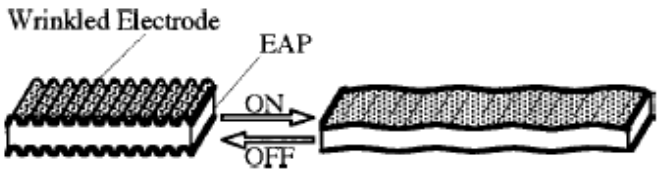

Figure 2.17. Polyurethane based actuator with wrinkled polypyrrole electrode [54]

Conducting Particles in a Polymer Matrix

Besides conducting polymers, polymer-particle systems have also been used as electrodes for dielectric elastomer actuators [10, 22, 57, 32, 33, 58]. Different polymer-particle systems have been reported such carbon black in silicone elastomer (grease electrode and rubber electrode) [22, 57, 32, 10], conductive grease containing silver powder [58] and conducting polyurethane (carbon black in polyurethane) [58]. Most commonly reported polymer-particle system is carbon black in silicone elastomer and electrodes made using this system have been called rubber or grease electrodes. The distinction between grease and rubber electrode is in their preparation technique and application method. To prepare grease electrodes, a suspension of carbon in a solvent (for the polymer media), prepared using ultrasound, is added to a polymer carrier (in compatible solvent). The resulting polymer-particle system is exposed to ultrasonic waves in an ultrasonic bath in order to breakdown the carbon particles to smaller size and get a homogeneous suspension. The mixture is then placed in a fume hood to allow the solvent to evaporate till optimum viscosity level is achieved. Grease electrodes can be applied to the actuator surface with a brush. In case of rubber electrodes the mixture of polymer carrier and carbon is applied to the actuator surface using an air-spray. Rubber electrode will be discussed in detail in section 4.2.1

2.3.3 Electrolytes

Electrolytes are chemical compounds that when dissolved in a solvent ionize and produce a conducting solution. Use of electrolytes as electrodes for dielectric elastomer actuators has been very limited and was found in literature at only one place.

Carpi and Rossi in their study on electromechanical characterization of planar acrylic based DEAs compared the performance of the prepared DEAs at different prestress levels and for

four different electrode materials, of which, one was a thickened electrolyte solution and the other three were graphite spray, graphite powder and carbon grease electrodes [16]. A thickened electrolyte solution was used as the electrode and was prepared in water (solvent) using NaCl as the electrolyte, polyethylene glycol as thickening agent and sodium laureth sulfate as surfactant. Capri and Rossi reported that thickened electrolyte solution gave best actuator performance for up to 20-25 V/μm (and appropriate pre-stress value), above that graphite spray electrodes were optimal (up to 50 V/μm). Maximum isotonic transverse strain of 5.3% at 21 V/μm and 29.4 kPa pre-stress, and isometric transverse stress of 29.5 kPa at 19 V/μm and 49 kPa pre-stress were reported for actuator with thickened electrolyte solution, whereas for actuator with graphite spray electrodes maximum isotonic transverse strain of 6% at 49 V/μm and 39.2 kPa pre-stress and isometric transverse stress of 49 kPa at 42 V/μm and 39.2 kPa pre-stress were reported.

3 RESEARCH OBJECTIVE

The objective of this research is to develop prototype fiber actuators using dielectric elastomers and study their actuation behavior under different boundary conditions. If developed, the fiber actuators can potentially be used to create textile structures that can alter its dimensions on demand. Additionally, these fibers can be the building blocks in developing various twisted or “laid” bundles for use as actuators for specific needs in robotics and elsewhere. It is hoped that the knowledge gained in this research will be of help in developing processes for making extruded fiber actuators in the future.

4 DEVELOPMENT AND EVALUATION

4.1 DESIGN

The design of a fiber actuator is based on the concept of cylindrical DEAs. The proposed fiber actuators are thin cylindrical fibers made of mostly dielectric polymer. These fibers consist of three parts: the conducting core, the dielectric actuating layer, and the conducting coating, see Figure 4.1 (a). The conducting components inside and outside of the fiber form the complaint electrodes required for actuation. In a way, the proposed design is similar to a cylindrical capacitor. The electrodes are connected to a high voltage supply such that there is a potential difference between the two electrodes. Because of the potential difference electrostatic pressure [33] develops between the two electrodes that squeezes the dielectric elastomer present between the two electrodes and changes the thickness and surface area of the fiber. This change in the dimensions of the fiber on application of an external voltage is called actuation and such a fiber that shows actuation in response to an electrical simulation is called a fiber actuator.

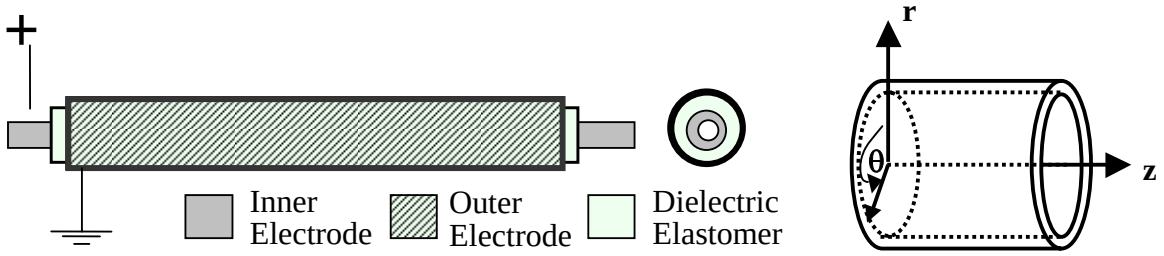

(a) (b)

Figure 4.1. Fiber actuator (a) schematics showing placement of dielectric material and compliant electrodes (b) cylindrical coordinates used for prototypes developed in this study, note that Z axis is coincident with the long axis of the fiber actuator.

4.2 FABRICATION OF PROTOTYPE

As mentioned earlier in the preceding section, prototype fiber actuators by design should have three components, with the core and the outer most layers form the electrodes. The dielectric elastomer layer in the middle is the actuating polymer. The three layers must be mechanically compatible, or should have similar mechanical behavior. Assuming that the required material properties are obtained in fiber forming polymers, using today's technology of multi-component fiber formation, the proposed fiber structure could potentially be extruded in a one step process. However, a number of important issues involving mechanical and dimensional characteristics of the fiber actuators must be explored prior to undertaking fiber manufacture. For those reasons, the prototype fiber actuators for this investigation were fabricated from commercially available components.

Commercially available, thin walled (100-200 microns) hollow dielectric elastomer tubes having inner and outer diameters around 500 to 900 microns respectively were used in fabrication of the prototype fiber actuator [see Table 4.1]. These tubes were same as hollow fibers but for their physical dimensions. Silicone and polyurethane tubes were chosen for fabrication of the prototypes (discussed in more detail in section 4.2.1). Of the various electrodes that were available, rubber electrode was found suitable for use as outer electrode and, depending on the type of prototype, conductive silver-grease and calcium chloride solution were found to be suitable for use as inner electrodes. The choice of electrodes and their preparation will be discussed in detail in section 4.2.1.2.

As the objective of this study was also to study the behavior of prototype fiber actuator under different boundary conditions, two types of prestrains were applied on the prototype during its fabrication: uniaxial prestrain (prestrain along only Z-direction, see Figure 4.1 (b)) and uniform prestrain. Different procedures were used to fabricate uniaxially prestrained prototypes and uniformly prestrained prototypes. Uniaxially prestrained prototypes were fabricated using both silicone and polyurethane tubes where as uniformly prestrained prototypes were fabricated with only silicone tubes. The fabrication procedures for the two types of prototypes will be discussed in detail in sections 4.2.3 and 4.2.4.

4.2.1 Materials

4.2.1.1 Dielectric elastomer tubes

Silicone and polyurethane dielectric elastomers were chosen for fabricating the prototype because they have good dielectric properties and can be potentially extruded in fiber form in the future. Silicone tubes were procured from Specialty Manufacturing Inc.[i] and Polyurethane tubes were procured from Precision Extrusion Inc. [ii]. Specifications of the two tubes are given in Table 4.1.

Table 4.1. Physical properties of dielectric elastomer tubes used in our study

Properties	Silicone Tube	Polyurethane Tube
Material	Dimethyl and Methylvinyl with reinforcing Silica*	Polytetramethyl glycol ether**
Hardness (Durometer)	50A[1a]	90A[1b]
Tensile Modulus (MPa) @ 100% Elongation	4.4[2]	33.4[3]
Outer Diameter (microns)	940[1a]	990[1b]
Inner Diameter (microns)	508[1a]	636[1b]
Wall Thickness (microns)	216	172

*Product Information sheet of Silastic® Biomedical Grade ETR Elastomers from Dow Corning, manufacturer of silicone elastomer.
** Product Information of Pellethane, Thermoplastic Polyurethane Elastomers from Dow Plastics, manufacturer of polyurethane elastomer.
[1a] Product information sheet from Specialty Manufacturing Inc.
[1b] Product information sheet from Extrusion Inc.
[2]Figure 4.3(a)
[3]Figure 4.3(b)

Tensile properties of dielectric elastomer tubes

It is known that elastomers have non-linear elastic behavior, also it is known that elastic modulus of the dielectric elastomer influences actuation behavior of the actuator (as discussed in section 2.2). As the objective of this study was to fabricate actuators using dielectric elastomers and study their actuation behavior under different boundary conditions (as discussed in section 3.0), which included applying high prestrains along the longitudinal

[i] Specialty Manufacturing Inc. 2210 Midland Road, Saginaw MI 48603
[ii] Precision Extrusion Inc. 12 Glens Falls Technical Park, Glens Falls, NY 12801 (http://www.precisionextrusion.com/)

axis (Z in Figure 4.1), it was important to determine the modulus of the dielectric elastomer tubes and understand its behavior as a function of strain.

Tensile modulus of the tubes was studied using a tensile testing machine (MTS 30/G). It was observed that the tensile behavior of the various tubes changed dramatically under cyclic loading and unloading, see Figure 4.2. In all cases, the drop in tensile modulus was significant after the first cycle. Upon subsequent cycles, the modulus and tensile behavior of the tubes remained the same but showed hysteresis. As the number of subsequent cycles was increased the hysteresis decreased and after a certain number of cycles no hysteresis was observed. Based on the initial trials, silicone tubes were cycled 25 times and polyurethane tubes were cycled 50 times before no hysteresis was observed in the load-strain curves of the loading-unloading cycles of these tubes (Figure 4.2). Hence, cycling the tubes served two purposes, firstly it reduced the modulus of the tubes, which was beneficial as a lower modulus tube was expected to give higher actuation strains in the prototype, and secondly it eliminated hysteresis from the tubes. Figure 4.3(a) and 4.3(b) show tensile modulus of a virgin silicone tube and silicone tube after 24 cycles and tensile modulus of a virgin polyurethane tube and polyurethane tube after 49 cycles respectively.

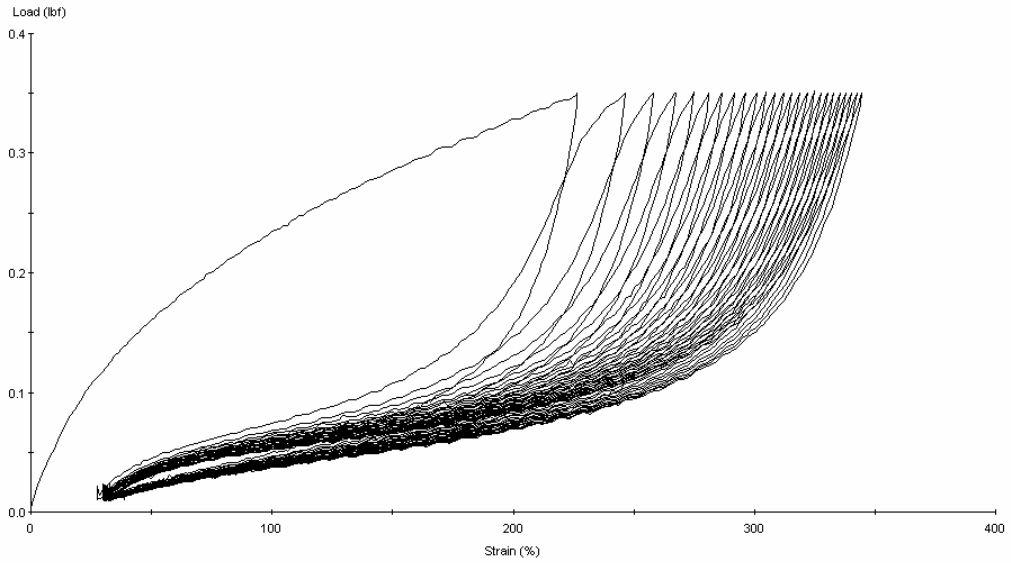

(a)

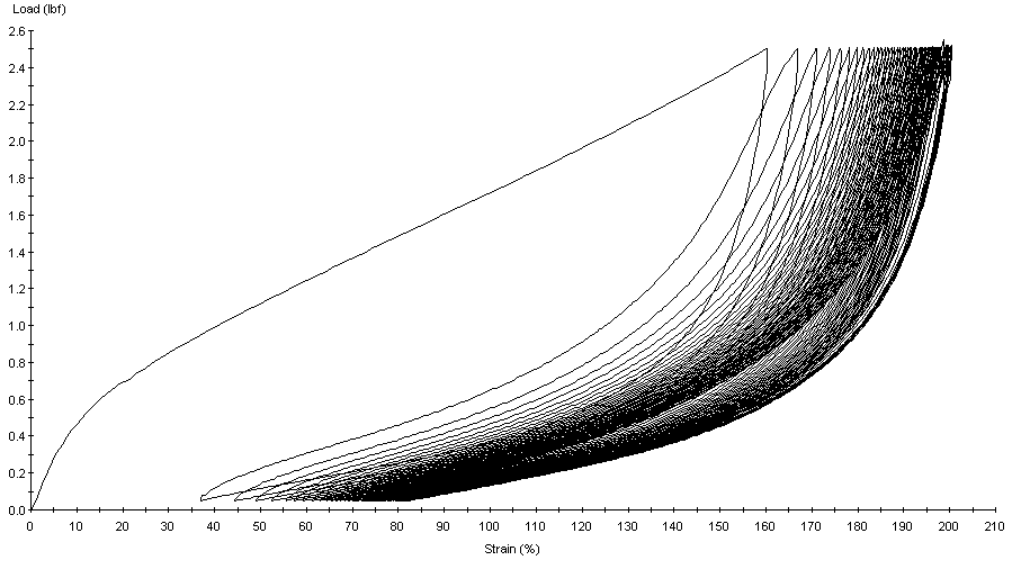

(b)

Figure 4.2 Load-strain curves for loading-unloading cycles of virgin dielectric elastomer tubes (a) load-strain curves for 25 loading-unloading cycles of virgin silicone tube (b) load-strain curves for 50 loading-unloading cycles of virgin polyurethane tube

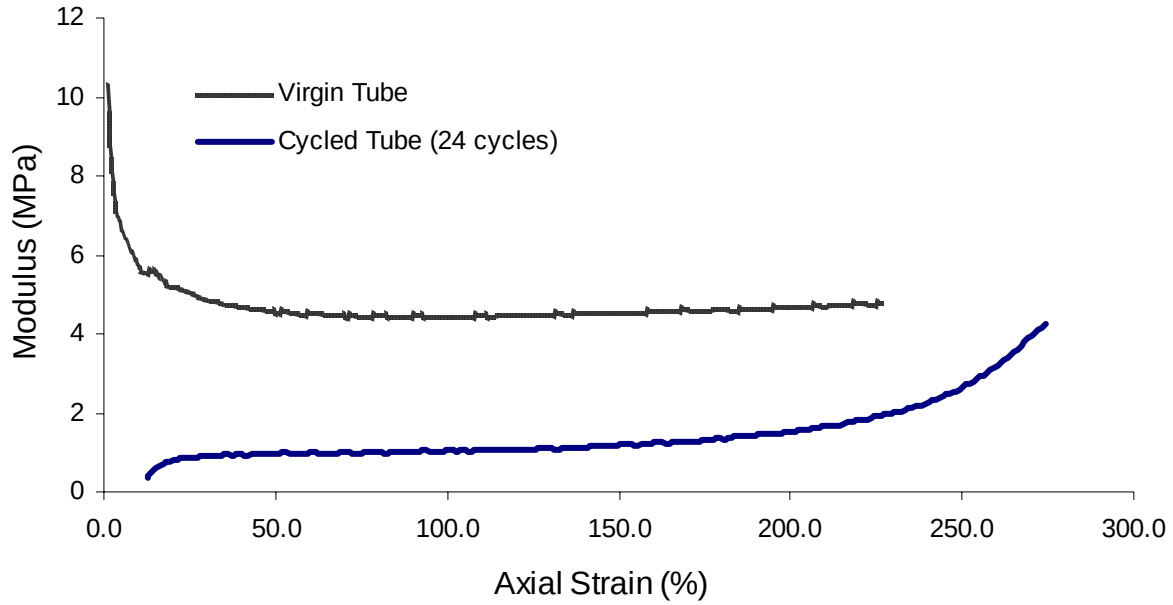

(a)

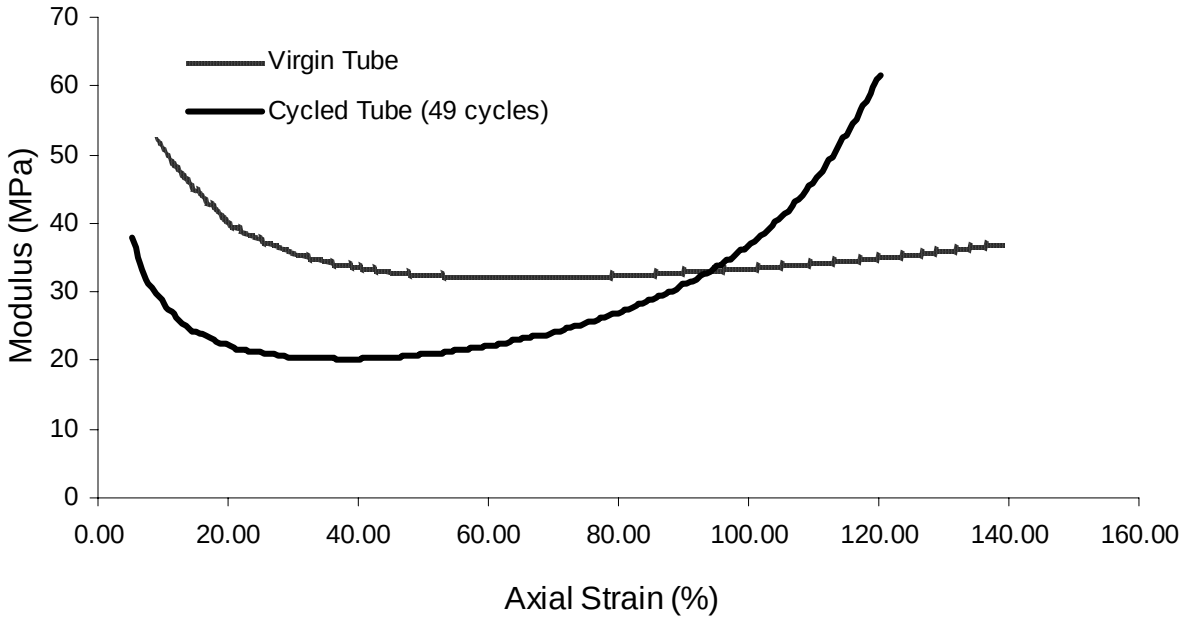

(b)

Figure 4.3. Tensile modulus of dielectric elastomer tubes at different axial strains before and after cycling (a) silicone tube (b) polyurethane tube

4.2.1.2 Electrodes

Various types of electrodes have been studied in the literature (see section 2.3 for details) including metallic and polymer based electrodes. Polymer based electrodes have proven to be more suitable for DEAs than metal electrodes because of their ability to maintain conductivity at high strains, elastic recovery, and ease of application. For these reasons, polymer based electrodes were chosen for fabricating the prototypes.

As mentioned earlier, the proposed prototype fiber actuators require two electrodes, an inner electrode and an outer electrode. In the present case, the inner electrode was filled in as a core of the dielectric elastomer tube whereas the outer electrode was applied on the surface of the tube as a thin uniform coating. Because the inner electrode was to be pushed into the inner cavity of the tube, it was desired that the electrode be either a liquid or a paste of low viscosity. The grease electrode, which is a silicone based conducting paste with carbon black as the conducting particle, has been used in various studies as the polymer based electrode for DEAs [57, 21]. But grease electrode was not suitable in this case as carbon black particles agglomerated and clogged the experimental set-up (discussed in details in next section) used to insert the inner electrode. Silicone based conducting paste containing silver as the conducting particle and having appropriate viscosity was tried as the inner electrode. It was observed that silver particles did not agglomerate and were easily inserted into the tubes. Hence silicone with silver particles was used as the inner electrode, it was commercially available from Chemtronics® under the trade name of CircuitWorks® conductive silver-grease.

In this study, the prototype fiber actuators have been studied under two different types of prestrains: uniaxial and uniform (as will be discussed in detail in sections 4.2.3 and 4.2.4). In case of uniaxially prestrained prototype, conductive silver-grease worked well as inner electrode. But in case of uniformly prestrained prototype, the inner electrode, besides acting as an electrode, was also used as a medium to inflate the tube (as will be discussed in detail in section 4.2.4). The pressure required to inflate the tube using conductive silver-grease paste was too high to achieve using the available set-up. The best alternative was to use a conducting liquid. Hence, an aqueous solution of calcium chloride, which is a strong electrolyte, was used as inner electrode in uniformly prestrained prototype. Calcium chloride was chosen for two reasons, firstly it ionizes completely in water and forms a strong

electrolyte, and secondly calcium chloride gives a stronger electrolyte than sodium or potassium chloride because it is known that strength of an electrolyte depends on the number of ions present in it and every molecule of calcium chloride disseminates into more number of ions (three) than each molecule of sodium or potassium chloride (two ions per molecule).
For the outer electrode, rubber electrode [57, 21] was chosen as it forms a uniform, thin electrode on the tube surface that maintains its conductivity at high strains. Details of preparation and application of electrodes are presented in the next section.

Rubber Electrode

Rubber electrode is a polymer-based electrode with conducting particles impregnated in a polymer matrix. We used silicone polymer and carbon black as the conducting particles to produce a conducting matrix. Based on previous studies [57], Sylgard® 186, a two component silicone elastomer, and 10% by weight carbon black were used to prepare the rubber electrode.

To prepare the rubber electrode 0.5g of carbon black was suspended in 100ml of heptane. The suspension was put into an ultrasonic bath for 10 hrs to breakdown the agglomerated carbon black particles. The two components of Sylgard® 186, silicone elastomer base and curing agent, were mixed in a ration of 10:1 and the viscosity of the mixture was reduced by adding a silicone based viscosity lowering agent, Fluid 200® FL 50 CST, in a 1:1 ratio. The total weight of the silicone mixture with viscosity lowering agent was 5gms. The resulting silicone mixture was then dissolved in 100ml of heptane and mixed with the heptane-carbon black suspension. The resulting mixture was stirred to homogeneously distribute the silicone polymer and carbon black particles in heptane. Thin layer of the above mixture was applied with an airbrush to the dielectric tube in order to form the rubber electrode. A commercially available air-spray gun from Campbell Hausfeld was used to spray the mixture on to the dielectric elastomer tubes.

Conductive Silver-grease

Conductive Silver-grease was procured from Chemtronics®. It is composed of 100% silver filled silicone oil. The conductivity [i] of the silver grease paste is <0.01 ohms-cm.

Calcium Chloride Solution

Aqueous solution of calcium chloride was prepared by dissolving calcium chloride anhydrate in 50ml of water at room temperature. The final solution had 74% by weight of calcium chloride in water. Conductivity of the final salt solution was 11.5 ohm-cm with a standard deviation of 0.04 ohm-cm. Conductivity measurements were made using ORION conductivity meter model 162 with 4-electrode cell technology.

4.2.2 UNIAXIALLY PRESTRAINED PROTOTYPE

Uniaxial prestrain was applied to change the boundary condition on the actuator in a biased manner and study the response of the actuator to this change. Uniaxial prestrain was applied along the length of the tube (Z-direction see Figure 4.1(b)). Fabrication, different prestrain levels and properties of tubes at different prestrain levels for the uniaxially prestrained prototype are discussed in the following sections.

4.2.2.1 Fabrication

Uniaxially prestrained prototypes were fabricated from a length of tube suitable to produce a prestrained final length of 10 cms after applying a predetermined level of prestrain. The prestrained length of 10 cms was appropriate for the rigid frame used to fabricate the actuator. To access the inner part of the tubes a hypodermic needle of appropriate dimension (20 gauge) was inserted from each end of the tubes. The dielectric elastomer tube between the two needles was stretched to a fixed length of 10 cm by pulling the two needles apart and holding them at a fixed distance from one another using a rigid frame, see Figure 4.4.

[i] Technical data sheet provided by Chemtronics® at http://www.chemtronics.com/products/americas/TDS/Cw7100tds.pdf

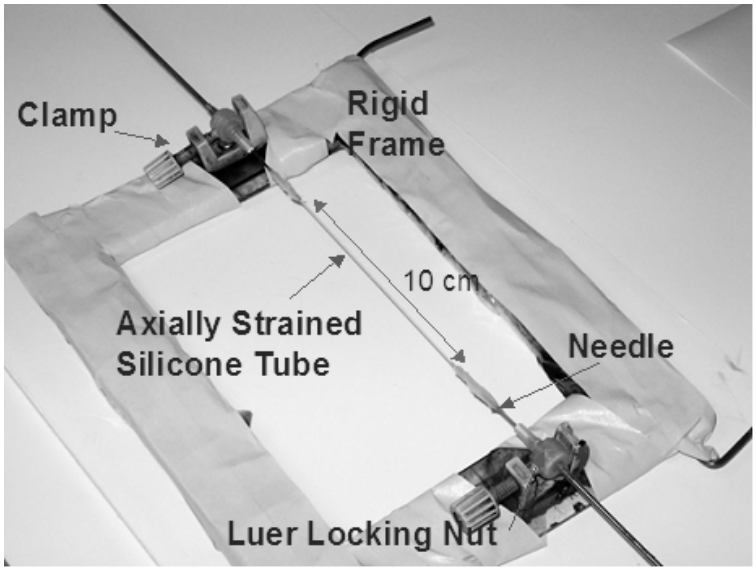

Figure 4.4. Set-up to apply uniaxial prestrain

Conductive silver grease (inner electrode) was inserted into the stretched tube from one end using a syringe attached to the inserted needle. The inner electrode was inserted up to 6cms along the length of the tube, from one end. This was done in order to avoid the inner electrode to get in contact with the needle at the other end of the tube that was to be used as the lead for the outer electrode. After inserting the inner electrode the whole set-up, except a 6 cm region on the tube from the edge opposite to the edge from which inner electrode was inserted, was masked using a tape. Rubber electrode was sprayed on the unmasked region using an air-spray gun. The rubber electrode formed the outer electrode of the fabricated actuator, though the active region was only that part of the tube where the inner and the outer electrodes overlapped. Thus the active region was at the center of the tube with a length of 2 cm, see Figure 4.5. Electrical connections were made to the inner and outer electrodes using the two needles as shown in Figure 4.5.

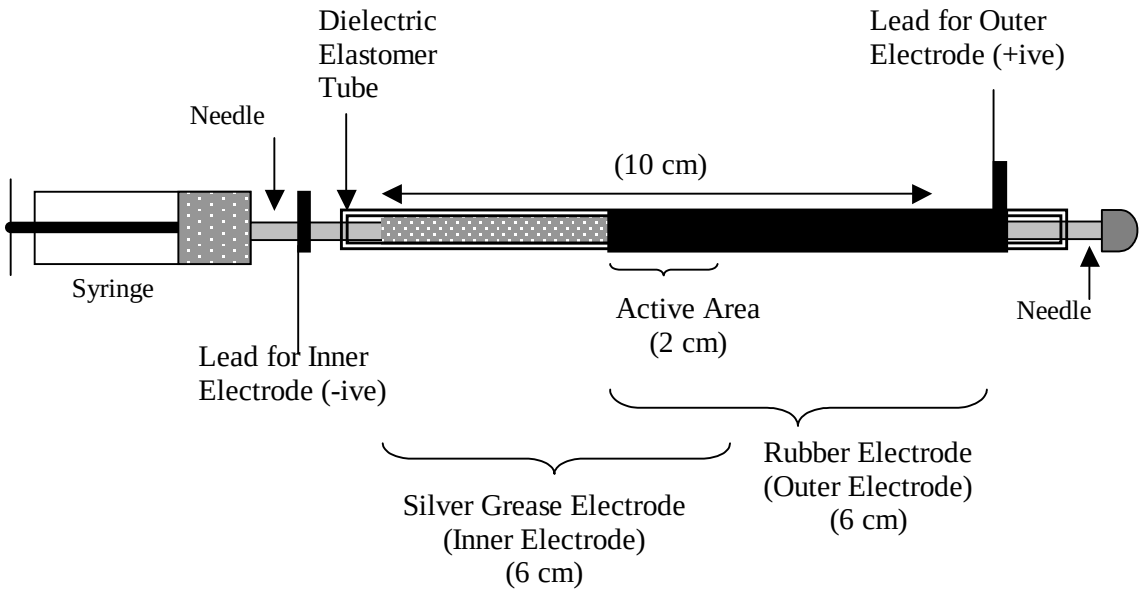

Figure 4.5. Schematic of a uniaxially strained prototype fiber actuator

4.2.2.2 Prestrain levels

As one of the objective of this research was to study the actuation behavior of the prototype fiber actuator under different boundary conditions, one of the ways in which boundary condition on the prototype was changed, besides changing the type of prestrain, was by applying different levels of prestrain. Different levels of uniaxial prestrains were applied by changing the initial length of the tube used to fabricate the prototype as discussed in the previous section. As the final length of the tube was fixed (10 cms) changing the initial length changed the applied prestrain on the tube.

In case of silicone tubes prestrains of 50%, 100%, 150%, 200% and 250% were applied and in case of polyurethane tube prestrains of 50% and 100% were applied. To apply strains greater than 100% on the polyurethane tube very high forces were required, which were not sustainable on our set-up used for applying prestrain. The prestrain levels were decided so as to cover different regions of the tensile modulus of the dielectric elastomer tube at different prestrains (Figure 4.3(a) and 4.3(b)).

4.2.2.3 Properties of tubes at different prestrain levels

When any elastomer is strained its mechanical and physical properties change. Hence, in this study, it was important to understand the change in properties of the dielectric elastomer tubes after application of prestrain.

Change in modulus and wall thickness of the tubes was studied as these two properties influence the actuation behavior of the prototype. Wall thickness determines the electric field developed between the two electrodes at a certain voltage, smaller the wall thickness higher is the electric field at the same voltage and higher is the electrostatic pressure at the same voltage. Modulus of the tube directly affects strains produced in the tube at a certain Maxwell's pressure, higher the modulus lowers is the strains produced in the tube at the same pressure.

Tube wall thickness at different prestrain levels

Wall thickness of the uniaxially prestrained tube decreased with the increase in prestrain level for both silicone and polyurethane tubes. Wall thickness was calculated using the constant volume assumption. That is, the volume of the dielectric elastomer remains the same before and after application of strain. For the purpose of calculations initial tube length, final tube length after applying the strain, initial outer and inner tube radii were known, and Poisson ratio of 0.5 was assumed. MAPLE mathematical software[i] was used to do the final wall thickness calculations based on constant volume assumption. Table 4.2 gives the wall thickness of dielectric elastomer tubes at different uniaxial prestrains used in our study.

Table 4.2. Wall thickness of dielectric elastomer tubes at different prestrain levels

Prestrain	Silicone Tube Wall Thickness (μm)	Polyurethane Tube Wall Thickness (μm)
0%	216	172
50%	176	145
100%	152	125.7
150%	136.5	n.a.*
200%	124.6	n.a.*
250%	115.4	n.a.*

* These prestrains are not applicable for polyurethane tube based actuators

[i] MAPLE 8.00. Copyright (c) 1981-2002 by Waterloo Maple Inc.

Modulus of tubes at different prestrain levels

Modulus along Z (axial) direction showed a non-linear behavior for both silicone and polyurethane tubes. At lower prestrain levels (50%-100%) modulus increased with increase in prestrain but not by much, at higher prestrains (>150%) there was an exponential increase in the modulus with increase in prestrain. Modulus along the θ (radial) direction could not be calculated because of difficulty in sampling, therefore the tube was assumed to be isotropic.

Modulus along Z (axial) direction of the uniaxially prestrained tubes was calculated from the load extension curves of the tubes. Dynamic stresses along the Z-direction and corresponding axial strains were used to calculate the modulus of the tube along Z-direction at different axial strains (Figure 4.3(a) and 4.3(b)). Table 4.3 gives the modulus of the silicone and polyurethane tube at different uniaxial prestrain levels used in our study.

Table 4.3. Modulus of dielectric elastomer tubes at different uniaxial prestrain levels.

Prestrain	Silicone Tube Tensile Modulus (MPa)	Polyurethane Tube Tensile Modulus (MPa)
50%	0.96	20
100%	1	40
150%	1.2	n.a*
200%	1.55	n.a.*
250%	2.756	n.a.*

* These prestrains are not applicable for polyurethane tube based actuators

4.2.3 UNIFORMLY PRESTRAINED PROTOTYPE

Uniform prestrain was applied in order to change the boundary conditions on the actuator in an unbiased manner and study the response of the actuator to this change. Uniform prestrain was applied by inflating the tube; hence the term ‘uniform prestrain’ used here indicates the applied prestrain due to inflation of the tube. The tube was inflated with calcium chloride solution that also acted as the inner electrode as discussed earlier. Only silicone elastomer

tubes were used as the dielectric in fabrication of uniformly prestrained prototype because of the constraints of our inflation set-up. The experimental set-up for inflation could not apply and sustain high enough pressures to inflate the polyurethane tubes because of their high modulus.

Direct measurement of the inflation pressure inside the tube was difficult during the fabrication of the prototype because when the tube was inflated with calcium chloride solution large pressure changes occurred across the inflation set-up, which had different elements like valves and elbows with different diameters through which the liquid passed, and made it impossible to know the actual pressure developed inside the tube. As an alternative, the inflation pressure was measured is a separate set of experiments using air as the inflation medium where length of the tube inflated tube was measured as a function of inflation pressure. Air was used as to measure pressure as it encounters least pressure changes across multiple diameter system because of its low viscosity. In another experiment, length of the inflated tube was measured as a function of amount of calcium chloride solution inserted inside the tube to inflate it. Then using inflated length of the tube as the common parameter, pressure measurements with air were correlated to the amount of calcium chloride solution inserted inside to determine the inflation pressure of the uniformly prestrained prototype. Details of inflation pressure determination, fabrication of uniformly prestrained prototype and proprieties of tube at different uniform prestrains (inflation pressures) are discussed in following sections.

4.2.3.1 Fabrication

As described earlier for uniaxially prestrained actuators, uniformly prestrained prototypes were also fabricated from a short length of tube. To access the inner part of the tubes a hypodermic needle of appropriate dimension (20 gauge) was inserted from each end of the tubes. The length of the tube between the two needles was always 4 cms. The length of 4 cms was decided based on the ease of inflation and final length of the actuator desired, which was around 10 cms based on the length of tube the frame used for applying outer electrode could accommodate. Two ends of the tube were firmly secured to the needles using a commercially available two-part epoxy. The needle at one end of the tube was attached to a syringe containing the inner electrode (Calcium chloride solution) that was attached to a syringe

pump. The needle at the other end was sealed using a locking nut. Before sealing the end, the whole system was flushed with the salt solution to push out all the air in the system. The tube was pressurized by pushing the calcium chloride solution into the system at a constant rate of 0.2 ml/min using the syringe pump. The syringe pump recorded the amount of calcium chloride solution inserted into the tube at each point of time. A slow rate of inflation was used to ensure a uniform inflation of the tube. High inflation rates lead to non-uniform inflation of the tube. This is believed to be because at slow inflation rates stresses in the tube are allowed sufficient to uniformly propagate through out the tube thus giving uniform tube inflation. Figure 4.6 shows the inflation set-up for this purpose.

It was observed that when the tube was inflated for the first time to a pressure of 23 psi, which induced an axial strain of nearly 325%, it did not recover its length completely upon deflation (Figure 4.7). The non-recovered length accounted for about 25% of the original length. For every inflation-deflation cycle thereafter, no such hysteresis was observed. It was also observed that the silicone tube behaved differently during inflation and deflation. When the tube was being inflated, at around 5 psi the tube first developed a bulge at the end that was closer to the source of inflation medium, then as the pressure was increased to around 7 psi the bulge propagated through the length of the tube, till the other end, resulting in a uniformly inflated tube. On further increase of the pressure the tube inflated uniformly. On the other hand, when the tube was being deflated it maintained a uniform diameter through out its length till the pressure was reduced to zero.

Based on the above observations, all the silicone tubes used for fabrication of uniformly prestrained prototype were taken through three inflation-deflation cycles to remove any hysteresis followed by inflating them to a very high pressure (around 23 psi) and then deflating them to the desired pressure required to set up the prestrain.

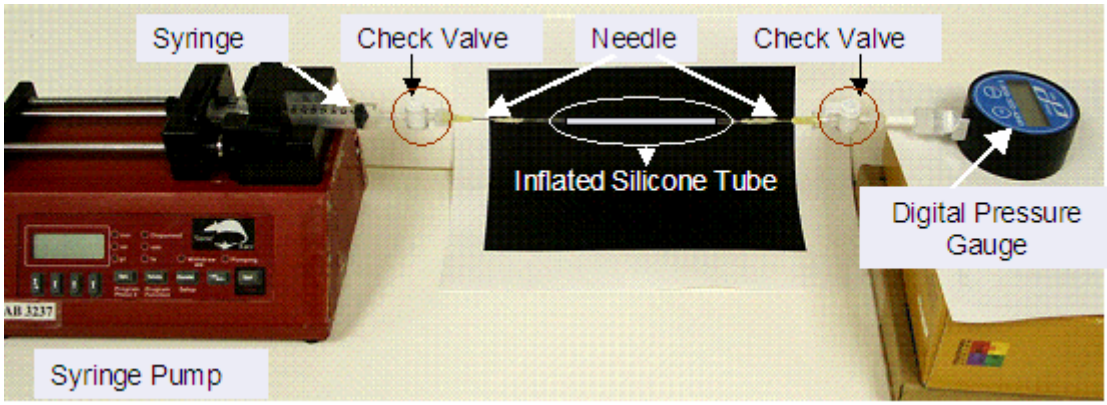

Figure 4.6. Inflation Set-up

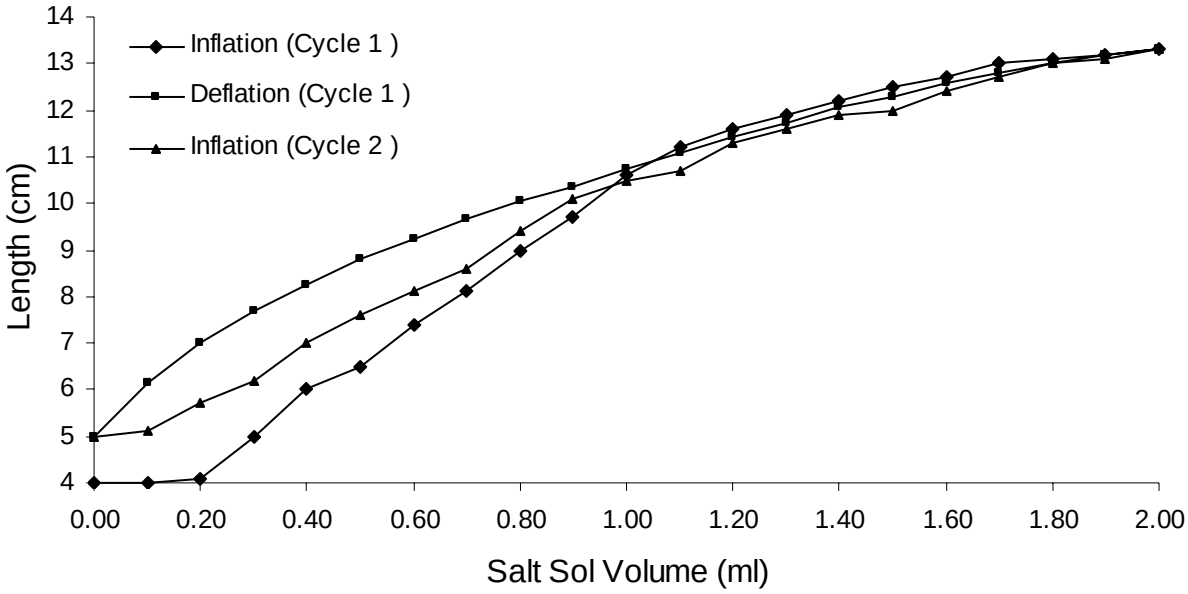

Figure 4.7. Hysteresis observed during multiple inflation cycles of axially cycled silicone tube.

After attaining the desired inflation pressure the check valves were closed and the inflated tube was separated from the inflation set-up. The tube, except a 2 cm region at the center, was then masked using a masking tape and rubber electrode (outer electrode) was sprayed on the unmasked region using an air-spray gun. The region with the rubber electrode formed the

active region (Figure 4.8). Electrical connection to the inner electrode was made using any one of the two needles and the outer electrode was connected using a thin copper wire.

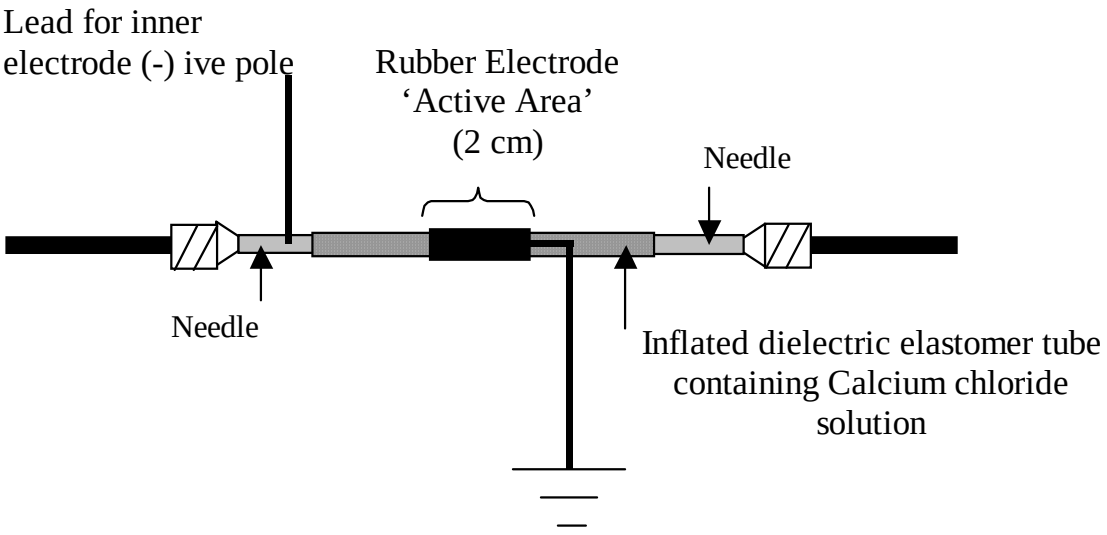

Figure 4.8. Schematic of a uniformly prestrained prototype fiber actuator

4.2.3.2 Prestrain levels

As has been discussed earlier, one of the ways of changing boundary conditions on the prototype fiber actuators was by applying different levels of prestrain. In case of uniformly prestrained prototypes different prestrain levels were achieved by changing the inflation pressure in the tubes. Four different inflation pressures were used 5.68 psi, 6.62 psi, 8.4 psi and 13.73 psi. Radial and axial prestrains at each inflation pressure were determined experimentally and are given in Table 4.4

Table 4.4 Inflation pressures used in uniformly prestrained prototype and corresponding radial and axial prestrains.

Inflation Pressure (psi)	**Radial Prestrain (%)**	**Axial Prestrain (%)**
5.68 psi	125.00%	104.00%
6.62 psi	155.00%	116.00%
8.4 psi	179.29%	136.00%
13.73 psi	216.43%	180.00%

As discussed before, inflation pressure in the tube was not measured directly during fabrication of the prototype, but in a separate set of experiments, using air as the inflation medium. During fabrication amount of calcium chloride salt solution inserted into the tube and corresponding axial strains were measured and during inflation experiments with air, pressure in the system and corresponding axial strains were measured. The measurements from the two experiments were then correlated using axial strains as the common parameter. The determination of inflation pressure is discussed in detail below.

Determination of Inflation Pressure

Figure 4.9 shows the step-by-step procedure used to derive a correlation between the inflation pressure and volume of salt solution pushed into the tube.

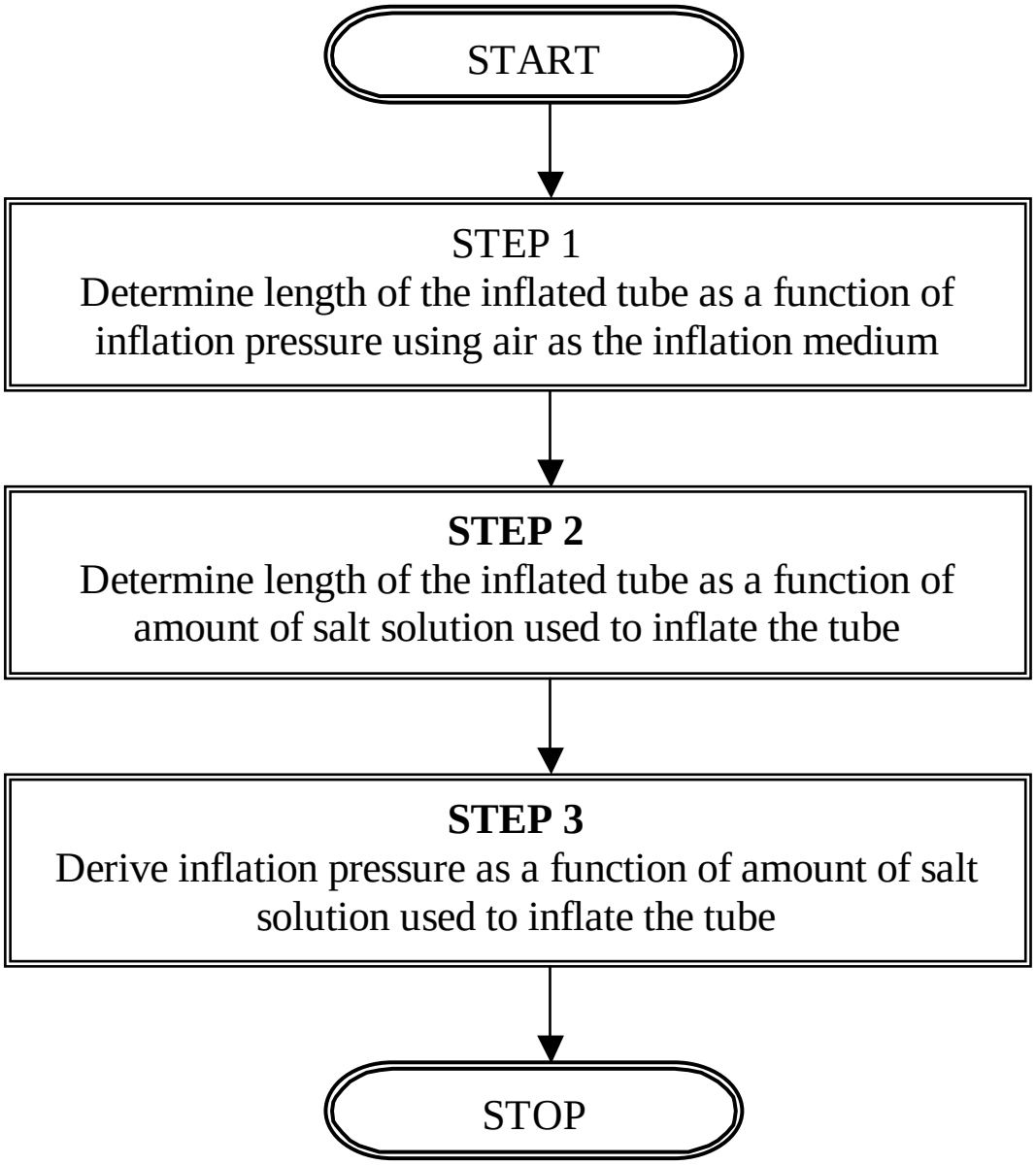

Figure 4.9. Step-by-step process to determine inflation pressure in the tube as a function of amount of salt solution used to inflate the tube

Step 1: Axial Strain as a function of Air Inflation Pressure

Axial strains in the tube were recorded as a function of air pressure in the tube (see Figure 4.10). The tube pressure was measured using a digital pressure gauge[i]. Here also axial strains and corresponding air pressures were recorded during the deflation of the tube as discussed earlier. The pressure values in figure 4.10 are average of pressures recorded during 3 deflation cycles at particular strain levels.

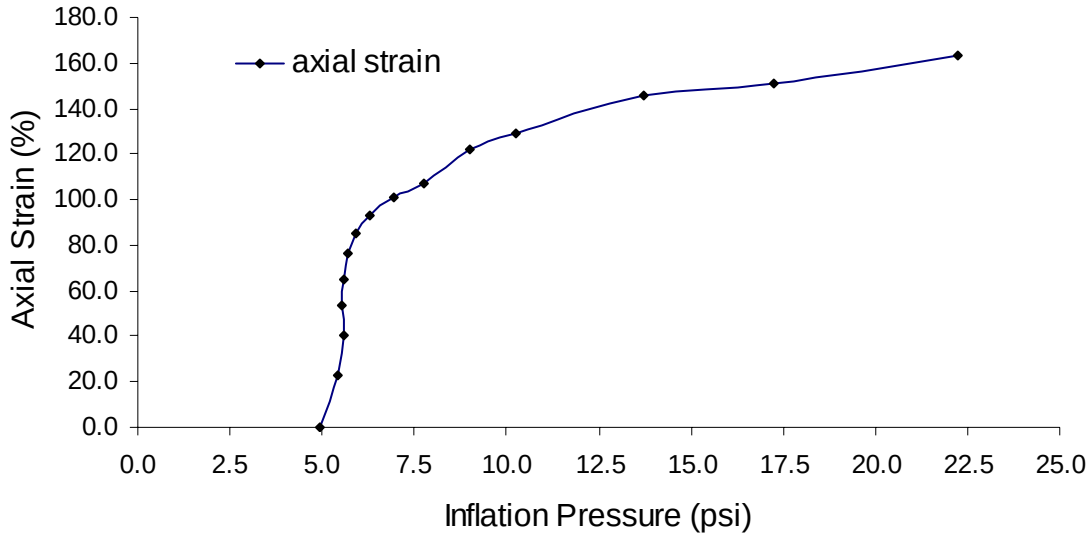

Figure 4.10. Axial strains produced in silicone tube as a function of salt solution volume inserted.

Step 2: Axial Strain as a function of Salt Solution Volume

Axial strain in the tube was recorded as a function of salt solution volume pushed into the tube for inflation (see Figure 4.11). Axial strain and corresponding salt solution volume was recorded during the deflation of the tube the reason for which has been discussed earlier in section 4.2.3.1. The deflation of the tube was carried out by removing the salt solution from the system at a constant rate of 0.2 ml/min. Axial strains of up to 170% were recorded for 2 ml of salt solution inserted into the tube.

[i] 68110-10, Digitial Pressure Gauge, 30 psi from Cole-Palmer® Instrument Company. www.coleparmer.com

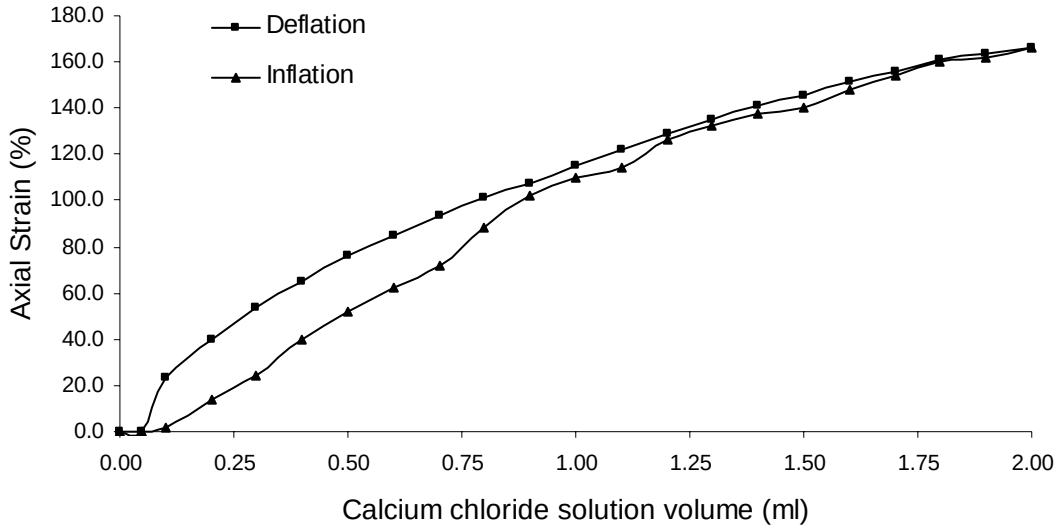

Figure 4.11. Axial strain in silicone tube as a function of air inflation pressure

Step 3: Correlating Inflation Pressure and Salt Solution Volume

Using relation between axial strains and inflation pressures (figure 4.10) and axial strains and salt solution volume (figure 4.11), a correlation between inflation pressure and salt solution volume was defined (figure 4.12). This allowed us to know the pressure developed inside the tube when a certain amount of salt solution was inserted into the tube to inflate it. The pressure values in figure 4.12 are average of pressures recorded during 3 deflation cycles.

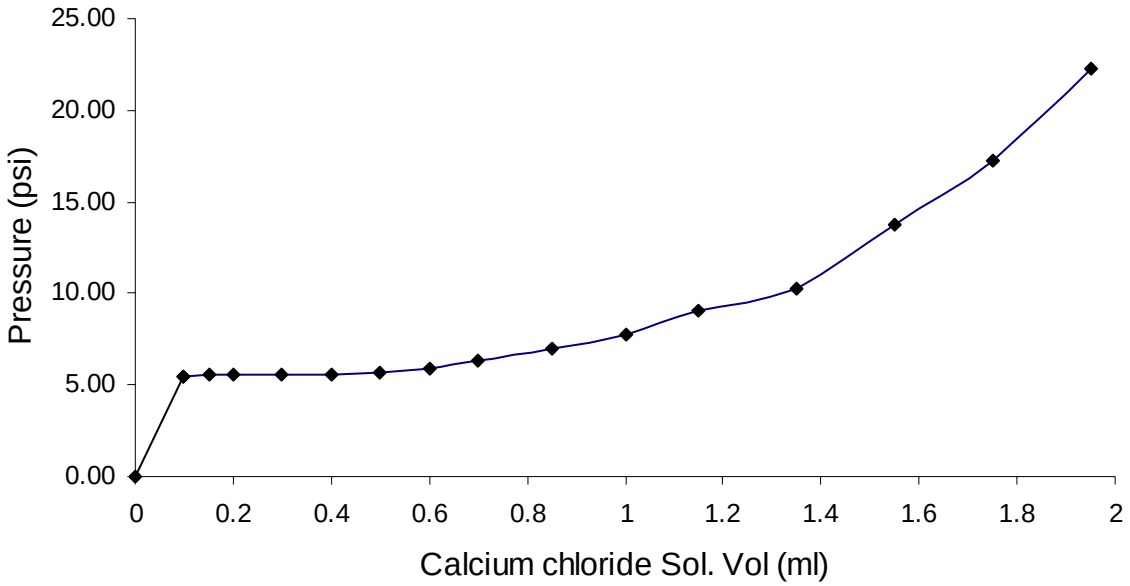

Figure 4.12. Inflation pressure as a function of salt solution volume used for inflating the tube.

4.2.3.3 Properties of silicone tube at different prestrain levels (inflation pressures)

As has been discussed before for uniaxially prestrained prototype, it was important to understand the change in modulus and wall thickness of the dielectric elastomer tubes after application of prestrain as these two properties influence the actuation behavior of the prototype. Wall thickness and modulus of silicone tube at different prestrain levels (inflation pressures) are discussed below.

Wall thickness of inflated tube at different prestrain levels (inflation pressures)

Wall thickness of the silicone tube decreased with the increase in prestrain levels (inflation pressures) based on the constant volume assumption. Wall thickness of the inflated tube was calculated by measuring outer diameter of the inflated tube and subtracting from it inner diameter of the tube, see Appendix A for details. Wall thickness of the inflated silicone tube at different prestrain levels (inflation pressures) used in our study, and corresponding inflation pressures, radial strains and axial strains, calculated using technique outlined in appendix A, are given in Table 4.5.

Table 4.5. Dimensions of the inflated silicone tube at different prestrain levels (inflation pressures)

Inflation Pressure (psi)	Salt Solution Vol. Inserted (ml)	Radial Prestrain (%)	Axial Prestrain (%)	Outer Radius (μm)	Inner Radius (μm)	Wall Thickness (μm)
5.68 psi	0.5 ml	125.00%	104.00%	1265	1237	28
6.62 psi	0.75 ml	155.00%	116.00%	1434	1411	23
8.4 psi	1 ml	179.29%	136.00%	1570	1552	18
13.73 psi	1.5 ml	216.43%	180.00%	1779	1765	14

Modulus of inflated tube at different prestrain levels (inflation pressures)

Modulus of tube increased along both θ (circumferential) and Z (axial) direction with increase in prestrain levels (inflation pressures).

Modulus of the inflated tube along θ (circumferential) and Z (axial) direction was calculated using well-known equations [53] for stresses developed in a pressurized thin cylinder. In general, a cylinder with a wall thickness $1/20^{th}$ time its diameter is considered as a thin cylinder. Because the wall thickness of the inflated tube was less than $1/20^{th}$ times its diameter, the following equations were considered valid.

$$\sigma_\theta = pr/t \quad \ldots (4.6)$$

$$\sigma_Z = pr/2t \quad \ldots (4.7)$$

Where σ_θ and σ_Z are stresses in the tube wall along the θ and Z directions respectively, p is the pressure inside the tube, r is the inner radius of the tube and t is the wall thickness (Figure 4.13).

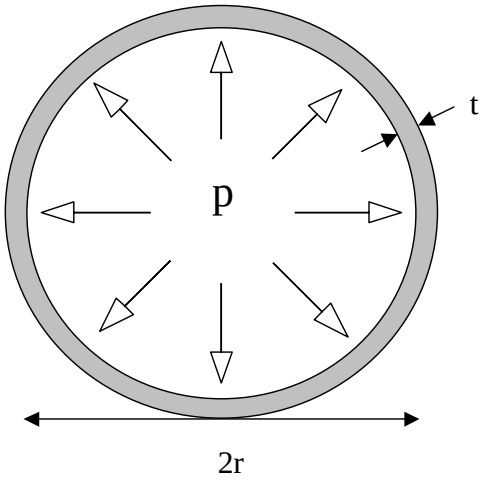

Figure 4.13. Top view of a pressurized thin walled cylinder

From equations 4.6 and 4.7, and values of wall thickness (t) and inner radius (r) of the tube given in Table 4.5, stresses in the tube along θ and Z coordinates were calculated at different inflation pressures. Modulus of the tube was calculated along both the directions at each inflation pressure using the stress values and strain values along the axial and circumferential (same as radial strains) directions (Table 4.6).

Table 4.6. Modulus of the inflated tube at different prestrain levels (inflation pressures)

Inflation pressure (psi)	**Radial (circumferential) prestrain (%)**	**Axial prestrain (%)**	**Modulus along circumferential direction (MPa)**	**Modulus along axial direction (MPa)**
5.68	125.00%	104.00%	1.36	0.82
6.62	155.00%	116.00%	1.85	1.24
8.4	179.29%	136.00%	2.70	1.78
13.73	216.43%	180.00%	5.47	3.29

4.3 EXPERIMENTAL SET-UP FOR EVALUATION OF PROTOTYPES

Prestrained prototypes that were developed, as discussed in section 4.2, were actuated using an external high voltage source and their resulting actuation behavior was measured. Three parameters were measured; axial strain, radial strain and blocking force (g). Axial strains were the strains produced in the active area of the prototypes along the z-direction (see Figure 4.1 (b)), radial strains were the strains produced in the active area of the prototypes along the radial direction (see Figure 4.1 (b)) and blocking forces were the reduction in force on actuation to maintain a constant length of the prototypes measured using a load cell coupled to the prototype. Experimental set-up designed to facilitate these measurements, details of how the actuation experiments were conducted and evaluation techniques used to measure the actuation behavior are discussed in following sections.

4.3.1 Experimental set-up

An experimental set-up was designed (Figure 4.14) to actuate the developed prototypes and measure the actuation behavior. The set-up included a 250N load cell that was mounted on a MTS® tensile testing machine. The load cell was coupled to the prototype using a pair of pneumatic grips that held the prototype in a vertical position, and was used to measure the actuation blocking force. Details of blocking force measurement technique will be discussed in detail in section 4.3.2. The active region of the actuator was imaged using a Pulnix Progressive Scan camera. The images from Pulnix camera, as will be discussed later in section 4.3.2, were used to calculate radial and axial actuation strains produced in the active area of the prototype. Electrical connections to inner and outer electrodes were made using alligator clamps attached to the hypodermic needles at the two ends of the prototype.

Actuation experiments were conducted by applying an appropriate DC voltage across the two electrodes of the prototype. The actuation voltage was applied in steps and taken from zero to peak actuation voltage of the prototype and then brought back to zero; for the purpose of this study this process was termed as ‘one actuation cycle’. Peak actuation voltage for a prototype was just below its breakdown voltage and varied with the level of prestrain. Breakdown voltage (or peak actuation voltage) depends on the level of prestrain because

changing the prestrain changes wall thickness of the tubes, as was discussed in sections 4.2.2 and 4.2.3, that in turn changes the electric field developed across the tube wall for the same applied voltage. As the prototypes fail at a specific electric field (depending on the type of dielectric elastomer used) and higher the prestrain lower the tube wall thickness (sections 4.2.2 and 4.2.3), high prestrained prototypes failed at lower actuation voltages as compared to low prestrained prototypes. Actuation voltage was applied in steps because the response time of the prototype was slow and to get full response at a particular voltage it was necessary to hold at that level for a few seconds. The axial strains, radial strains and blocking forces developed in the prototypes during an actuation cycle were measured using evaluation techniques that will be discussed in detail in section 4.3.2. For each prototype, three measurements each were made for axial actuation strains and radial actuation strains to get a statistical average. Blocking force was measured during every actuation cycle alongside actuation strain measurements.

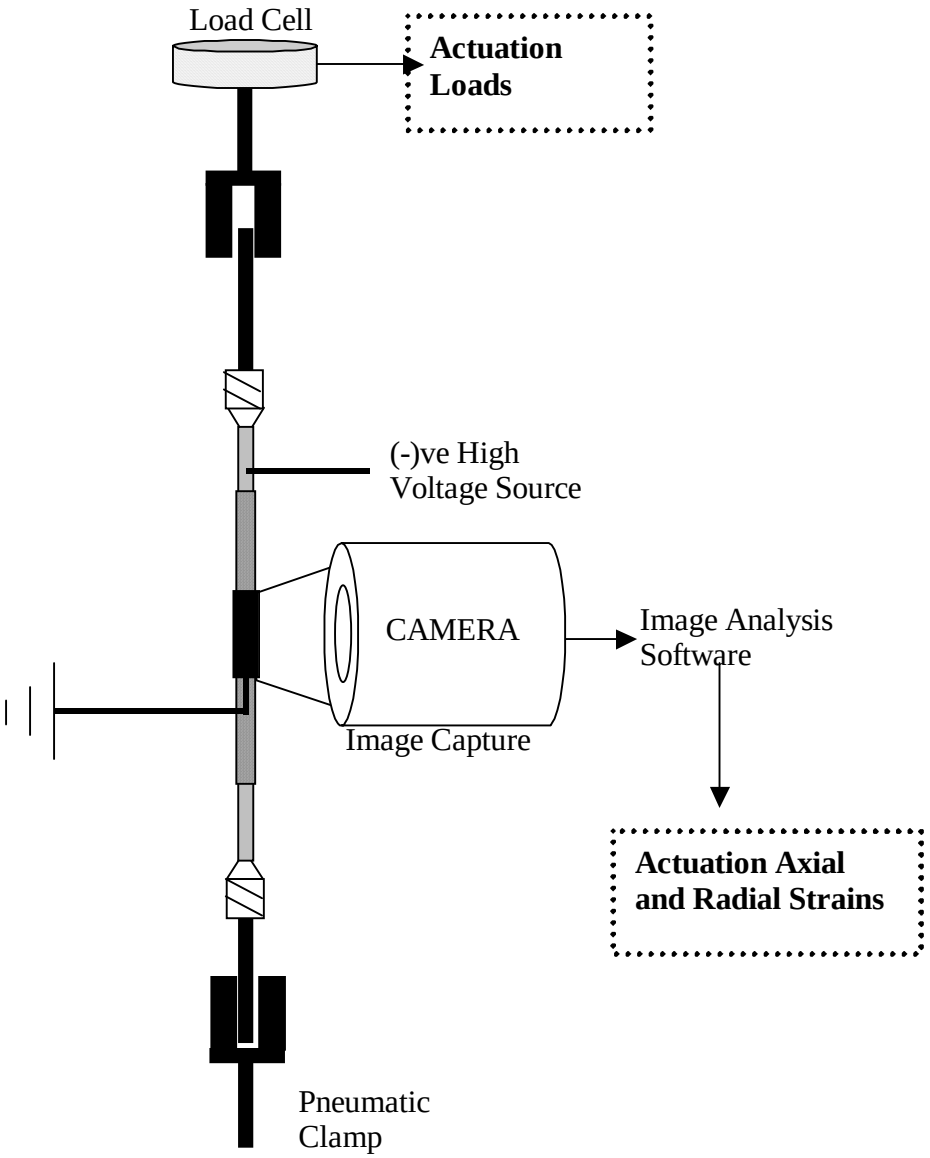

Figure 4.14. Experimental Set-up

4.3.2 Evaluation Techniques

Different evaluation techniques were used to measure the actuating behavior of developed prototypes. Blocking force was measured using a 250N load cell whereas axial and radial strains were measured by acquiring and analyzing images of active area of the prototype during actuation. Evaluation techniques are discussed in detail below.

Measurement of axial actuation strain

In order to measure the strain along the longitudinal axis of the actuator tube, two silver paint dots or markers were placed on the active area of the fabricated actuator, one near each end, see Figure 4.15. Each marker was placed at a distance of 2mm from the edge of the active area and the axial actuation strains were measured by recording the change in distance between the two markers. Video of active area during actuation was obtained by using a Pulnix Progressive Scan camera working at 7 frames per second. The image of the active area was captured in a way such that the two markers (silver paint dots) were visible as bright spots on a black background, see Figure 4.16. Blob analysis of these images was done, where the markers were identified as blobs, and position of these markers was recorded for each image. By analyzing consecutive images, the movement of the center of markers with time was recorded. A macro was written (Appendix B) to analyze image taken every second and record position of the markers at every second from the recorded video. Axial actuation strains were obtained by calculating change in distance between the two markers with time. This gave axial actuation strains as a function of time. But the objective was to know the actuation behavior as a function of applied voltage (electric field). This was achieved by recording applied voltage as a function of time and then correlating it with axial actuation strains as a function of time. How this correlation was done will be discussed in detail later in this section.

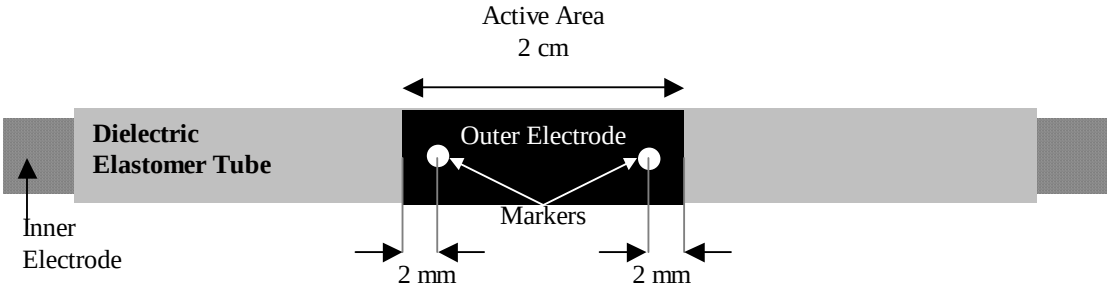

Figure 4.15. Schematic of active area with silver paint markers

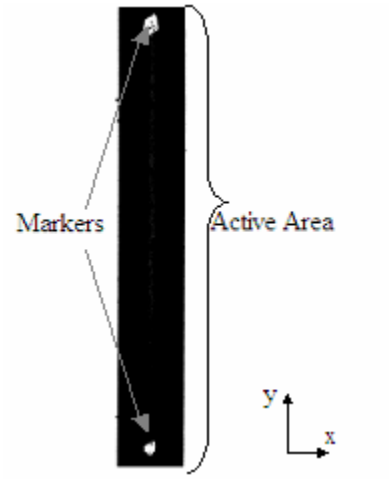

Figure 4.16. Image taken for axial actuation strain measurement using blob analysis

Measurement of radial actuation strain

To measure radial strains, the two boundaries of the active area were imaged and change in distance between the two boundaries was calculated. The same imaging system described earlier was used for the radial strain measurement. The image was taken in a way such that the active region was distinctively darker than the background, see Figure 4.17. Blob analysis of the images taken at every second was done and the area of the dark region (active area) was recorded. A macro was written (Appendix C) to do the image analysis of the image taken at every second. The area of the dark region when divided by its length, which was fixed, gave the distance between the two boundaries of the dark region or the outer diameter of the actuator. Hence, by analyzing images taken at every second, outer diameter of the actuator was recorded with time. Radial actuation strains were obtained by calculating the change in diameter. This gave radial actuation strains as a function of time. But, as discussed before, the objective was to know the actuation behavior as a function of applied voltage (electric field) that was achieved by recording applied voltage as a function of time and then correlating it with radial actuation strains as a function of time. How this correlation was done will be discussed in detail later in this section.

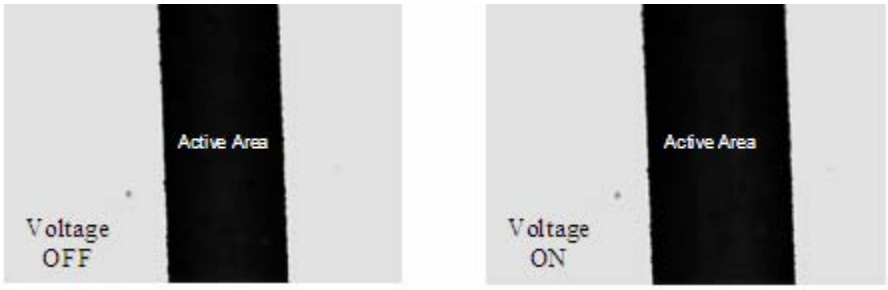

Figure 4.17. Images taken for radial actuation strain measurement using blob analysis

Measurement of actuation blocking force

Blocking force is the force required to prevent any actuator displacement [42]. The blocking force is also the maximum force that is generated when the actuator is held at constant length, also known as isometric actuator operation. As mentioned earlier, in evaluating the actuation behavior, the test samples were held under constant prestrain (and at the corresponding force). The reduction in force on actuation to maintain the length is considered here as the blocking force. Actuation blocking force was measured using the load cell on the MTS tensile testing machine on which the prototype fiber actuators were mounted. As all the actuators were prestrained, they applied a downward load on the load cell. Upon actuation this load applied on the load cell by the actuator changed. Load as a function of time was recorded using TestWorks® software. Actuation blocking force was calculated as the change in load with time. Actuation blocking force as a function of applied electric field was determined as mentioned for axial and radial actuation strains and will be discussed in detail below.

Correlating actuation behavior and applied voltage

In order to correlate applied voltage with load and strain measurements of the actuator a time line was constructed. This was done by recording time of every event with reference to a starting point. The starting point in all experiments was the starting of recording of load values from the load cell. Using this timeline, applied voltage, axial strain, radial strain and load were known as a function of time. Hence actuation behavior of the prototype was known as a function of applied voltage. A time line of events in an actuation experiment is shown in Figure 4.18.

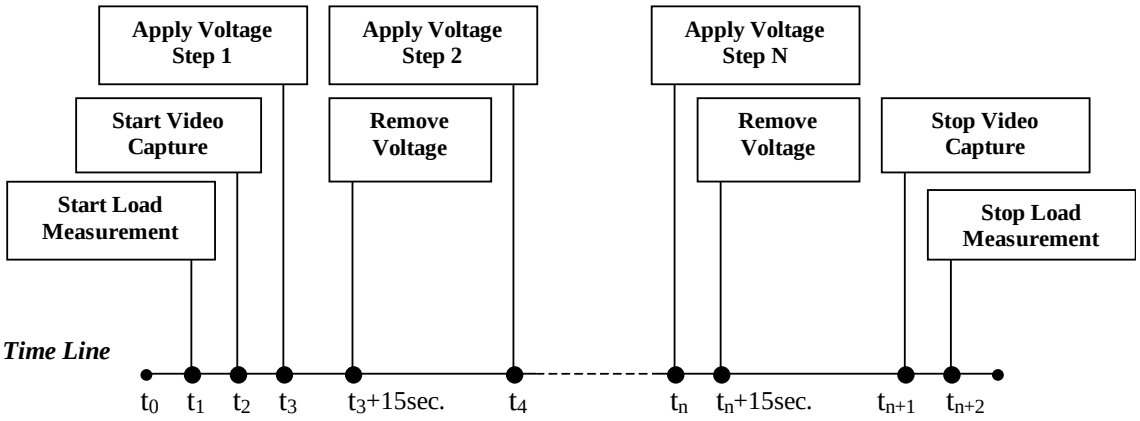

Figure 4.18. Timeline of events during conduct of actuation experiments

5 RESULTS AND DISCUSSIONS

Uniaxially and uniformly prestrained prototypes, fabricated as discussed in section 4.2, were evaluated for their actuation behavior using the experimental set-up discussed in section 4.3.2. The experiments performed are described in detail in section 4.3.3. Actuation strains and blocking forces were measured during actuation experiments of the fabricated prototypes and are discussed in the following sections.

As the actuation behavior of a test sample is measured over multiple actuation cycles (as discussed in section 4.3.3) it is important to test the prototypes for any hysteresis, especially because elastomers used here are known to show hysteresis (discussed in section 4.2.1). The test samples were tested for hysteresis by taking them through multiple actuation cycles (>20) and observing for any change in their actuation behavior. The results of hysteresis test are discussed in detail in section 5.3.

Please note that in the context of the experiments and results described here the term "uniformly prestrained" is used to indicate applied prestrain due to inflation of the tube.

5.1 ACTUATION BEHAVIOR OF UNIAXIALLY PRESTRAINED PROTOTYPE

The uniaxially prestrained prototype (discussed in section 4.2.2) actuators were subjected to multiple actuation cycles. During each actuation cycle a DC voltage was applied across the two electrodes of the test sample in steps of 1 kV or 2 kV (depending on the breakdown voltage of the prototype) up to just under its breakdown voltage. The breakdown voltage was determined experimentally for each prototype. For samples with high prestrains (200% and 250% for silicone tube and 100% for polyurethane tube), which failed at much lower voltages (as discussed in section 4.3.3), steps of 1 kV were used in order to get enough data points for analysis. For all other samples steps of 2 kV were used. At every step, the applied voltage was held constant for 15 seconds. This was done to get the full response of the prototype at that particular voltage. After 15 seconds the voltage was brought down to zero and maintained at zero volts for a few seconds to allow for actuator recovery and charge dissipation before it was subjected to the next level of potential.

The actuation behavior of uniaxially prestrained silicone and polyurethane based prototypes at different levels of prestrain is discussed in detail below.

5.1.1 Axial actuation strains

Axial actuation strains produced by silicone and polyurethane based uniaxially prestrained samples plotted as a function of applied electric field are shown in Figures 5.1(a) and 5.1(b) respectively. The data points in the graphs in Figure 5.1 are axial actuation strains at each step of the actuation cycles and the lines are fitted curves through these points. Applied voltage was converted to applied electric field for each prototype by dividing applied voltage by corresponding tube wall thickness.

A parabolic relationship was observed between applied electric field and axial actuation strains, as was expected from the equation (2.1) for electrostatic pressure in DEAs. The relationship is parabolic for all prestrain levels and for both silicone and polyurethane based samples. It is also observed that increasing the prestrain decreased the axial actuation strains produced in both silicone and polyurethane based prototypes. The distribution of strain caused by the pressure in the radial direction of the tubular sample is dependent on the anisotropy of the tube wall. Application of prestrain in the longitudinal direction (see Figure 4.3) of the tube further increases the elastic modulus of the tube in the longitudinal direction, introducing additional anisotropy in the tube. As the electrostatic pressure develops along the radial (r) direction, the resulting strain therefore is smaller along the longitudinal direction (x) because of the higher modulus in this direction. Following the same reasoning the resulting strain is higher in the circumferential direction (theta) of the tube wall as will be seen later in section 5.1.2. This reasoning is reinforced by the observation that axial actuation strains observed in prototypes fabricated using polyurethane tube, which have higher tensile modulus than silicone tube, are much smaller than actuation strains observed in silicone tube based prototypes.

As shown in Figure 5.1, maximum axial actuation strain of 6.9% at 80 V/μm was observed for silicone tube with 50% prestrain (Figure 5.1 (a)). In case of polyurethane based actuators maximum axial actuation strain observed was 0.58% at 125V/μm for the same level of prestrain (Figure 5.1 (b)). The obvious reason for the difference is explained earlier. A set of images showing axial actuation strain in silicone based prototype is given in Appendix E.

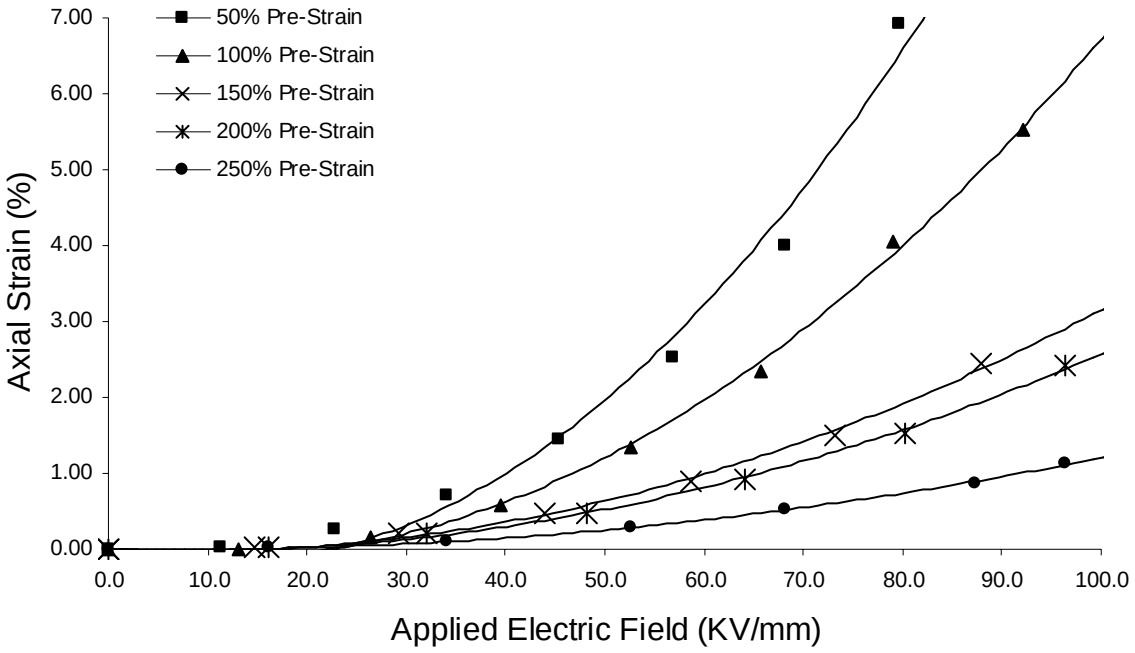

(a)

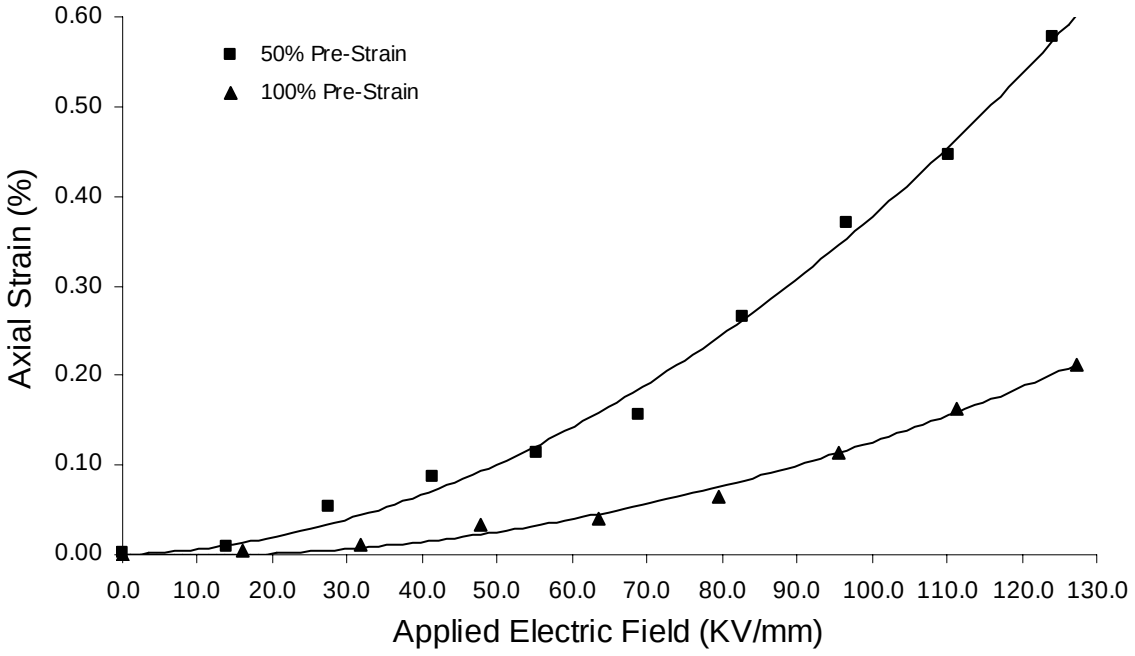

(b)

Figure 5.1. Axial actuation strains as a function of applied electric field in uniaxially prestrained prototypes for different prestrain levels (a) silicone tube based actuator (b) polyurethane based actuator

5.1.2 Radial actuation strains

Radial actuation strains produced at different prestrain levels of silicone and polyurethane based uniaxially prestrained prototype are plotted as a function of applied electric field are shown in Figures 5.2(a) and 5.2(b) respectively. The data points in Figure 5.2 are radial actuation strains at each step of the actuation cycles and the lines are fitted curves through these points. As before, applied voltage is converted to electric field for each prototype by dividing applied voltage by corresponding tube wall thickness.

As expected, a parabolic relationship between radial actuation strain and applied electric field is obtained. Contrary to the observation with axial actuation strains, radial actuation strains generally increased with increase in axial prestrain for both silicone and polyurethane based prototypes. The reason for increase in radial strain with higher prestrain is explained earlier in section 5.1.1. It is also important to note that, higher radial strains are observed in silicone-based prototypes as compared to polyurethane tube based prototypes; similar to what was observed for axial actuation strains. The reason is believed to be lower elastic modulus of silicone tube than polyurethane tube. As was discussed earlier, a higher modulus results in lower strain response.

As shown in Figure 5.2, maximum radial actuation strain observed was 18.31% for 200% axial prestrain in case of silicone-based actuator at 96V/μm, see Figure 5.2(a). With polyurethane based actuator the maximum radial actuation strain observed was 2.04% for 100% axial prestrain at 127V/μm, see Figure 5.2 (b). A set of images showing radial actuation strain in silicone based prototype is given in Appendix E.

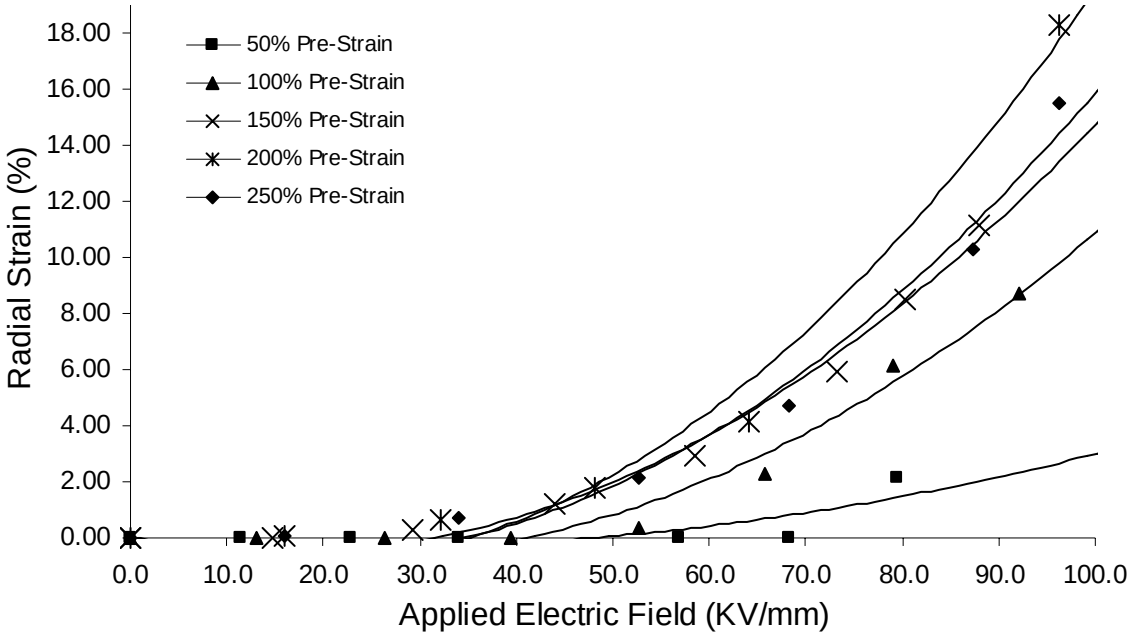

(a)

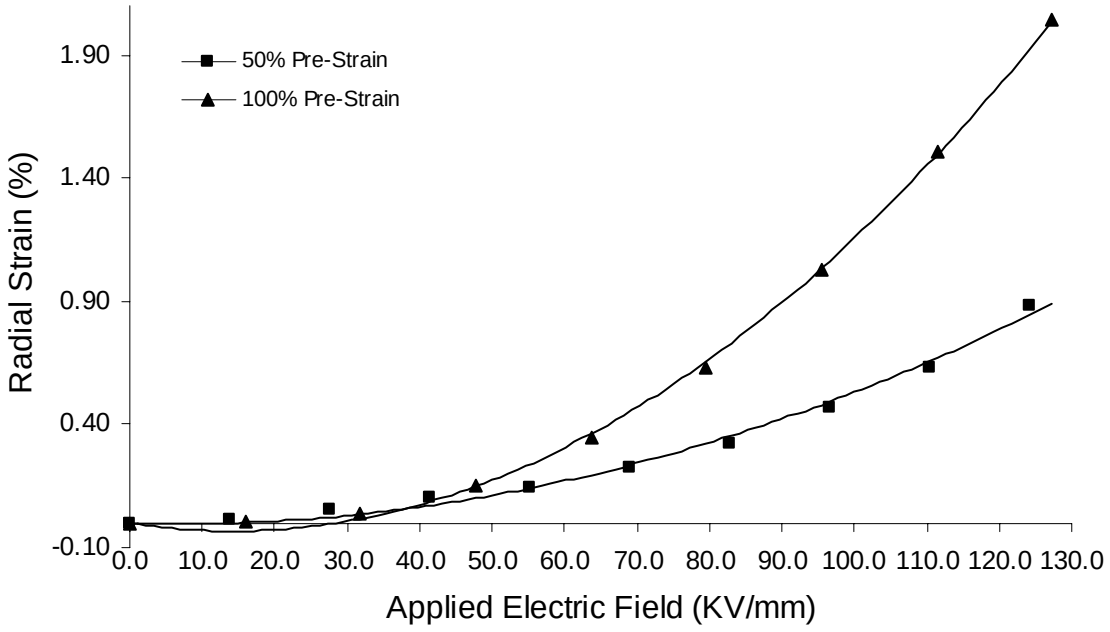

(b)

Figure 5.2. Radial actuation strains as a function of applied electric field in uniaxially strained prototype fiber actuators for different prestrain levels (a) silicone tube based actuator (b) polyurethane based actuator

5.1.3 Blocking force

Blocking force, as discussed earlier in sections 2.2.2 and 4.3.1, is the force developed in the prototype fiber actuator along its axial direction upon actuation. It was calculated by subtracting the force on the load cell at each step of the actuation cycle from its nominal value at the start of actuation. Blocking force produced at different prestrain levels of silicone and polyurethane based uniaxially prestrained samples are plotted as a function of applied electric field and are shown in Figures 5.3(a) and 5.3 (b), respectively. As earlier, the data points in the graphs in Figure 5.3 are blocking force at each step of the actuation cycles and the lines are fitted curves through these points. Applied voltage was converted to applied electric field for each prototype by dividing applied voltage by corresponding tube wall thickness.

A parabolic relationship between the actuation blocking force (change in load) and applied electric field is observed, see Figures 5.3a and 5.3b. With increase in prestrain the actuation blocking force decreased for both silicone and polyurethane based prototypes. The observation of lower blocking force in case of higher prestrains is primarily due to the change in mechanical behavior of elastomers on prestraining. The effect of prestraining on the mechanical properties of the tubular structure are likely to be two fold, first in the direction(s) of applied strain the modulus should be higher in the prestrained state. Additionally, the prestrain induced deformation will also cause the modulus in the radial direction (along the tube wall thickness) to be higher. The measured blocking force is a result of the electrostatic pressure generated by the applied electrical field. The coupling between the electrostatic pressure along the radial direction and the resulting magnitude of constant volume deformation of the tube walls is manifested in the measured “blocking force,” and is likely to be weaker for a relatively rigid tube.

It was also observed that higher actuation blocking forces were developed in polyurethane based prototypes. The dimensions of the two tubes used for this investigation are comparable; however, the elastic modulus of the polyurethane tube is about 10 times greater than that of the silicone tube. Using the explanation presented before on the effect of prestrain, it would seem to be an anomaly. However, the most plausible explanation of higher blocking force for polyurethane is in its greater dielectric constant (ε~6-7, [44]) compared to silicone (ε~2-4, [18]). Higher dielectric constant helps generate a greater

electrostatic force on the polyurethane tube walls resulting in higher measured blocking force (see Equation 2.2).

Maximum actuation blocking force of 5.26 g was observed in 50% prestrain Polyurethane based prototypes at 125V/μm, see Figure 5.3(b). In silicone based prototypes the maximum actuation blocking force observed was 1.69 g for 100% prestrain level at 92V/μm. At the same electric field, actual value of actuation blocking force for 50% prestrain silicone based prototype was not available but the expected value came out to be 1.79 g, which is higher than 100% prestrain level as expected, see Figure 5.3 (a).

Another perspective to look at blocking force is to look at percent change in preload (due to prestrain) upon actuation. In which case it is observed that percent change in preload is much higher for silicone based prototype than for polyurethane based prototype (Appendix D). The reason being that preloads (due to prestrain) in silicone tube were very low, because of its low modulus, as compared to polyurethane based prototypes.

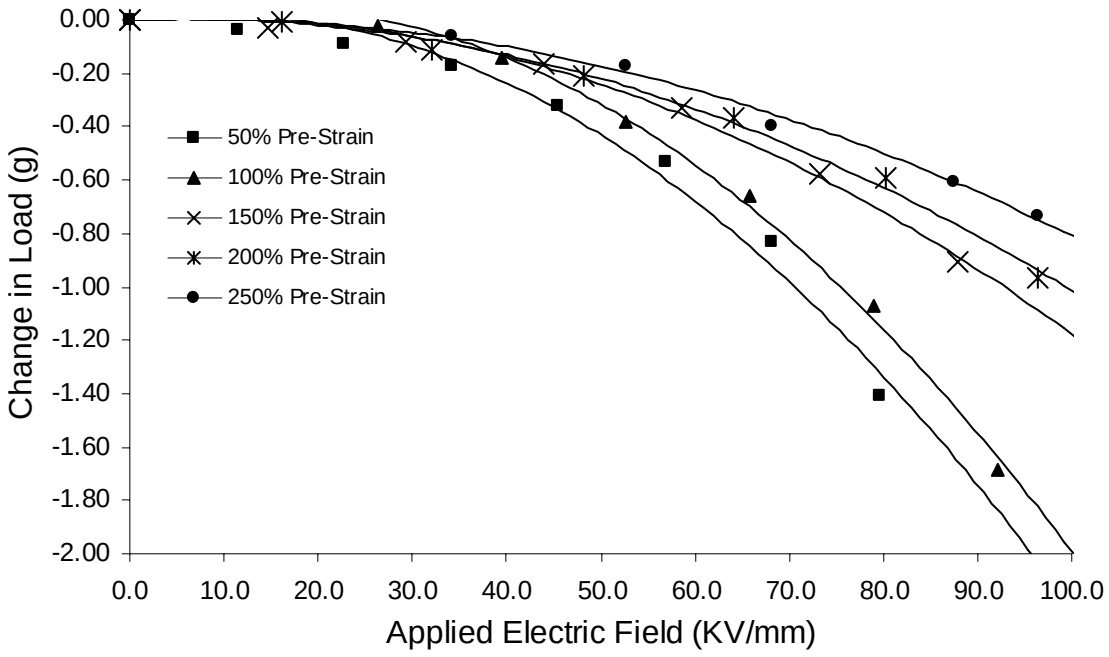

(a)

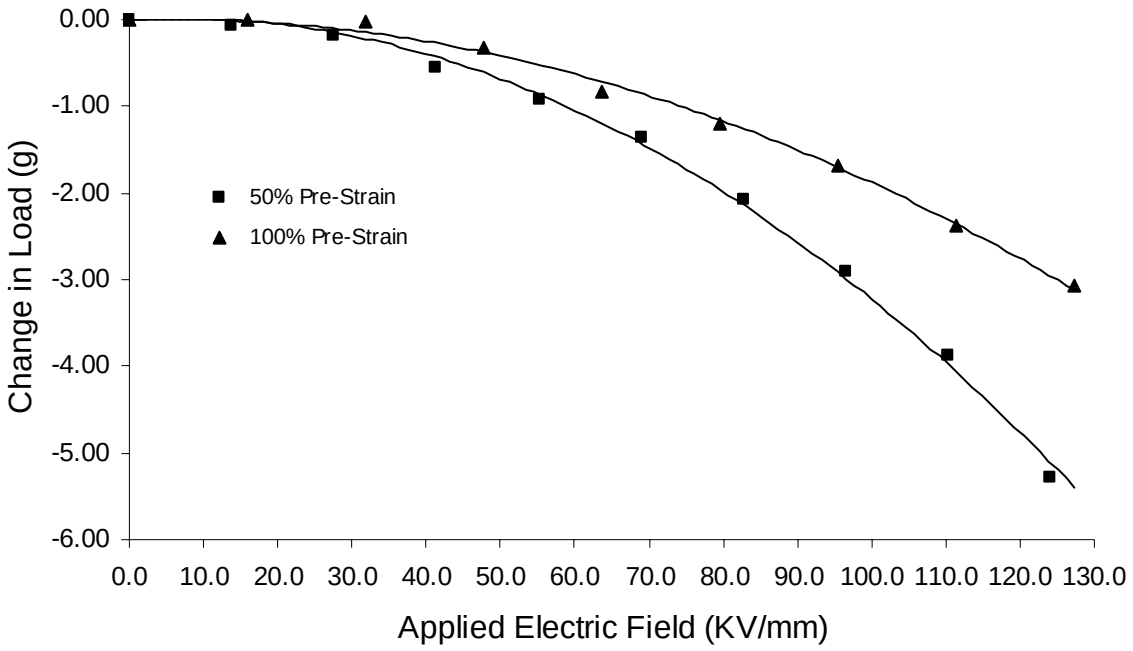

(b)

Figure 5.3. Change in load on the load cell as a function of applied electric field in uniaxially strained prototypes for different prestrain levels (a) silicone tube based prototype (b) polyurethane based prototype

5.2 ACTUATION BEHAVIOR OF UNIFORMLY PRESTRAINED PROTOTYPE

Much like uniaxially prestrained prototype samples, after fabricating uniformly prestrained prototypes (discussed in section 4.2.3), the test samples were subjected to multiple actuation cycles. Only silicone tube based prototypes were evaluated under uniform prestrain because polyurethane tubes required very high inflation pressures that were not achievable with the available test set-up. During each actuation cycle a DC voltage was applied across the two electrodes of the prototype in steps of 0.5 KV or 0.25 KV (depending on the breakdown voltage of the prototype) up to just under the breakdown voltage of the sample. Note that steps used here were very small compared to the ones used in actuation experiments of uniaxially prestrained prototypes because breakdown voltages for uniformly prestrained prototypes (<4 KV) were much lower than uniaxially prestrained prototypes (>14 KV). The

breakdown voltage was determined experimentally for each prestrain level. For highly prestrained prototypes at 8.4 psi (179% radial prestrain, 136% axial prestrain) and 13.73 psi (216% radial prestrain and 180% axial prestrain), which failed at much lower voltages (<2.5 KV) as compared to samples at lower prestrains, steps of 0.25 KV were used in order to get enough data points for analysis. Similar to actuation experiments of uniaxially prestrained prototypes, at every step, the applied voltage was held for 15 seconds before bringing it back to zero volts, where it was again held for a few seconds to allow for actuator recovery, and then taken to the next level.

The actuation behavior of uniformly prestrained silicone based prototypes at different levels of prestrain is discussed in detail below.

5.2.1 Axial actuation strains

Axial actuation strains produced at different prestrain levels (inflation pressures) of silicone based uniformly prestrained samples are plotted against applied electric field and are shown in Figure 5.4. As earlier, the data points in the graphs in Figure 5.4 are axial actuation strains at each step of the actuation cycles and the lines are fitted curves through these points. Applied voltage was converted to applied electric field for each prototype by dividing applied voltage by corresponding tube wall thickness.

As was observed earlier in case of uniaxially prestrained prototype fiber actuators, axial actuation strains for uniformly prestrained prototypes also show a parabolic relationship with applied electric field and decrease with increasing levels of uniform prestrain. Reason for such behavior, as mentioned in case of uniaxially prestrained prototypes, is increase in modulus of the silicone tube with increasing prestrain. Maximum axial actuation strain of 6.78% for 6.62 psi inflation pressure (155% radial prestrain and 116% axial prestrain) at 134 V/μm was observed, see Figure 5.4. A set of images showing axial actuation strain in uniformly prestrained prototype is given in Appendix E.

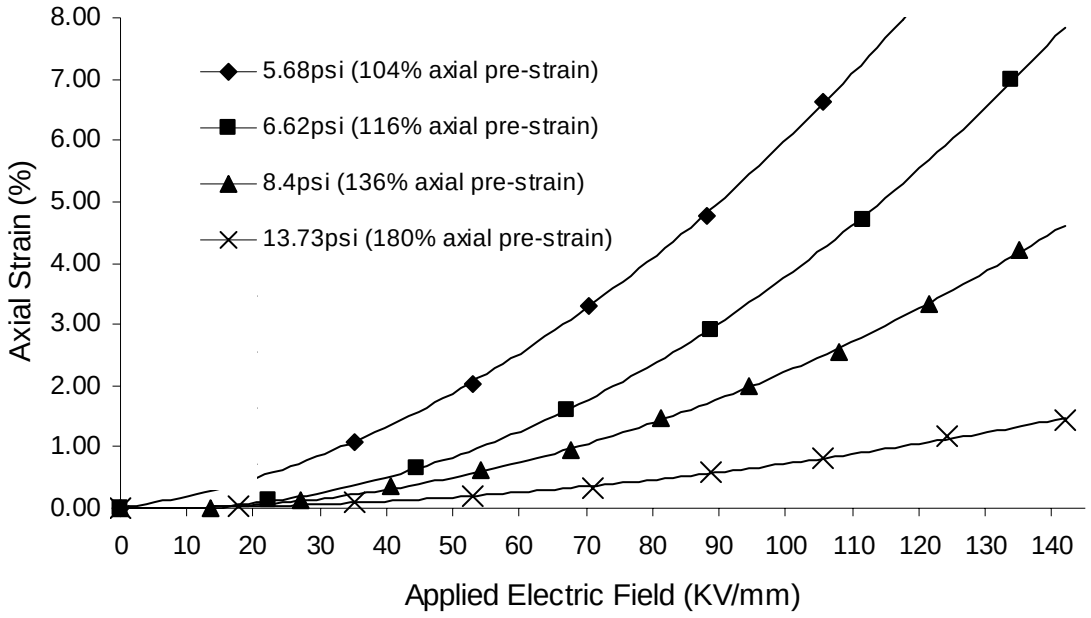

Figure 5.4. Axial actuation strains as a function of applied electric field in uniformly prestrained silicone based prototypes at different inflation pressures (uniform prestrains)

5.2.2 Radial actuation strains

Figure 5.5 shows, radial actuation strains produced at different uniform prestrain levels by silicone based uniformly prestrained samples as a function of applied electric field. The data points in the graphs in Figure 5.5 are radial actuation strains at each step of the actuation cycles and the lines are fitted curves through these points. Applied voltage was converted to applied electric field for each prototype by dividing applied voltage by corresponding tube wall thickness.

Similar to axial actuation strains, radial actuation strains for uniformly prestrained prototypes also show a parabolic relationship with applied electric field and decrease with increasing prestrain levels. Once again, this is due to the increase in modulus of the silicone tube with increase in prestrain, see section 4.2.3.3. Maximum radial actuation strain observed was 6.70% for 5.68 psi inflation pressure at 34V/μm (125% radial prestrain and 104% axial prestrain), see Figure 5.5. A set of images showing radial actuation strain in uniformly prestrained prototype is given in Appendix E.

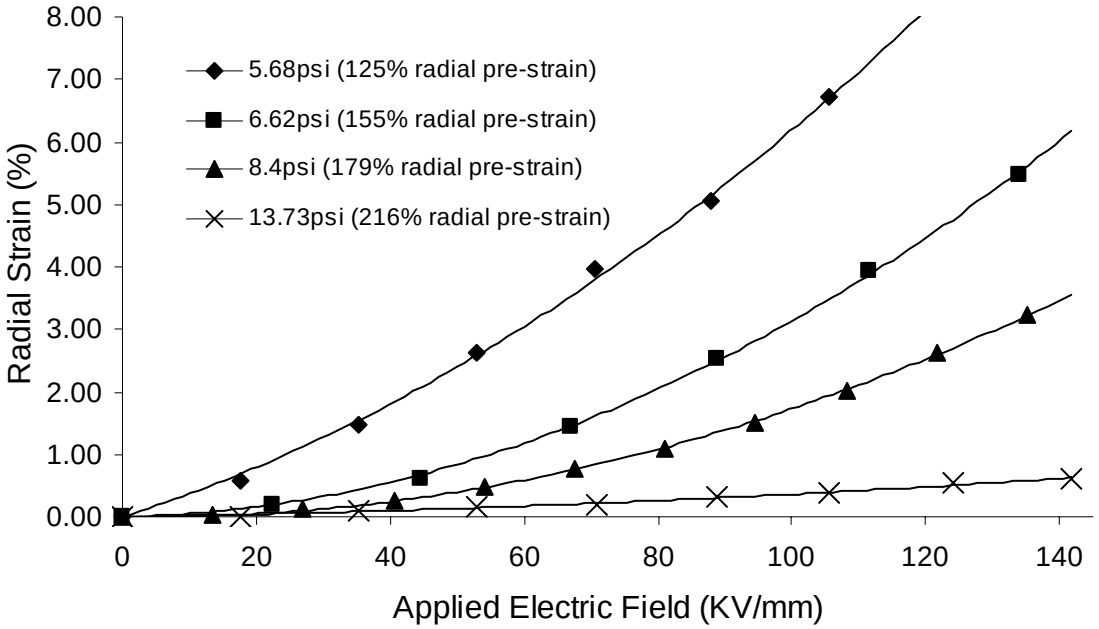

Figure 5.5. Radial actuation strains as a function of applied electric field in uniformly prestrained silicone based prototypes at different inflation pressures (uniform prestrains)

5.2.3 Blocking force

Blocking force produced at different prestrain levels (inflation pressures) of silicone based uniformly prestrained prototype are plotted against applied electric field and are shown in Figure 5.6. Actuation blocking force developed in uniformly prestrained prototypes show similar behavior as uniaxially prestrained prototype fiber actuators. It has a parabolic relationship with applied electric field and the blocking force decreases with increase in prestrain level. Maximum actuation blocking force developed was 1.61 g for actuator with 6.62 psi inflation pressure (155% radial prestrain and 116% axial prestrain) at 52V/μm; maximum predicted actuation blocking force at 52V/μm is 3.32 g for 5.68 psi inflation pressure (125% radial prestrain and 104% axial prestrain), see Figure 5.6.

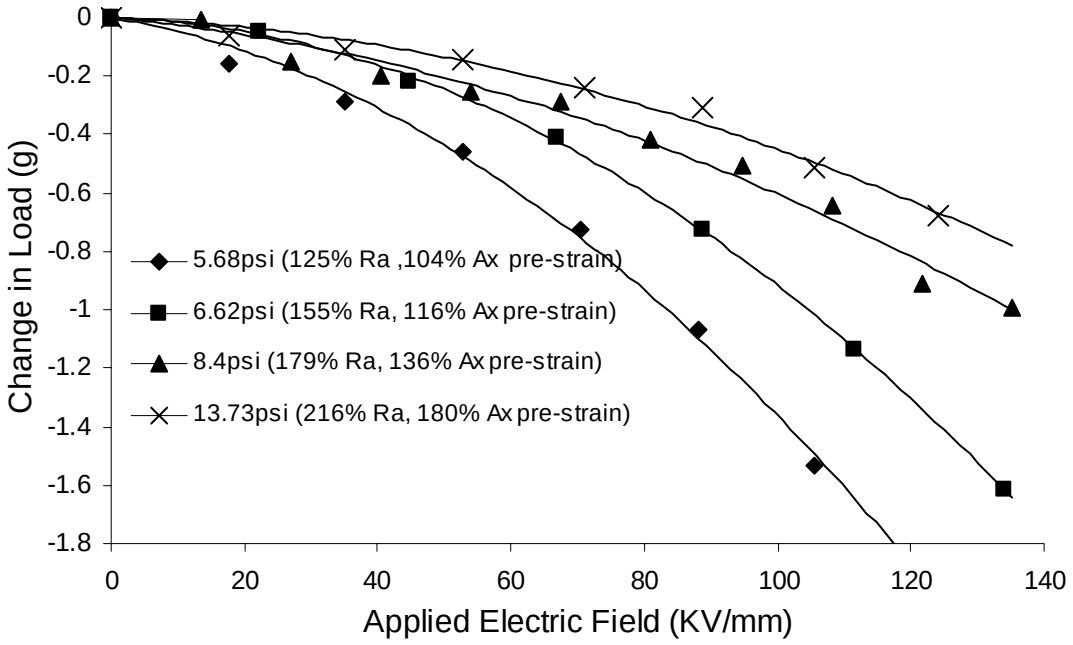

Note: Ra and Ax in the legend stand for Radial and Axial respectively.

Figure 5.6. Blocking force as a function of applied electric field in uniformly prestrained silicone based prototype at different inflation pressures (uniform prestrain levels).

So, in summary, we observed that uniformly prestrained prototypes showed different actuation behavior as compared to uniaxially prestrained prototypes. The actuation strains produced in uniformly prestrained prototypes were approximately equal in both radial and axial directions, and decreased with increase in prestrain level. Whereas in cases of uniaxially prestrained prototypes we had observed that actuation strains along axial and radial directions were very different and followed opposite trends with the increase in prestrain, that is, axial strains decreased and radial strains increased with the increase in prestrain level. On the other hand, similar levels of blocking forces were observed for both uniaxial and uniformly prestrained prototypes, which followed similar trends with the increase in prestrain level. From a broader perspective, what we observe here is that the actuation strains and blocking force decrease with increase in modulus of the dielectric elastomer and, if the system is anisotropic, the strains are higher along the direction with lower modulus. Similar observations have been made in the literature for planar DEAs [31,32, 22]

5.3 HYSTERESIS IN PROTOTYPE FIBER ACTUATORS

Hysteresis is a measure of loss of energy that occurs under cyclical loading and unloading. In this case the loading and unloading (or deformation cycles) is caused by repeated actuation. Evaluation of hysteresis in this context is therefore important for two reasons; first to characterize the tubular actuators for their utility and secondly to validate the experimental technique used in this study. The characterization of actuation behavior of the prototypes was done over multiple actuation cycles and any change in behavior from one cycle to another would make the interpretation of data more difficult. To study hysteresis, 24 and 21 actuation cycles were performed on 150% prestrain silicone tube based and 50% prestrain polyurethane tube based uniaxially strained prototypes respectively. Hysteresis was not studied for all prestrain levels or for inflated prototype fiber actuators as hysteresis is a material property and is not believed to be dependent on the boundary conditions of the prototype.

5.3.1 Hysteresis in silicone based prototypes

Upon taking the silicone based prototype fiber actuator though multiple actuation cycles we observed that the diameter of the actuator showed hysteresis. That is, the diameter did not recover completely even after the applied voltage was removed. The diameter of the actuator at zero electric field kept increasing, to a very small extent (< 2.6% change in diameter over 24 cycles), with every actuation cycle (Figure 5.7(a)). Interestingly, it was observed that even though the diameter of the actuator showed some hysteresis, the net change in diameter for each actuation cycle was constant (Figure 5.7(b)). Because in our study of actuation behavior of prototype fiber actuators we are only concerned with the change in diameter and not absolute diameter of the actuator, any hysteresis in diameter did not have any effect on our results.

Similar observation was made for the actuation blocking force (g) developed in the actuator over multiple actuation cycles. The load values showed some hysteresis (< 0.7% change in absolute load over 24 actuation cycles) but change in load for every cycle remained constant (Figure 5.7 (c) and (d)).

Hence, multiple actuation cycles of the silicone dielectric elastomer based prototype fiber actuators during experimentation had no effect on our actuation behavior measurements.

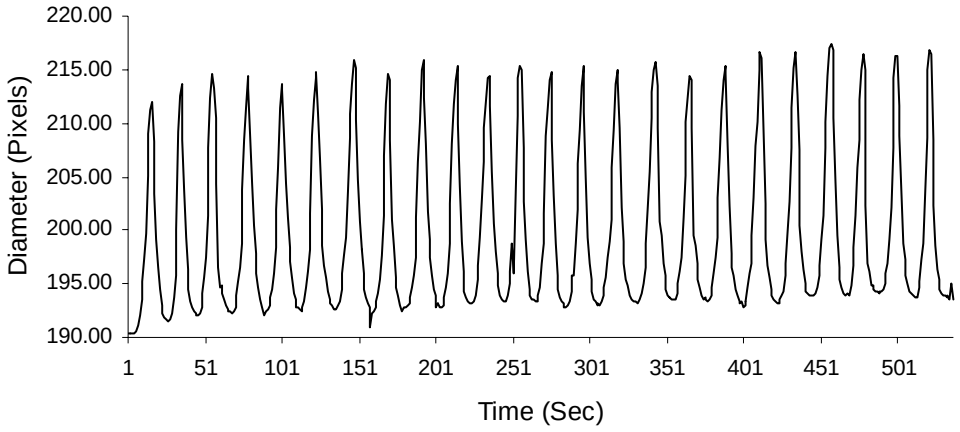

(a)

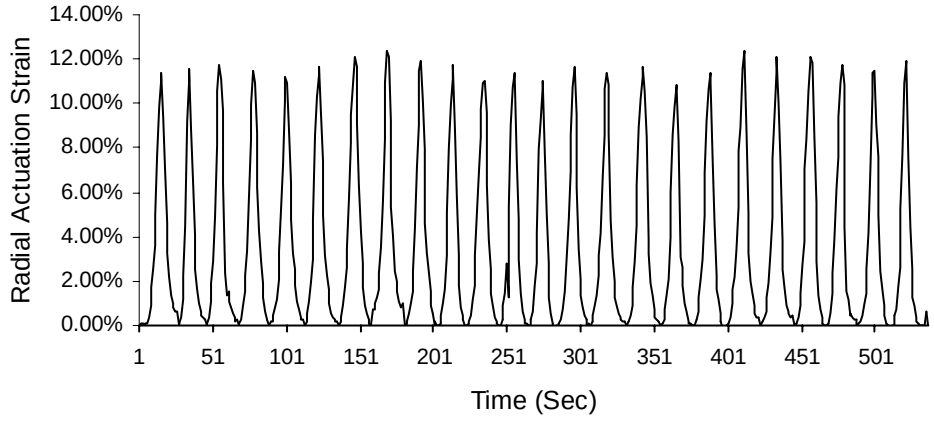

(b)

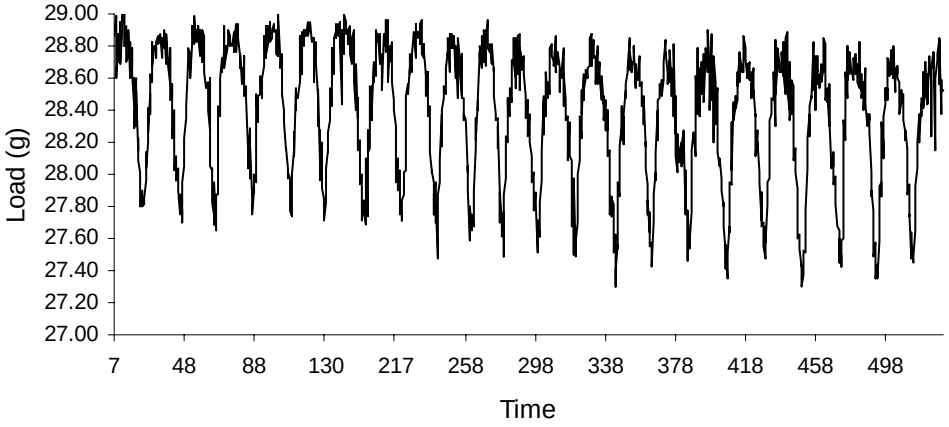

(c)

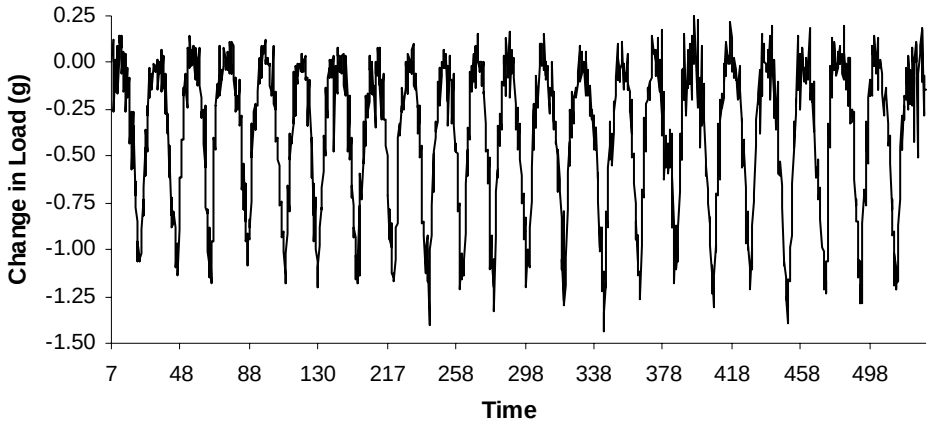

(d)

Figure 5.7. Actuation behavior of silicone dielectric elastomer based prototype fiber actuator over multiple actuation cycles (a) actuator diameter over multiple actuation cycles (b) radial actuation strains over multiple actuation cycles (c) loads on load cell over multiple actuation cycles (d) change in loads over multiple actuation cycles

5.3.2 Hysteresis in polyurethane based prototypes

Polyurethane dielectric elastomer based prototype fiber actuators showed similar hysteresis behavior as silicone based actuators (section 4.3.1). The diameter of the actuator showed hysteresis over multiple actuation cycles, though the hysteresis was lower as compared to silicone based actuator (< 0.5% change in diameter over 22 actuation cycles), but the net change in diameter in each cycle remained constant (Figure 5.8 (a) and (b)). Similarly, load values showed some hysteresis (< 0.45% change in absolute load over 22 actuation cycles) but change in load for every cycle remained constant (Figure 5.8 (c) and (d)).

Hence, multiple actuation cycles of the polyurethane dielectric elastomer based prototype fiber actuators during experimentation had no effect on our actuation behavior measurements.

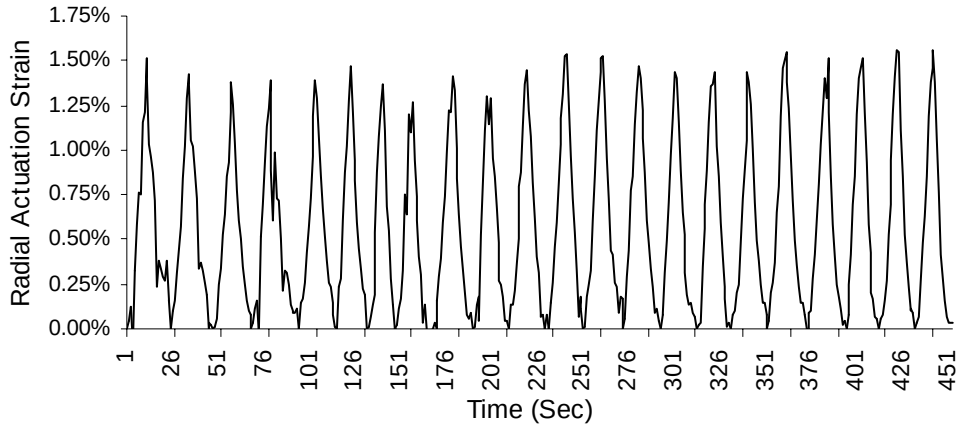
Radial Actuation Strain
1.75%
1.50%
1.25%
1.00%
0.75%
0.50%
0.25%
0.00%
1
26
51
76
101
126
151
176
201
226
251
276
301
326
351
376
401
426
451
Time (Sec)

(a)

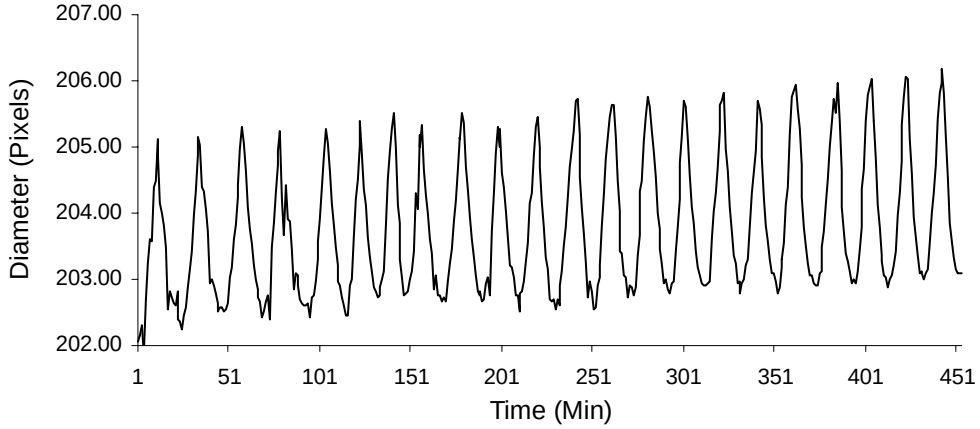
Diameter (Pixels)
207.00
206.00
205.00
204.00
203.00
202.00
1
51
101
151
201
251
301
351
401
451
Time (Min)

(b)

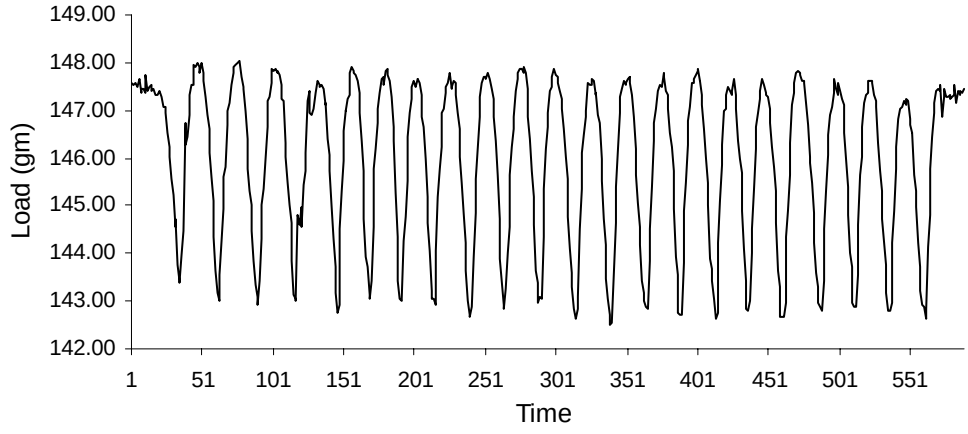
Load (gm)
149.00
148.00
147.00
146.00
145.00
144.00
143.00
142.00
1
51
101
151
201
251
301
351
401
451
501
551
Time

(c)

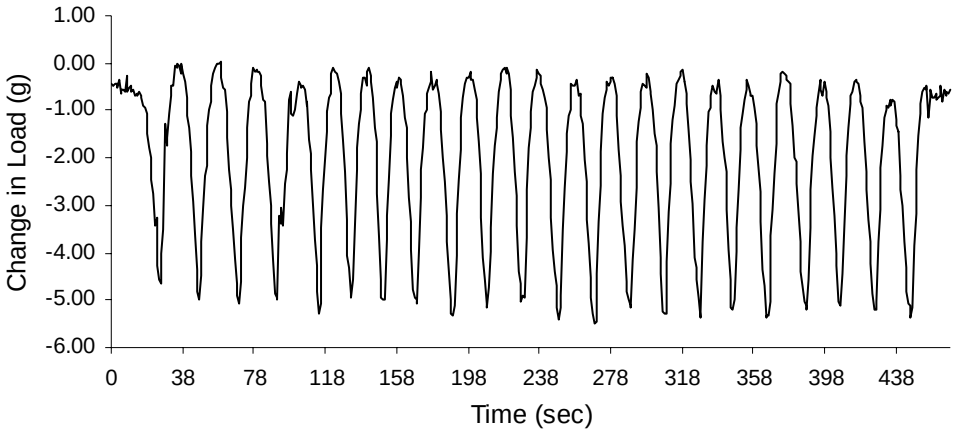

(d)

Figure 5.8. Actuation behavior of polyurethane dielectric elastomer based prototype fiber actuator over multiple actuation cycles (a) actuator diameter over multiple actuation cycles (b) radial actuation strains over multiple actuation cycles (c) loads on load cell over multiple actuation cycles (d) change in loads over multiple actuation cycles

6 CONCLUSIONS

Prototype of a fiber actuator was fabricated using silicone and polyurethane dielectric elastomer tubes with appropriate compliant electrodes on the inner and outer walls of the tube. When an external electric field was applied across the electrodes, the prototype fiber actuator responded with an increase in its physical dimensions in both length and diameter, and developed blocking force.

Strain softening was used as a means to stabilize the mechanical behavior of the elastomeric tubes by eliminating what is known as Mullin's effect. Prestraining the dielectric elastomer tube changed the mechanical properties and physical dimensions (wall thickness and cross-sectional area) of the dielectric elastomer tube, which in-turn changed the actuation behavior of the prototype fiber actuator depending on the type of prestrain and the level of prestrain applied. Two types of prestrains were applied, uniaxial prestrain by straining the tube along its length (along z-direction) and uniform prestrain by inflating the tube. Upon actuation of the developed prototypes by applying an external electric field it was observed that both actuation strains and blocking force followed a parabolic relationship with applied electric field.

In case of uniaxially prestrained prototypes, an increase in prestrain level resulted in a decrease in axial actuation strains accompanied with an increase in radial actuation strains and decrease in actuation blocking force. Such opposite behavior of axial and radial actuation strains is observed because of increased anisotropy of the tube material due to application of axial prestrain. In an anisotropic system actuation occurs primarily along the direction with lower modulus. Decrease in actuation blocking force with increase in prestrain level is believed to be because of change in mechanical properties of the tubes. It was also observed that dielectric elastomer used for fabrication of the prototype had an effect on its actuation behavior. Higher actuation strains were observed in silicone based prototypes as compared to polyurethane based prototypes whereas higher actuation blocking forces were developed in polyurethane based prototypes. Higher actuation strains in silicone based prototypes are believed to be because of its lower modulus than polyurethane elastomer. Based on the theory of linear elasticity, higher strains are developed in materials with lower modulus under same level of Maxwell stress. Higher actuation blocking forces in polyurethane based

prototypes are believed to be because of relatively higher dielectric constant of the polyurethane elastomer. A higher dielectric constant results in higher electrostatic pressure in polyurethane as compared to silicone.

For uniformly prestrained prototype fiber actuator, increase in the uniform prestrains (inflation pressure) resulted in a decrease in all the three actuation behavior parameters; axial actuation strains, radial actuation strains and actuation blocking force. This is observed because increase in uniform prestrains (inflation pressure) increases the modulus of the tube along axial direction (z) as well as along radial direction (θ).

Both silicone and polyurethane based prototypes were tested for hysteresis in their actuation response. No hysteresis was observed.

To understand the actuation behavior of the fiber or tubular actuators more accurately, appropriate theoretical models should be developed. The proposed analysis should account for high strains and anisotropy of the tube materials. In this vein, the work of Carpi and Rossi (2004) has been a step in the right direction. However, their assumptions of linear elastic behavior and isotropy are severely limiting.

7 REFERENCES

[1] Andreas Wingert, Matthew Lichter, Steven Dubowsky, Moustapha Hafez, "Hyper-Redundant Robot Manipulators Actuated by Optimized Binary Dielectric Polymers", Smart Structures and Materials Symposium 2002: Electroactive Polymer Actuators and Devices, Proc. SPIE, Vol. 4695, pp

[2] Bar-Cohen Y., S. Leary, K. Oguro, S. Tadokoro, J. Harrison, J. Smith and J. Su, "Challenges to the transition of IPMC artificial muscles to practical application," Proceedings of the 1999 fall MRS symposium, Vol. 600, (1999).

[3] Bar-Cohen Y., T. Xue and S.-S., Lih, "Polymer piezoelectric transducers for ultrasonic NDE," First international internet workshop on ultrasonic NDE. Subject: Transducers, organized by R. Diederichs, Utonline Journal, Germany, http://www.ndt.net/article/yosi/yosi.htm (Sept.1996)

[4] Yoseph Bar-Cohen, " EAP actuators as Artificial muscle", SPIE-International Society for Optical Engine, October 2001.

[5] Baughman Ray H., Changxing Cui, Anvar A. Zakhidov, Zafar Iqbal, Joseph N. Barisci, Geoff M. Spinks, Gordon G. Wallace, Alberto Mazzoldi, Danilo De Rossi, Andrew G. Rinzler, Oliver Jaschinski, Siegmar Roth, Miklos Kertesz, "Carbon Nanotube Actuators", *Science*, Vol 284, Issue 5418, 1340-1344, 21 May 1999.

[6] Benslimane M., Gravesen P. (2002) "Mechanical properties of Dielectric Elastomer Actuators with smart metallic compliant electrodes" *Smart Structures and Materials: Electroactive Polymer Actuators and Devices, Proc. SPIE*, Vol. 4695 (2002), pp150-157

[7] Calvert P., J. O'Kelly, C. Souvignier, "Solid freeform fabrication of organic-inorganic hybrid materials," Material Science and Engineering, Vol. C6, (1998), PP. 167-174.

[8] Cheng Z.Y., H. S. Xu, J. Su, Q. M. Zhang, P. –C. Wang and Alan G. MacDiarmid, "High performance of all-polymer electrostrictive systems" Smart Structures and Materials 1999: Electroactive Polymer Actuators and Devices, Proc. SPIE, Vol. 3669, pp140-148

[9] Cheng Z.Y., H. S. Xu, V. Bharti, Q. M. Zhang and S. Wang, “Transverse strain response in the electrostrictive Poly(vinylidene fluoride-trifluoroethylene) copolymer”, Applied Physics Letters, Vol. 74 (1999), pp 1901-1903.

[10] C. Lui, Y. Bar-Cohen, and S. Leary, “Electro-statically stricted polymers (ESSP)”, Part of SPIE Conference on EAP Actuators and devices (1999), Vol. 3669, pp.186-190.

[11] Davis, L.C., “Model of magnetorheological elastomers,” Journal of Applied Physics, Vol. 85, No.6 (1999), pp.3348-3351.

[12] “EAP-based artificial muscles as an alternative to space mechanisms” Study Report by University of Pisa, University of Rome & Kayser Italia S.r.l.

[13] Eckerle, J., J.S. Stanford, J. Marlow, Roger Schmidt, S. Oh, T. Low, and V. Shastri. 2001. “A biologically inspired hexapedal robot using field-effect electroactive elastomer artificial muscles,” *Proc. SPIE, Smart Structures and Materials 2001: Industrial and Commercial Applications of Smart Structures Technologies*, Vol. 4332.

[14] Eguchi M., “On permanent electret”, Philosophical Magazine, Vol.49, (1925) pp178.

[15] European Patent WO2004109817

[16] F. Carpi, D. De Rossi, “Theoretical description and fabrication of a new dielectric elastomer actuator showing linear contractions”, *Proc. of Actuator 2004*, Bremen 14-16 June 2004, pp. 344-347.

[17] F. Carpi, D. De Rossi, “Electromechanical characterization of dielectric elastomer planar actuators: comparative evaluation of different electrode materials and different counter loads”, Sensors and Actuators A 107 (2003), pp. 85-95

[18] F.Carpi, D. De Rossi, “Dielectric elastomer cylindrical actuators: electromechanical modeling and experimental evaluation”, Materials Science and Engineering C 24 (2004) 555–562

[19] Gandhi M. R., P.Murray, G. M. Spinks, and G.G. Wallace, “Mechanisms of electromechanical actuation in Polypyrrole,” Synthetic Metals, Vol.75 (1995), pp. 247-256.

[20] Hirai T, M. Watanabe, M. Yamaguchi, “PVC gel deforms like a tongue by applying an electric field,” WW-EAP Newsletter, Vol. 1, No.2, 1999, pp. 7-8.

[21] Kofod G., “Dielectric elastomer actuators” The Technical University of Denmark, Ph.D. thesis, September 2001

[22] Kofod G., Roy Kornbluh, Ron Pelrine, and Peter Sommer-Larsen, “Actuation response of Polyacrylate dielectric elastomers” Journal of Intelligent Material Systems and structures, Vol. 14, No. 12, 787-793 (2003)

[23] Kornbluh R., et. al. (1999) “High-field electrostriction of elastomeric polymer dielectrics for actuation” *Smart Structures and Materials 1999: Electroactive Polymer Actuators and Devices, Proc. SPIE,* Vol. 3669, pp149-161

[24] Kornbluh R. “Ultrahigh strain response of field-actuated elastomeric polymers” *Smart Structures and Materials 2000:Electroactive Polymer Actuators and Devices, Proc. SPIE*, Vol. 3987, pp51-63

[25] Kornbluh R., Harsha Prahlad, Ron Pelrine, Scott Stanford, Marcus A. Rosenthal, Philip A. von Guggenberg, “Rubber to rigid, clamped to undamped: towards composite materials with wide-range controllable stiffness and damping”, Smart Structures and Materials 2004: Industrial and Commercial Applications of Smart Structures Technologies, ed. E. Anderson, Proc. SPIE, Vol. 5388, p. 372-386.

[26] Kornbluh R. “Application of Dielectric Elastomer Actuators” Smart Structures and Materials 2001:Electroactive Polymer Actuators and Devices, Proc. SPIE, Vol. 4329.

[27] Lui Z. and P. Calvert, “Multilayer hydrogels and muscle-like actuators,” Advanced Materials, Vol. 12, No.4 (2000), pp. 288-291.

[28] M A ZHENYI et.al ,”High Field Electrostrictive Response of Polymers” Journal of Polymer Science: Part B: Polymer Physics, Vol. 32,2721-2731 (1994)

[29] Osada Y., and R. Murphy, “Intelligent Gels,” Scientific American, 268, (1993), pp. 82-87.

[30] Otero T. F., and Sansenena, J. M., “Soft and wet conducting polymers for artificial muscles,” Adv. Materials 10 (6), (1998) pp. 491-494.

[31] Pelrine R., Roy Kornbluh, G. Kofod, “High-strain actuator materials based on dielectric elastomers”, Advanced Materials (2000), 12, No. 16, pp 1223-1225.

[32] Pelrine R., Roy Kornbluh, Qibing Pei, Jose P. Joseph, “High- Speed Electrically Actuated Elastomers with Strain Greater Than 100% ” Science, Vol. 287 (2000), pp 836-839

[33] Pelrine R., Roy Kornbluh, Jose P. Joseph, “Electrostriction of polymer dielectrics with compliant electrodes as a means of actuation”, Sensors and Actuators A 64 (1998) 77-85.

[34] Pelrine R., Peter Sommer-Larsen, Roy Kornbluh, Richard Heydt, Guggi Kofod, Qibing Pei, Peter Gravesen, “Applications of Dielectric Elastomer Actuators”, Proceedings of SPIE, Smart Structures and Materials, 2001, Vol. 4329.

[35] Pelrine R., Roy Kornbluh, Qibing Pei, Scott Stanford, Seajin Oh, Joe Eckerle , “Dielectric Elastomer Artificial Muscle Actuators: Toward Biomimetic Motion”, Smart Structures and Materials 2002: Electroactive Polymer Actuators and Devices (EAPAD), Proceedings of SPIE Vol. 4695 (2002)

[36] Pei Q., R. Pelrine, S. Stanford, R. Kornbluh, M. Rosenthal, K. Meijer, and R. Full, “Multifunctional electroelastomer rolls and their application for biomimetic robots,” *Proc. SPIE, Smart Structures and Materials 2003: Electroactive Polymer Actuators and Devices (EAPAD)*, ed. Y. Bar-Cohen.

[37] Pei Q., R. Pelrine, S. Stanford, R. Kornbluh, M. Rosenthal, “Electroelastomer rolls and their application for biomimetic walking robots”, Synthetic Metals 135-136 (2003), pp. 129-131.

[38] Pei Q., M. Rosenthal, Harsha Prahlad, Ron Pelrine, Scott Stanford, "Multiple degrees of freedom electroelastomer roll actuators", Smart Materials and Structures 13 (2004) N86-N92.

[39] Ratna B. R., "Liquid crystalline elastomers as artificial muscles: role of side chain-backbone coupling," Proceedings of the SPIE's 8th Annual International Symposium on Smart Structures and Materials, EAPAD Conf. (2001).

[40] Shiga, T. "Deformation and viscoelastic behavior of polymer gels in electric fields," adv. Polym. Sci. Vol.134, (1997), pp.131-163

[41] Shahinpoor M., "Elastically-activated artificial muscles made with liquid crystal elastomers," Y. Bar-Cohen, (Ed.), Proceedings of SPIE's EAPAD conf., part of the 7th Annual International Symposium on Smart Structures and Materials, SPIE Proc. Vol. 3987, (2000) pp 187-192.

[42] Spinks G. M., Campbell T. E., and Gordon G. G., "Force Generation from polypyrrole actuators", Smart Materials and Structures, 14 (2005) 406-412

[43] Sue, Zhang and Ting, "Space Charge Enhanced Electro Mechanical Response in Thin Film Polyurethane Elastomers" Applied Physics Letters, Vol.**71** (3), 21 July 1997

[44] Su J., Qiming Zhang, Pen-Cheng Wang, Alan. G. MacDiarmid and Kenneth J. Wynne, "Preparation and Characterization of Electrostrictive Polyurethane Films with Conductive Polymer Electrodes" Polymers for Advanced Technologies, Vol. 9 (1998), pp 317-321

[45] US Patent 6,891,317

[46] US Patent 6,586,859

[47] US Patent 6,343,129

[48] US Patent 6,545,384

[49] US Patent 6,583,533

[50] US Patent 6.812,624

[51] US Patent 4400634

[52] US Patent 6,876,135

[53] Treloar L. R. G., “The physics of rubber elasticity”, Oxford University Press 1958.

[54] Watanabe M., et. al. (2002) “ Wrinkled Polypyrrole Electrode for Electroactive Polymer Actuators” *Journal of Applied Physics*, Vol 92, number 8, pp 4631-4637.

[55] Winslow, W.M. ,”Induced fibrillation of suspensions,’ Journal of Applied Physics, Vol.20, (1949), pp.1137.

[56] Zrinyi M., D. Szabo and J.Feher, “Comparative studies of electro- and magnetic field sensitive polymer gels,” Y. Bar-Cohen, (Ed.), Proceedings of the SPIE’s 6th Annual International Symposium of Smart Structures and Materials, EAPAD Conf., SPIE Proc. Vol. 3669 (1999) pp.406-413.

[57] Akbay, M. C., “Performance of compliant electrodes in electro active polymer (EAP) actuators”, Masters thesis, North Carolina State University, 2004.

[58] Kim H., Hwang S., Choi H. R., Kim M. H., Jeon J. W., Nam J., “Field actuated behavior of polymers as dielectric material”, Proceedings of SPIE, Smart Structures and Materials, 2001: Electro active Polymer Actuators and Devices, Vol. 4329 pp 491-498.

APPENDIX A. Wall thickness calculation for uniformly prestrained prototype.

Wall thickness of the inflated tube was calculated by measuring outer diameter of the inflated tube and subtracting from it inner diameter of the tube. Outer diameter of the inflated tube (OD_2) was calculated by taking image of the inflated tube at different prestrain levels (inflation pressures) and comparing them with image of a standard linear scale of least count 1mm. All the images were taken at the same magnification. The diameter of the inflated tube was measured in number of pixels and physical dimension of one pixel in the image was calculated using the image of the standard scale. MATROX® Image analysis software was used to do the image analysis. Inner diameter of the inflated tube was calculated by using the constant volume assumption for the dielectric elastomer. Initial volume of the dielectric elastomer for a specific length was calculated using the inner and outer diameter provided by the supplier. Initial tube volume was equated to the tube volume after inflation, where inner diameter was the unknown. Length of the inflated tube was measured using a ruler and outer diameter of the inflated tube measured using image analysis, as mentioned above. Following set of equations show the calculations performed to calculate the inner diameter of the inflated tube:

V_2 (Volume of Inflated Tube) = V_1 (Initial Volume of the Tube) …*(G.1)*

$$V_2 = \pi \times ((OD_2/2)^2 - (ID_2/2)^2) \times l_2 \quad \text{…(G.2)}$$

$$V_1 = \pi \times ((OD_1/2)^2 - (ID_1/2)^2) \times l_1 \quad \text{…(G.3)}$$

From (3.1), (3.2) and (3.3)

$$ID_2 = 2 \times \sqrt{(OD_2/2)^2 - (\{\pi \times ((OD_1/2)^2 - (ID_1/2)^2 \times l_1\}/ (\pi \times l_2))} \quad \text{…(G.4)}$$

$$\text{Final Wall Thickness} = (OD_2 - ID_2)/2 \quad \text{…(G.5)}$$

Where:

ID_2 = Inner Diameter of inflated tube

OD_2 = Outer diameter of the inflated tube

l_2= Length of inflated tube

ID_1 = Inner Diameter of un-inflated tube

OD_1 = Outer diameter of the un-inflated tube

l_1 (Length of un-inflated tube) = 4 cm

APPENDIX B: Macro written in MATROX® Inspector to measure the distance between two reference points on the active area of the prototype fiber actuator using blob analysis.

```
Def TwoPtAxialStr(S_VHL_S1_AX_1_AVI)
{
for( i=1;i<=2365;i=i+7)
{
SeqSetCurEx(S_VHL_S1_AX_1_AVI,0+i);
ImgSetCurrent(S_VHL_S1_AX_1_AVI, R_Def, ALL_BANDS);
B_BLOBSET2 = BlobNew();
BlobSetCur(B_BLOBSET2);
BlobSetRemEdge(FALSE, FALSE, FALSE, FALSE);
BlobEnableMaxArea(TRUE);
BlobSetMaxArea(1000);
BlobSetThreshEx (0, 220);
BlobFeatSelect(BLOB_AREA, FALSE);
BlobFeatSelect(BLOB_CENTER_OF_GRAVITY_X_BIN, TRUE);
BlobFeatSelect(BLOB_CENTER_OF_GRAVITY_Y_BIN, TRUE);
BlobCount();
T_TABLE1 = MeasNew();
MeasSetCur(T_TABLE1);
BlobTransferOneEx(0, "");
BlobTransferOneEx(1, "");
MeasSelect(1);
MeasSelect(2);
MeasCalcLine(0, -1);
MeasExportResult(3, "Book1|Sheet1|A1|R|B|N|F");
MeasClose();
BlobCloseAllRes();
BlobClose();
delete B_BLOBSET2;
}
}
```

APPENDIX C: Macro written in MATROX® Inspector to measure area of the active region of the prototype fiber actuator using blob analysis.

```
Def ScrRec2(S_HL_S1_RA_1_AVI)
{
for( i=1;i<=2416;i=i+7 )
{
SeqSetCurEx(S_HL_S1_RA_1_AVI, 0+i);
ImgSetCurrent(S_HL_S1_RA_1_AVI, R_Def, ALL_BANDS);
B_BLOBSET3 = BlobNew();
BlobSetCur(B_BLOBSET3);
BlobSetRemEdge(FALSE, FALSE, FALSE, FALSE);
BlobSetMinArea(2000);
BlobSetForeground(0);
BlobCount();
BlobExportResults(BLOB_ALL, BLOB_NONE, "", "Book7|Sheet1|A1|R|B|N|F");
BlobCloseAllRes();
BlobClose();
delete B_BLOBSET3;
}
}
```

APPENDIX D. Percent change in load upon actuation of uniaxially prestrained prototypes.

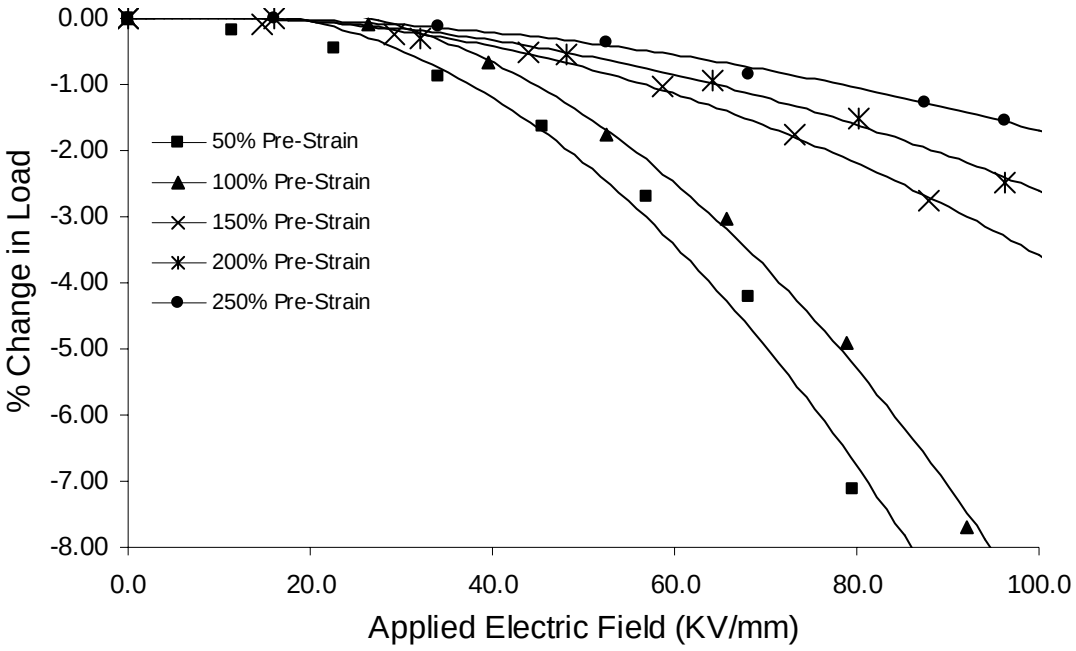

(a)

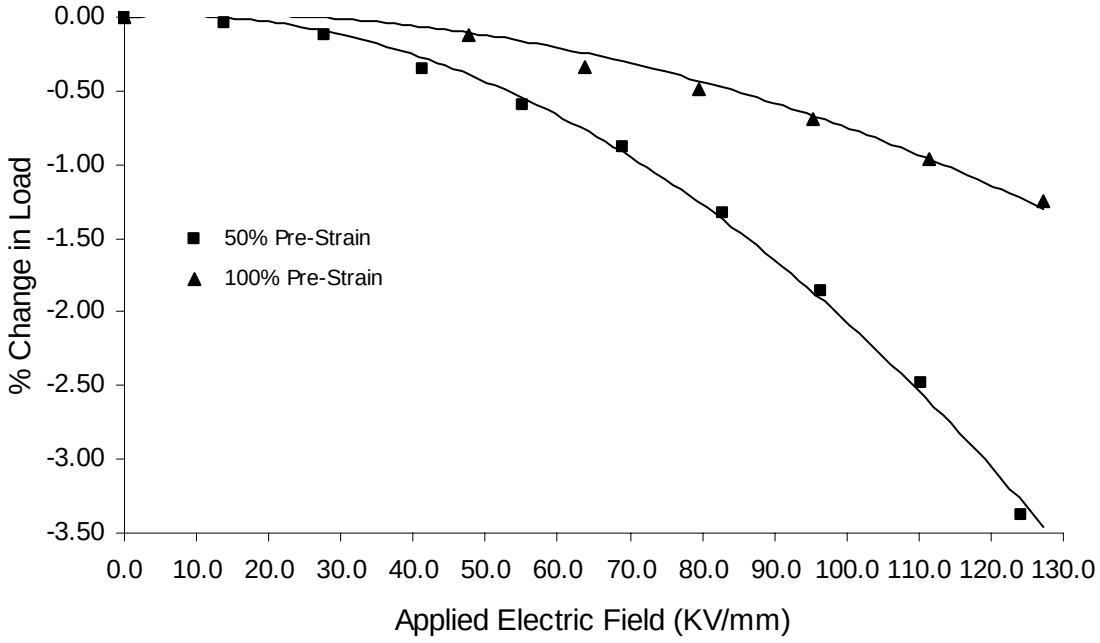

(b)

Figure D.1 Percent change in load in uniaxially prestrained prototypes (a) silicone based prototype (b) polyurethane based prototype

APPENDIX E: Images depicting actuation strains in silicone based uniaxially prestrained and uniformly prestrained prototypes.

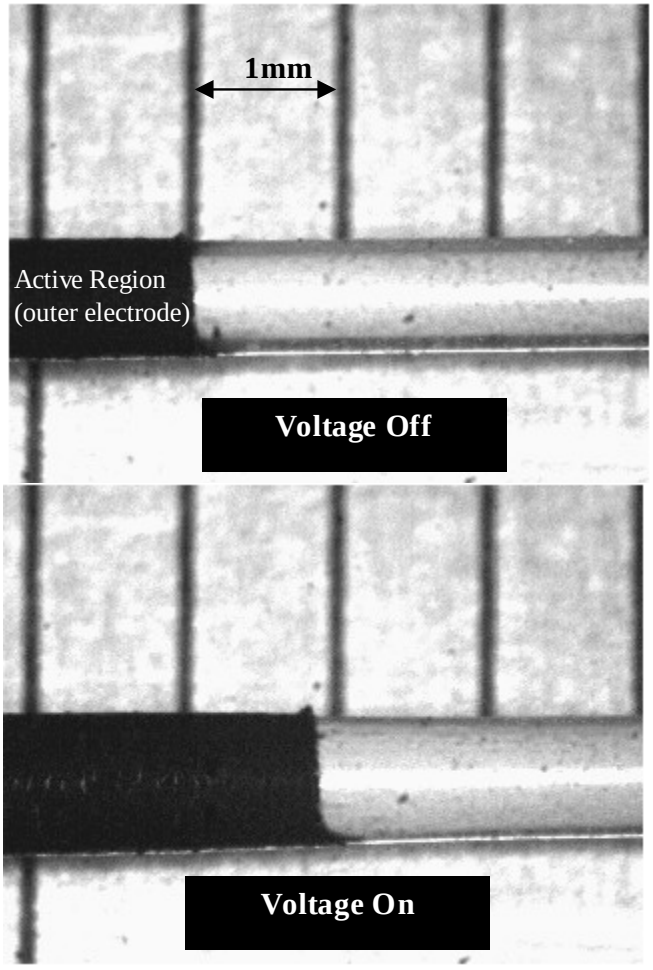

Figure E.1. Axial actuation strain produced in uniaxially prestrained silicone based prototype (50% prestrain level and having an active region of 20mm) at an electric field of 102V/μm. The images show an axial actuation strain of 10%.

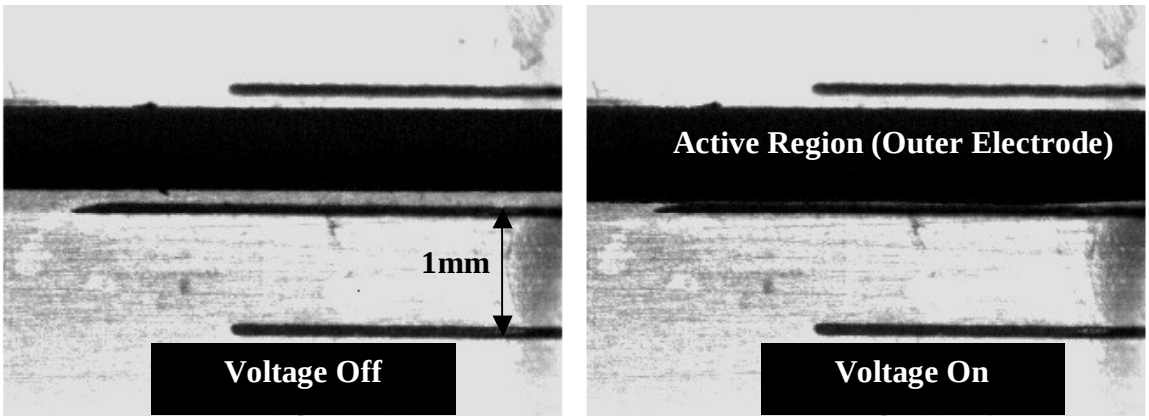

Figure E.2. Radial actuation strain produced in uniaxially prestrained silicone based prototype (150% prestrain level and having an active region of 20mm) at an electric field of 103V/μm. The images show radial actuation strain of 16%.

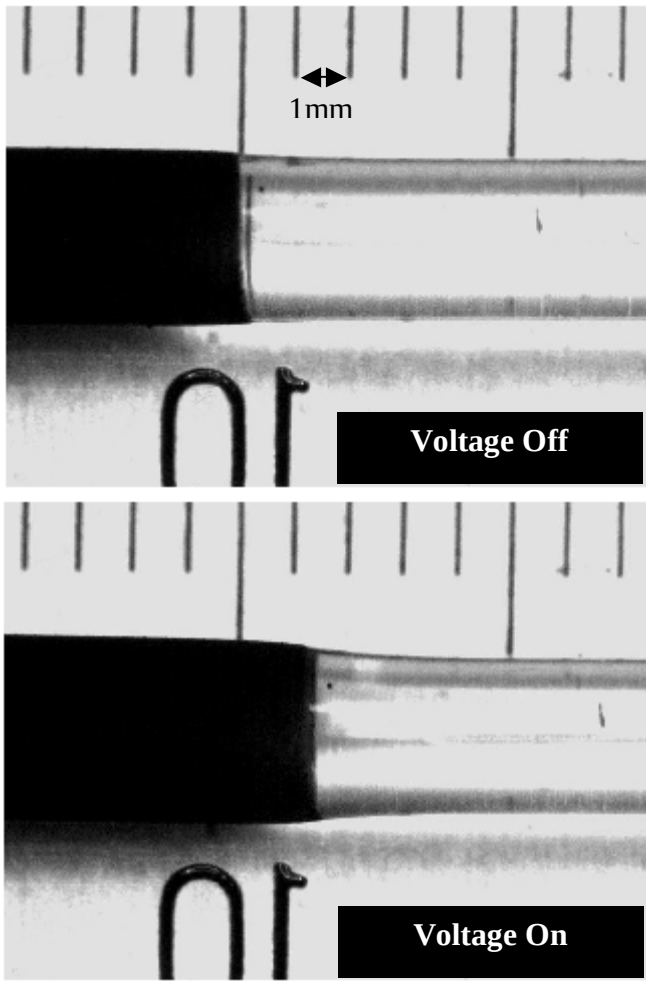

Figure E.3. Axial actuation strain produced in uniformly prestrained silicone based prototype (6.62 psi (155% radial prestrain and 116% axial prestrain) and having an active region of 20mm) at an electric field of 167 V/μm. The images show axial actuation strain of 18%.

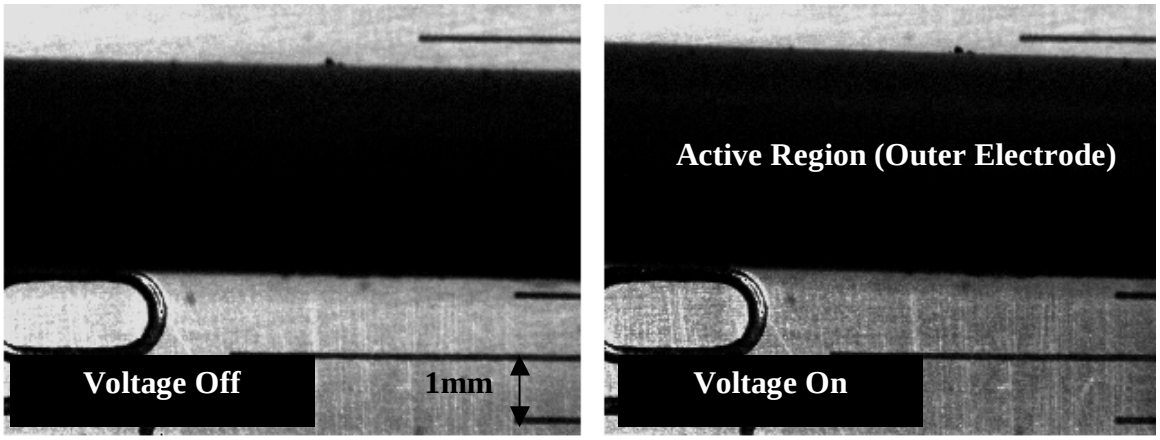

Figure E.4. Radial actuation strain produced in uniformly prestrained silicone based prototype (6.62 psi (155% radial prestrain and 116% axial prestrain) and having an active region of 20mm) at an electric field of 112 V/μm. The images show axial actuation strain of 4.2%.